THE UNIVERSITY OF MANITOBA

HETEROBIMETALLIC DICYCLOHEXYLPHOSPHIDO-BRIDGED COMPLEXES

BY

HILARY ANNE JENKINS

A THESIS

SUBMITTED TO THE FACULTY OF GRADUATE STUDIES

IN PARTIAL FULFILLMENT OF THE REQUIREMENTS FOR THE DEGREE OF

MASTER OF SCIENCE

DEPARTMENT OF CHEMISTRY

WINNIPEG, MANITOBA

1987

ISBN 0-315-44139-9

HETEROBIMETALLIC DICYCLOHEXYLPHOSPHIDO-BRIDGED COMPLEXES

BY

HILARY ANNE JENKINS

A thesis submitted to the Faculty of Graduate Studies of the University of Manitoba in partial fulfillment of the requirements of the degree of

MASTER OF SCIENCE

ABSTRACT

This thesis describes the synthesis, characterization, and reaction studies of several heterobimetallic dicyclohexylphosphido-bridged complexes. Heteronuclear compounds are of current interest because unique reactivity features may result from linking together metals with different substrate reactivities. Di- and polynuclear complexes that contain bridging ligands such as diorganophosphido groups are particularily desirable since these ligands may prevent fragmentation of the complexes during reactions. The bridge-assisted method of synthesis is used to prepare the complexes described herein. This method employs a phosphide ligand to bring two metal centres together by nucleophilic displacement of a chloride ligand by the phosphido group, which than serves as a bridge between the metals. The complexes prepared are studied through the use of $^{31}P\{^{1}H\}$, $^{13}C\{^{1}H\}$, and ^{1}H nmr, infrared spectroscopy, and X-ray crystallography.

The doubly-bridged complexes of the type $(CO)_4M(\mu\text{-}PCy_2)_2M'(PPh_3)$ (M = Mo, W; M' = Ni, Pd, Pt) serve as a preliminary study to introduce concepts such as the relationship between $^{31}P\{^{1}H\}$ nmr and X-ray diffraction studies, and the metal-metal interaction. Several Fe-Ir and Fe-Rh complexes are prepared, due to similarities between these compounds and well-known catalysts, such as Wilkinson's catalyst, $RhCl(PPh_3)_3$[63]. Coordinatively saturated $(CO)_3(PPh_3)Fe(\mu\text{-}PCy_2)Ir(PPh_3)(CO)_2$ undergoes several substitution reactions with

trialkyl phosphines; we observed that the molecule behaves as a single entity rather than as two separate metal centres. The coordinatively unsaturated complex $(CO)_4Fe(\mu\text{-}PCy_2)Ir(COD)$ was prepared, and was found to catalytically hydrogenate styrene to ethyl benzene. Finally, the coordinatively unsaturated complexes $(CO)_3(PPh_3)Fe(\mu\text{-}PCy_2)Rh(PPh_3)(CO)$ and $(CO)_4Fe(\mu\text{-}PCy_2)Rh(COD)$ were prepared. These complexes readily undergo substitution, addition, and oxidative-addition reactions, and certainly warrant further study.

to my dad

there are no failed experiments,

there are only more data.

ACKNOWLEDGEMENTS

The author is deeply grateful for the guidance, patience, and friendship of Dr. Stephen Loeb, without whom this work would not have been possible. Dr. Loeb's unique personality and sense of humour allowed him to make the best of any situation, and the time that I've worked with him will remain etched in my memory always.

Many thanks also to the Chemistry Department at the University of Winnipeg, especially to Broer de Groot for the help with the GC-MS studies, and to Kirk Marat and Terry Woloweic at the University of Manitoba for all the nmr time.

Finally, a special thanks to all my friends for their support over the past two years, especially to Debbie, Vic, and Kent, who helped me keep my sense of humour, and to Matt and Ginny, who brought bright sunshine into my life.

TABLE OF CONTENTS

Page

Page

Page

Page

Page

Page

LIST OF TABLES

LIST OF FIGURES

KEY ABBREVIATIONS

Me	methyl
Et	ethyl
Ph	phenyl
Cy	cyclohexyl
Bz	benzyl
i-Pr	isopropyl
n-Bu	n-butyl
t-Bu	tert-butyl
dppe	bis(diphenylphosphino) ethane
dppm	bis(diphenylphosphino) methane
PR_3	trialkyl phosphine
THF	tetrahydrofuran
COD or 1,5-COD	1,5-cyclooctadiene
DMA	dimethylacetamide

CHAPTER ONE

INTRODUCTION

1.1 Preamble

The ability of a transition metal complex to activate small molecules is enhanced when a metal atom is surrounded by electron-donating, sterically demanding trialkylphosphine ligands[1]. Two-coordinate, 14 electron complexes of the type $[M(PR_3)_2]$ (M = Pd, Pt; R = *i*-Pr, *t*-Bu, Cy), three-coordinate, 14 electron complexes of the type $[RhH(PR_3)_2]$ (R = *i*-Pr, *t*-Bu, Cy), and five-coordinate, 16 electron complexes of the type *trans*-$M(PR_3)_2(CO)_3$ (M = Mo, W; R = *i*-Pr, Cy), are excellent examples of systems where the bulky trialkylphosphines have been used to promote coordinative unsaturation and increased reactivity with small substrate molecules[2-5]. These complexes are known to react with N_2, H_2, C_2H_4, CO, SO_2, and CO_2.

This specific reactivity toward substrates such as the small molecules named above should be possible for multi-centred complexes if a balance between steric and electronic properties is achieved. The approach used in this thesis is the use of bulky dialkylphosphido-bridging ligands in combination with various large ancillary ligands (such as PR_3) to produce coordinatively unsaturated heterobimetallic complexes. These complexes are interesting because, as explained in

Section 1.2, unique chemical reactivity may result from the close proximity of two different metals with different substrate activity.

1.2 Heteronuclear Metal-Metal Bonded Compounds

The past 10 to 15 years have seen increasing interest in the preparation and study of heteronuclear compounds with metal-metal bonds. The reactions of these complexes are especially interesting because of their potential applications in catalysis[6]. For example, heteronuclear compounds can function in the following ways: 1) metal-metal bonded compounds ought to show special reactivity features as a result of cooperation between adjacent metals and these could then function as unique homogeneous catalysts, 2) metal-metal bonded compounds, particularily those containing three or more metal atoms, may also function as 'storehouses' for the release and take-up of catalytically active fragments. Such clusters are also being used to model the bonding and reactions of substrates on metal surfaces.

In this study, we will be looking at heterobimetallic compounds only. There is increasing evidence that binuclear transition metal complexes will play at least two important roles in the systematic development of organotransition metal chemistry. Firstly, relatively simple compounds can serve as models for more complex systems, where fundamental studies of binuclear oxidative-additions, reductive-eliminations, and migratory insertions should add significantly to the development and interpretation of polymetallic- or cluster-catalyzed reactions. Secondly, reactions of bimetallic compounds should prove

unique and useful in their own right. This potential has been suggested by recent studies involving bimetallic mechanisms in reactions previously believed to take place at a single metal site[7].

Finally, heterobimetallic compounds should show unique reactivity features as a result of combining the different reactivity properties of constituent metals[6]. For example, dinuclear compounds with early-late transition metal combinations might be able to polarize and activate substrates such as CO. Alternatively, and from a mechanistic point of view, the low symmetry which heteronuclear compounds inherently possess has been shown to be extremely useful for elucidating specific sites of reactivity and can provide important insight into mechanistic detail[8].

1.3 Synthesis of Heteronuclear Metal-Metal Bonded Complexes

The first heteronuclear metal-metal bonded compound was prepared in 1933 by Schubert, as in Figure 1.1 and Equation 1.1 below[9], and was formulated as $AgCo(CO)_4 \cdot xH_2O$ based on chemical analysis alone. A more recent study[10] has indicated that the structure is likely that of a tetrameric complex with alternating Ag and $Co(CO)_4$ units linked via Ag-Co bonds in an eight-membered ring.

$$K_2[Co(cysteine)_2] \xrightarrow[ii)\ AgNO_3]{i)\ CO} AgCo(CO)_4 \cdot xH_2O \qquad (1.1)$$

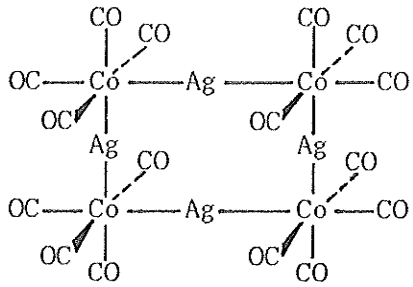

Figure 1.1: The first heteronuclear metal-metal bonded compound, prepared by Schubert in 1933.

In 1959, Chini[11] prepared the first heterometallic transition-metal cluster, $[FeCo_3(CO)_{12}]^-$, by the reaction of $Co_2(CO)_8$ and $Fe(CO)_5$ in acetone at 60°C, as shown in Equation 1.2.

$$7/2\ Co_2(CO)_8 + 2\ Fe(CO)_5 \longrightarrow [Co(acetone)_6][FeCo_3(CO)_{12}]_2 \quad (1.2)$$

Since this time of course, many heteronuclear species have been prepared, often where the only factor controlling the reaction is chance. In fact, in many cases where heteronuclear cluster compounds have been prepared, the only 'method' was to put all the reagents in a flask to see what products would be obtained. While this method often provided for novel, interesting complexes, it was obvious that for the synthesis of specific transition metal compounds a more direct approach would have to be taken. The most useful and rational approach for synthesizing a polymetallic complex would be to work by a stepwise synthesis: adding one metal at a time using monomeric organometallic compounds as building blocks, as in Figure 1.2[6].

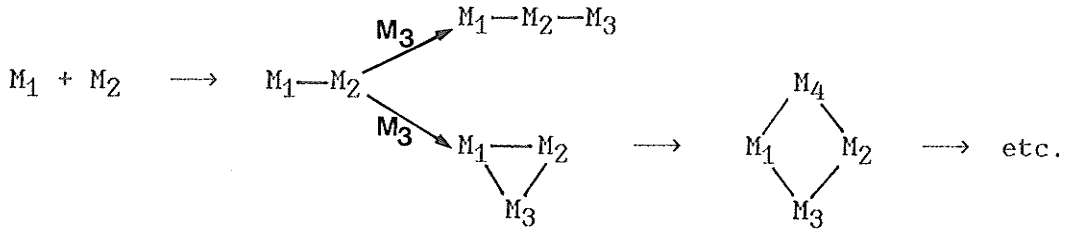

Figure 1.2: Stepwise synthesis of heteronuclear compounds.

For the systems in this paper the best synthetic approach was the bridge-assisted synthesis, outlined below in Figure 1.3. A bridge-assisted reaction is one which employs a ligand to bring two metal centres together where that ligand then functions as a bridge between the two metals in the final product. Specifically, we have employed the bridge-assisted substitution, the most widely used synthetic route to diorganophosphido-bridged heterobimetallic complexes[12]. Two types of ligand systems that most often participate in bridge-assisted substitution reactions are derivatives of group 15 and 16 elements, P, As, and S. A chalcogen atom bound to a single metal centre always has a lone pair of electrons which potentially can be used to donate to a second metal. The metallo-ligands can therefore displace a ligand (such as a halide) on another metal centre[13]. The interest in organophosphido (R_2P) or arsenido (R_2As) groups can be attributed to the realization that these metal-bridging ligands have a stability that is independent of bonding interactions between the metal atoms. This stability is of particular interest in homogeneous cluster catalysis where metal-metal bond breaking and formation play an important part in the catalytic mechanism. Utilization of organophosphido or arsenido bridging ligands may prevent undesirable fragmentation of the cluster

unit or reaction with substrate molecules thus stabilizing the catalyst complex[14].

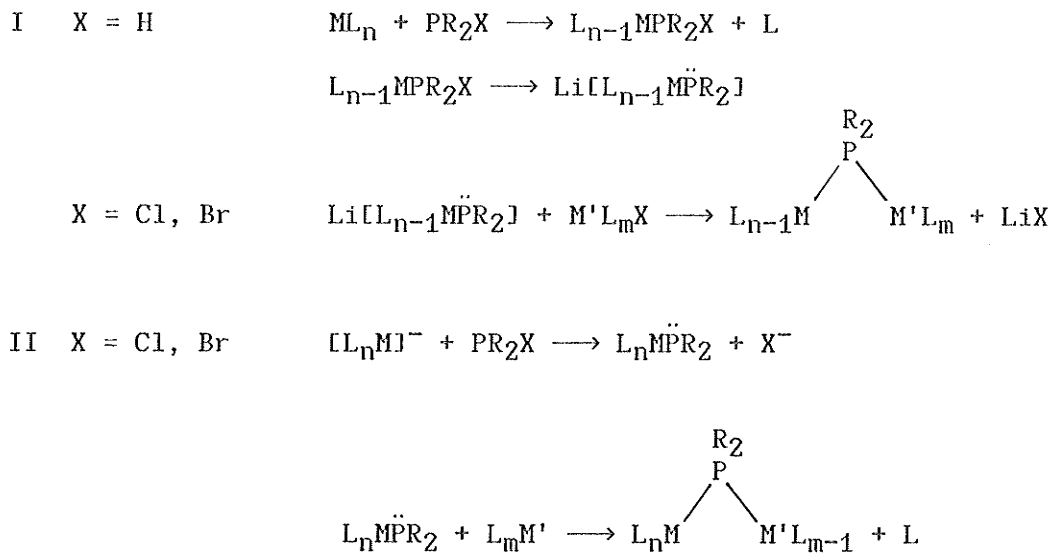

Figure 1.3: Bridge-assisted substitution methods.

According to Carty[15] et.al. the major drawback to the use of metal cluster compounds as homogeneous catalysts is their inherent tendency to degrade under conditions appropriate for effective catalysis. Therefore many high nuclearity carbonyl clusters undergo fragmentation under pressure of CO or in the presence of Lewis bases[16]. A solution to this problem has been sought via the design of molecules with stable, flexible supporting bridges capable of maintaining the integrity of a cluster framework while allowing facile metal-metal bond cleavage and reformation.

The formation of the metal-metal bond is dictated by the metals and the ligand set involved in the particular reactions. For example group 15 derivatives usually only possess one lone pair of electrons, used to

bind the ligand to the metal centre. To create a second lone pair of electrons on the pnicogen atom it must be modified as in Figure 1.3. The initial dinuclear product formed does not necessarily have a metal-metal bond. The bond can often be generated by heating or irradiating the dinuclear product to induce ligand loss followed by closure. The reactions below illustrate Method 1, the method of choice for this thesis. Equations 1.4 and 1.5 illustrate formation of an initial product without a metal-metal bond and its subsequent transformation into a complex with a metal-metal bond[11].

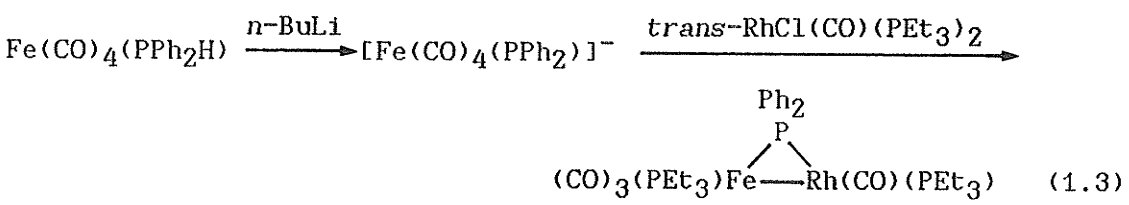

(1.3)

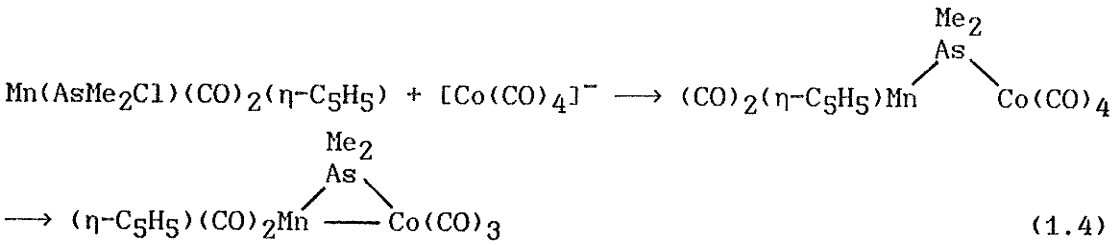

(1.4)

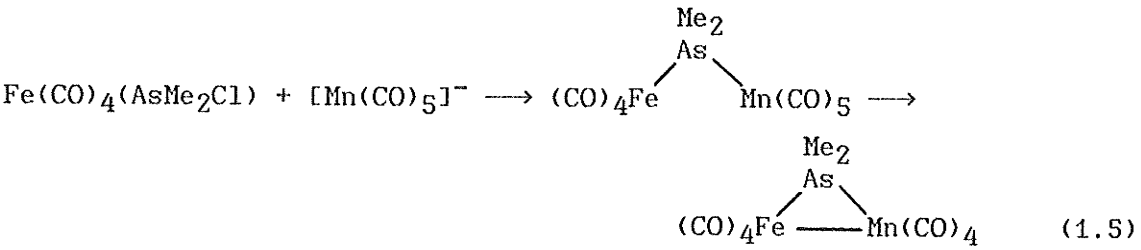

(1.5)

1.4 Phosphide Bridges

The first diphenylphosphido complexes were prepared by Hayter[17] and Chatt[18] 25 years ago, though it is only recently that interest in the use of organophosphido groups has increased. This is probably due to the following factors: 1) a tremendous recent interest in catalysis by transition metal clusters, 2) the realization that organophosphido groups form stable bridges between two metals similar to the mercaptide ligands, and 3) the increased use of $^{31}P\{^{1}H\}$ nmr spectra for characterization and structure elucidation of the resulting products[19]. Some of the general advantages of using phosphide bridges have already been mentioned, for example, they are among the most useful ligands for bridge-assisted substitution reactions.

Two different transition metals brought into close proximity in a bimetallic complex may display chemistry unique from that found in the individual separated fragments. Heterobimetallic centres have been formed and stabilized in such altered environments by construction of metal-metal bonds, ligand bridges, or a combination of both structural features. In this regard, phosphido ligands have been found in some instances to provide particularily stable bridge anchors which retard fragmentation of the bimetallic unit[20]. In most cases in fact, the phosphido-bridge will not react with substrate molecules, however, this is not always the case, as for example with the complex $(MeCp)(CO)_2Mn(\mu\text{-}t\text{-}Bu_2P)Ir(COD)$ (COD = 1,5-cyclooctadiene). In reactions with H_2 the phosphide bridge adds hydrogen to form $Mn(MeCp)(CO)_2(t\text{-}Bu_2PH)$[21].

As was mentioned at the beginning of this chapter, it is well-known

that bulky phosphine ligands can impart added stability to coordinatively unsaturated transition metal compounds. Diphenylphosphido-bridged complexes are quite common, due to their ease of preparation and the ability to compare diphenylphosphide with the common ancillary ligand, triphenylphosphine. This study employs the dicyclohexylphosphide ligand, for two reasons. Firstly, in comparison with diphenylphosphide, dicyclohexylphosphide is a much more bulky ligand, which may facilitate coordinative unsaturation in the final products, an important factor in oxidative-addition reactions. Secondly, the dicyclohexylphosphide ligand, being an alkyl ligand, is more basic that diphenylphosphide, and therefore electron density between the two metal atoms should be greater, and should increase the stability of the bimetallic complex. Like phosphines, the differences between phosphides depends on both steric and electronic properties.

1.5 Chemical Reactivity

Until 1982, syntheses of heteronuclear complexes far outweighed studies of their reactivity. More recently, specific reactions of heteronuclear compounds have been investigated, though in many cases mechanistic details are still not understood. The following section outlines the different reactions that can be carried out with bimetallic species. Some mechanistic details are given where they are known and understood.

i) Substitution Reactions

Substitution chemistry of ligand-bridged compounds has been studied in some detail. Substitution, by definition, implies the replacement of one ligand in a complex for another[6]. In nearly all the heteronuclear complexes whose substitution reactions have been studied, the leaving group has been CO, and the entering group has been PR_3.

In the case of ligand-bridged complexes the metal-metal bond may be thought of as reserving a position for the incoming ligand by occupying a coordination site. The bridging ligand itself can facilitate an electronic redistribution so that a stable intermediate without a metal-metal bond, which is often isolable, can be formed. In cases such as these, subsequent heating or irradiation can induce loss of a ligand and reformation of the metal-metal bond.

In the example shown in Figure 1.4, Vahrenkamp[22] has studied the substitution of phosphine for CO. Initial phosphine addition seems to occur at the Mn centre, and then through isomerization the phosphine ligand migrates to Fe. The mechanisms for this reaction are not understood since the isomerization can involve intramolecular ligand exchange or ligand dissociation. Indeed, it is not even known how the initial substitution occurs, since the PR_3 ligand can add either to the Mn centre of an intermediate where there is no metal-metal bond, or through PR_3 association with the intact metal-metal bonded complex to cause the bond to break.

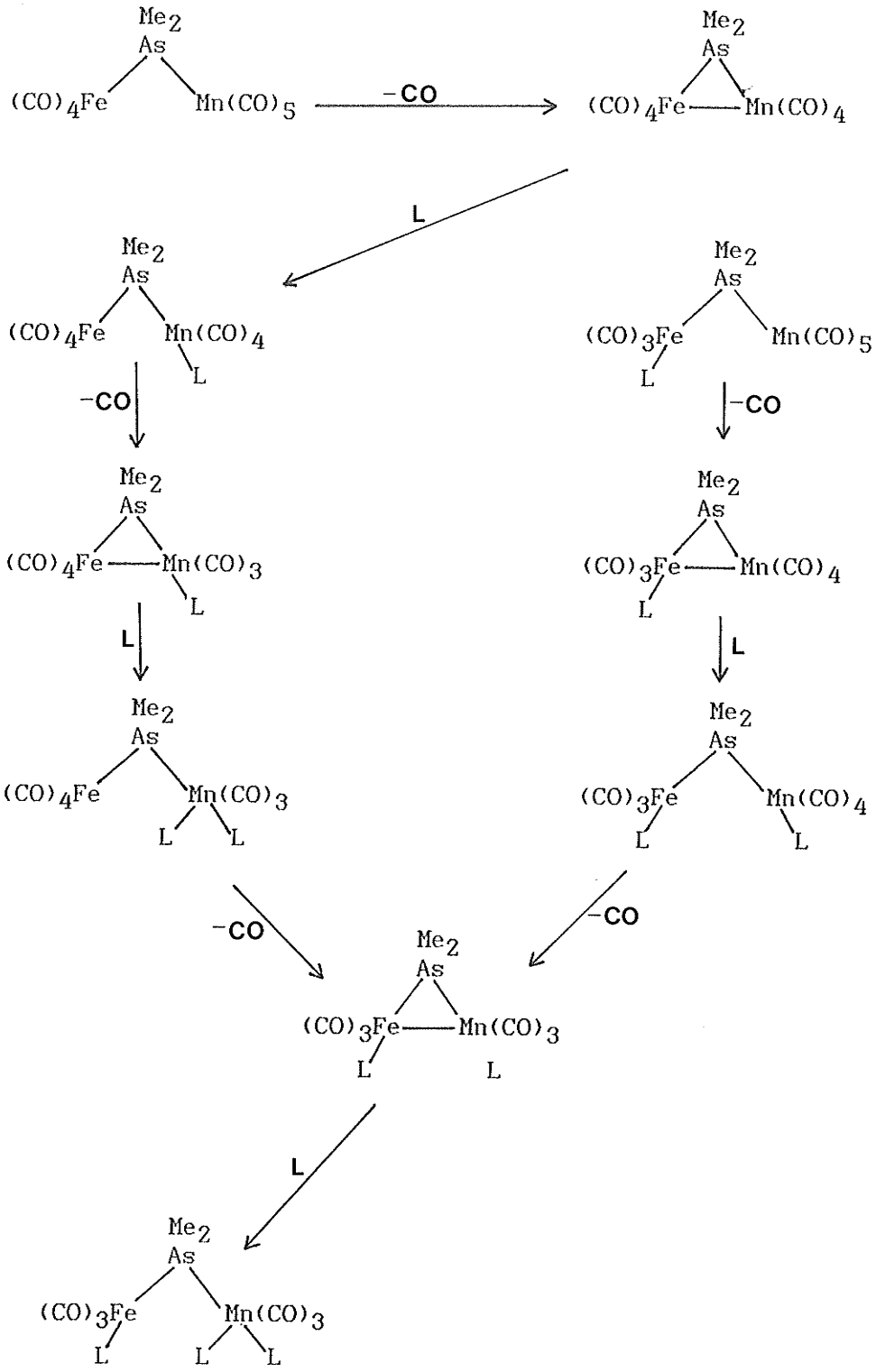

Figure 1.4: Substitution of L = PPh_3 for CO in the complex $(CO)_4Fe(\mu\text{-}AsMe_3)Mn(CO)_5$.

ii) Addition Reactions

An addition reaction is one where a complex incorporates a ligand without loss of any other ligand. There are two types of addition reactions for heteronuclear compounds: a) those where a ligand adds at a coordinatively unsaturated centre without any disruption of the metal-metal bond, and b) those where the incoming ligand adds across the metal-metal bond to displace it. Type a) reactions are similar to the mononuclear oxidative-addition reactions typical of planar Rh(I) and Ir(I) complexes. An example of such a reaction is shown in Equation 1.6[23].

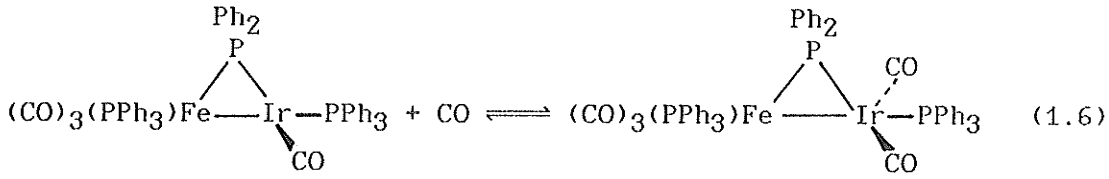

(1.6)

The second type of addition reaction involves the formal reduction in the metal-metal bond order. Using the example above, if another CO molecule adds at the Ir centre the metal-metal bond is cleaved, as in Equation 1.7.

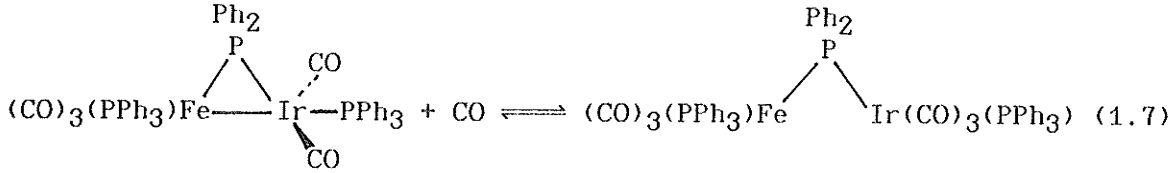

(1.7)

Cleavage of the bond occurs where a single bond exists; a reduction in bond order would occur for a multiply-bonded complex. Where a

bridging ligand is present the compound will, in general, remain intact. However, where no bridge exists the heteronuclear compound dissociates to its mononucuclear components.

The two reactions shown above illustrate how in an appropriately designed system reversible addition of two two-electron donor molecules can occur without loss of integrity of the complex. Such reactions are unique to polynuclear complexes and would seem to make them extremely useful in catalytic reactions.

iii) Acid-Base Reactions

In this case, acid/base reactions are examined from the Brönsted sense, i.e. protonation and deprotonation. From studies of homometallic compounds it is known that protonation can occur at the metal-metal bond or at one of the metal centres[24]. Because the proton brings in no electrons and does not alter the electron count of a compound, it might be expected that addition (or removal) of a proton from a metal-metal bonded compound would have little effect in regard to the metal-metal bond. However, subtle electronic effects do exist, where the added proton changes electronic distribution by attracting electron density to itself.

If straightforward protonation is desired, then acids with non- or weakly-coordinating anions such as H_2SO_4, H_3PO_4, HPF_6, or HBF_4 should be employed. Coordinating acids such as hydrohalic acids can cause disruption of the metal-metal bond with coordination of the anion.

Ligand-bridged or cluster compounds are typically more stable to

protonation than complexes with unsupported metal-metal bonds. Anionic clusters are often protonated under mild conditions to give their hydride analogues, as in Equation 1.8[25]. Protonations such as these are usually carried out using non-complexing acids such as H_3PO_4, for the reasons outlined above.

$$[CoRu_3(CO)_{13}]^- \xrightarrow{H_3PO_4} [CoRu_3H(CO)_{13}] \qquad (1.8)$$

iv) Oxidation-Reduction Reactions

Oxidative-addition and reductive-elimination reactions are important because nearly all catalytic and many useful stoichiometric processes involve these two types of reactions. Oxidative-addition is a term used to describe an ubiquitous class of reactions where a group A-B adds to, and thus oxidizes, a metal complex M. For these types of reactions both the oxidation state and the coordination number of the metal increase. The reverse reactions are reductive-eliminations, where both the oxidation state and the coordination number of the metal decrease[26].

For heteronuclear complexes oxidative-addiditon or reductive elimination reactions can occur at one of the metal centres or across the metal-metal bond. Reactions that occur at the metal centre would require coordinative unsaturation and open coordination sites at the metal. These reactions resemble oxidative-additions/reductive-eliminations that occur for the square-planar complexes containing group 9 metals such as $RhCl(PPh_3)_3$[27] and *trans*-$IrCl(CO)(PPh_3)_2$[28].

Equation 1.9[23] is an example of oxidative-addition at one metal centre for a heterobimetallic complex.

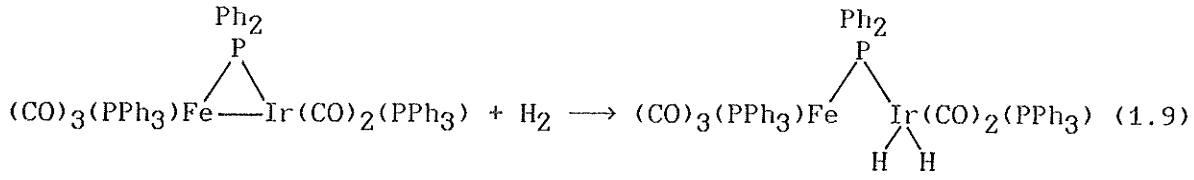

(1.9)

The addition of H_2 to the Fe-Ir compound has also displaced the metal-metal bond, though this is not always the case. The iridium atom has changed oxidation states from Ir(I) to Ir(III), and from coordination number four (neglecting the metal-metal bond) to coordination number six.

Oxidation-reduction reactions can also occur at the metal-metal bond of a heteronuclear complex, by increasing or decreasing the bond order. For example, for the complex $MnRe(CO)_{10}$[29], two new compounds can be designed through oxidation or reduction of the Mn-Re bond. As it is, each metal achieves its 18 electron valency through the metal-metal bond, but if the complex were oxidized, a doubly-bonded compound would be formed to satisfy the electron counts of the metals. Similarly, if the complex were reduced, the metal-metal bond would no longer be needed, and two mononuclear products would be formed, as in Equation 1.10.

$$(Mn{=}Re)(CO)_{10} + 2e^- \longrightarrow MnRe(CO)_{10} + 2e^- \longrightarrow [Mn(CO)_5]^- + [Re(CO)_5]^- \qquad (1.10)$$

Of course, if the heteronuclear complex being reduced contains a bridging ligand, cleavage of the metal-metal bond would not form two mononuclear complexes. Instead, as in the oxidative-addition reaction of Equation 1.9, the integrity of the original complex would be preserved.

CHAPTER TWO

DOUBLY-BRIDGED COMPLEXES OF Mo-Ni, Mo-Pd, Mo-Pt, W-Ni, W-Pd, and W-Pt

2.1 Introduction

The initial investigations into the use of dicyclohexylphosphido-bridging ligands in heterobimetallic complexes are reported in this chapter. At the time of preparation of $(CO)_4M(\mu\text{-}PCy_2)_2M'(PPh_3)$, (M = Mo, W; M' = Ni, Pd, Pt), very few dicyclohexylphosphido-bridged complexes had appeared in the literature: $[Ni(\mu\text{-}PCy_2)(PCy_2Ph)_2]_2$[29], $[Ni(\mu\text{-}PCy_2)(CO)_2]_2$[29], and $ZrFe(\mu\text{-}PCy_2)_2Cp_2(CO)_3$[30], and none had been structurally characterized by X-ray diffraction. The synthesis and characterization of these complexes are described in this chapter, along with the molecular structure of $(CO)_4Mo(\mu\text{-}PCy_2)_2Pd(PPh_3)$.

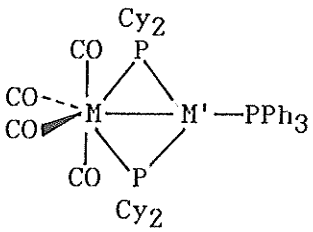

M	M'
Mo	Ni, Pd, Pt
W	Ni, Pd, Pt

We believed initially that a doubly-bridging PCy_2 unit would impart more stability to heterobimetallic compounds due to the increased

basicity of the cyclohexyl group, (as compared to the phenyl rings in PPh_2) and increased steric bulk of the ligand. As discussed in Chapter One, it is well known that variations in the size of R groups of trialkyl- or triarylphosphines can dramatically alter the chemical and physical properties of their transition metal complexes[31]. A bis-bridging system, being sterically more demanding than a mono-bridging system, would make coordinative unsaturation at one of the metal centres more likely, increasing the likelihood of oxidative-addition reactions at that metal centre.

Finally, in our initial investigations we have paired Mo or W with Ni, Pd, or Pt. These early-late transition metal combinations should prove interesting since the group 10 elements readily undergo oxidative-addition/reductive-elimination reactions and are catalytically relevant. The effect of a second metal on the more reactive site can be studied when we synthesize these metal-metal bonded compounds.

2.2 Experimental

i) General

cis-$PtCl_2(PPh_3)_2$[32], $PdCl_2(PPh_3)_2$[32], $NiCl_2(PPh_3)_2$[33], *cis*-$Mo(CO)_4(NHC_5H_{10})_2$[34], and *cis*-$W(CO)_4(NHC_5H_{10})_2$[34], (NHC_5H_{10} = piperidine) were prepared by literature methods. $NiCl_2 \cdot 6H_2O$ (Baker), $Mo(CO)_6$, $W(CO)_6$, K_2PtCl_4, PCy_2H, K_2PdCl_4 (Strem), *n*-BuLi, and PPh_3 (Aldrich) were purchased and used as received. THF (tetrahydrofuran) and toluene

were dried by distillation from Na-benzophenone ketyl under N_2; CH_2Cl_2 was dried by distillation from P_2O_5 under N_2; *n*-hexane was dried over molecular sieves and degassed with N_2 prior to use. All reactions were conducted under an atmosphere of N_2 by standard Schlenk techniques[49], using a double gas/vacuum manifold, syringes for transferring liquids, and side-arm round bottom flasks designed for working under an inert atmosphere.

$^{31}P\{^1H\}$ nmr spectra were obtained at 36.4 MHz on a Bruker WH90 spectrometer at 300K with an external D_2O lock. Phosphorous chemical shifts were measured relative to external 85% H_3PO_4 with positive shifts downfield. Infrared spectra were recorded on a Perkin-Elmer 787 grating spectrometer. Chemical analyses were performed at Guelph Chemical Laboratories, Guelph, Ontario.

ii) Preparation of *cis*-$Mo(CO)_4(PCy_2H)_2$ (1)

PCy_2H (7.51 mL, 36.4 mmol) was added to a suspension of *cis*-$Mo(CO)_4(NHC_5H_{10})_2$ (6.37 g, 18.2 mmol) in toluene (40 mL). The mixture was stirred overnight at room temperature and the solvent removed in vacuo. The resultant off-white solid was washed with cold diethyl ether (2 X 10 mL) and dried in vacuo, yielding white crystalline product (7.81 g, 71%). ^{31}P nmr (CH_2Cl_2): δ 25.9 (d, J_{P-H} = 301.1 Hz). Anal. calc'd. for $C_{28}H_{46}MoO_4P_2$: C, 55.62; H, 7.68. Found: C, 56.02; H, 7.48.

iii) Preparation of *cis*-$W(CO)_4(PCy_2H)_2$ (2)

PCy_2H (3.08 mL, 14.9 mmol) was added to a suspension of *cis*-$W(CO)_4(NHC_5H_{10})_2$ (3.21g, 7.45 mmol) in toluene (30 mL). The mixture was stirred with warming to approximately 60°C for four hours, cooled to room temperature, filtered, and the solvent removed in vacuo. The resulting bright yellow solid was recrystallized from toluene, yielding 3.51 g (68%) product. ^{31}P nmr (CH_2Cl_2): δ 10.0 (d of t, J_{P-H} = 312.6 Hz, J_{W-P} = 214.5 Hz). Anal. calc'd. for $C_{28}H_{46}O_4P_2W$: C, 48.56; H, 6.71. Found: C, 48.71; H, 6.66.

iv) Preparation of $(CO)_4Mo(\mu\text{-}PCy_2)_2Ni(PPh_3)$ (3)

n-BuLi (1.55M in hexanes, 5.38 mL, 8.34 mmol) was added via syringe to a THF (20 mL) solution of **1** (2.52 g, 4.17 mmol) at 23°C. After it was stirred 10 minutes, this solution was added dropwise over 30 minutes, to a suspension of $NiCl_2(PPh_3)_2$ (2.73 g, 4.17 mmol) in THF (30 mL)at 0°C. An immediate colour change from green to dark orange was observed. The solution was warmed to room temperature and stirred for two hours and the solvent removed in vacuo. The resulting dark orange-red solid was extracted with cold *n*-hexane (6 X 10 mL) and cooled to -20°C for 8 hours. The orange-red microcrystalline product was isolated by keeping the recrystallization flask at about -10°C, removing the mother liquor, and drying the solid in vacuo. (If the solution is warmed to room temperature during the isolation process, only brown oily products result.) This

yielded 2.15 g of **3** (56%). Anal. calc'd. for $C_{46}H_{59}MoNiO_4P_3$: C, 59.93; H, 6.46. Found: C, 59.39; H, 6.45.

v) Preparation of $(CO)_4Mo(\mu\text{-}PCy_2)_2Pd(PPh_3)$ (4)

n-BuLi (1.55M in hexanes, 2.67 mL, 4.14 mmol) was added via syringe to a THF (20 mL) solution of **1** (1.18 g, 2.07 mmol) at 23°C. After it was stirred for 10 minutes, this solution was added dropwise, over 30 minutes, to a suspension of $PdCl_2(PPh_3)_2$ (1.40 g, 2.07 mmol) in THF (30 mL) at 0°C. The resulting dark red solution was stirred at room temperature for four hours and the solvent removed in vacuo. The residue was extracted with *n*-hexane (7 X 10 mL) and the solution volume reduced to 40 mL. After the solution was cooled to -20°C for 12 hours red crystals of **4** were isolated; yield 0.99 g (48%). Anal. calc'd. for $C_{46}H_{59}MoO_4P_3Pd$: C, 56.88; H, 6.14. Found: C, 57.01, H, 6.23.

vi) Preparation of $(CO)_4Mo(\mu\text{-}PCy_2)_2Pt(PPh_3)$ (5)

n-BuLi (1.55 M in hexanes, 0.65 mL, 1.01 mmol) was added via syringe to a THF (20 mL) solution of **1** (0.31 g, 0.51 mmol) at 23°C. After it was stirred for 10 minutes, this solution was added dropwise, over 30 minutes, to a suspension of *cis*-$PtCl_2(PPh_3)_2$ (0.40 g, 051 mmol) in THF (30 mL) at 23°C. The resulting dark orange solution was stirred for 24 hours at room temperature and the solvent removed in vacuo. The residue was extracted with *n*-hexane (5 X 10 mL) and the volume of the

solution reduced to 20 mL. After the solution was cooled to -20°C for 36 hours, orange micorcrystals of **5** were isolated, yield 0.22 g (41%). Anal. calc'd. for $C_{46}H_{59}MoO_4P_3Pt$: C, 52.10; H, 5.62. Found: C, 52.44; H, 5.57.

vii) Preparation of $(CO)_4W(\mu\text{-}PCy_2)_2Ni(PPh_3)$ (6)

n-BuLi (1.55 M in hexanes, 3.73 mL, 5.78 mmol) was added via syringe to a THF (20 mL) solution of **2** (2.00g, 2.89 mmol) at 23°C. After it was stirred for 10 minutes, this solution was added dropwise, over 30 minutes, to a suspension of $NiCl_2(PPh_3)_2$ (1.89 g, 2.89 mmol) in THF (30 mL) at 0°C. The dark red-orange solution was warmed to room temperature and stirred for three hours. The solvent was removed in vacuo, and the solid residue was extracted with *n*-hexane (4 X 10 mL). After the solution volume was reduced slightly and the solution was cooled to -20°C for 10 hours, red-brown microcrystals of **6** were isolated; yield 1.75 g (60%). This procedure was performed at -10°C as for **3**. Anal. calc'd. for $C_{46}H_{59}NiO_4P_3W$: C,54.71; H, 5.90. Found: C, 54.72; H, 5.82.

viii) Preparation of $(CO)_4W(\mu\text{-}PCy_2)_2Pd(PPh_3)$ (7)

n-BuLi (1.55M in hexanes, 3.16 mL, 4.90 mmol) was added via syringe to a THF (20 mL) solution of **2** (1.70 g, 2.45 mmol) at 23°C. After it was stirred for 10 minutes, this solution was added dropwise, over 30

minutes, to a suspension of $PdCl_2(PPh_3)_2$ (1.72 g, 2.45 mmol) in THF (30 mL) at 0°C. The dark orange-red solution was warmed to room temperature and stirred for six hours. The THF was removed in vacuo and the solid residue extracted with *n*-hexane (6 X 10 mL). The solution was filtered and the volume reduced to 30 mL. After the solution was cooled to -20°C for 12 hours, orange-red crystals of **7** were isolated; yield 1.14 g, (44%). Anal. calc'd. for $C_{46}H_{59}O_4P_3PdW$: C, 52.14; H, 5.62. Found: C, 52.00; H, 5.71.

ix) Preparation of $(CO)_4W(\mu\text{-}PCy_2)_2Pt(PPh_3)$ (8)

n-BuLi (1.55 M in hexanes, 0.64 mL, 0.99 mmol) was added via syringe to a THF (40 mL) solution of **2** (0.34 g, 0.49 mmol) at 23°C. After it was stirred for 10 minutes, this solution was added dropwise, over 15 minutes, to a suspension of *cis*-$PtCl_2(PPh_3)_2$ (0.39 g, 0.49 mmol) in THF (15 mL) at 23°C. The dark orange-brown solution was stirred for 19 hours at room temperature. The THF was removed in vacuo and the orange-brown residue extracted with *n*-hexane (7 X 5 mL) The volume of the solution was reduced to 5 mL, and orange microcrystals formed after cooling to -20°C for 16 hours; yield 0.240 g (42%). Anal. calc'd. for $C_{46}H_{59}O_4P_3PtW$: C,48.11; H, 5.19. Found: C, 48.33; H, 5.09.

x) Reactions with Small Molecules: CO, H_2, Acetylene

a) CO

Complex **4**, (0.050 g, 0.05 mmoles) was dissolved in *n*-hexane (3 mL) and stirre under CO (1 atmosphere) for one hour at 23°C. The solution remained orange-red in colour. The $^{31}P\{^{1}H\}$ nmr spectrum was recorded under CO, and showed that no reaction with CO had occurred.

b) H_2

Complex **4**, (0.050 g, 0.05 mmoles, was dissolved in *n*-hexane as above and stirred under H_2 (1 atmosphere) for one hour at 23°C. The solution again showed no colour change. $^{31}P\{^{1}H\}$ nmr under H_2 showed no reaction had occurred.

c) Dimethylacetylene Dicarboxylate ($CH_3CO_2C{\equiv}CCO_2CH_3$)

Complex **4**, (0.180 g, 0.186 mmoles) was dissolved in CH_2Cl_2 (5 mL). To this was added dimethylacetylene dicarboxylate (0.036 mL, 0.372 mmoles). The solution was stirred for 1 hour, and turned light orange from orange-red. The volume of the solution was reduced to approximately three mL and the $^{31}P\{^{1}H\}$ nmr spectrum recorded, revealing no identifiable phosphide-bridged products.

2.3 Synthesis and Characterization of Complexes 1-8

In 1978 Darensbourg and Kump[34] devised a convenient and inexpensive method of preparing complexes of the type *cis*-$M(CO)_4L_2$ where M = Mo, W; L = group 15 ligand. They had observed that preparation of disubstituted Lewis base derivatives of the group 6 hexacarbonyls was not a trivial task due to *cis-trans* isomerization of the final products. The process they developed was based on the ready availability of *cis*-$M(CO)_4(NHC_5H_{10})_2$ in large quantities and the very facile replacement of the piperidine ligands in these species by phosphines. Geoffroy[36] has also employed this method to prepare *cis*-$W(CO)_4(PPh_2H)_2$, and we have used it here to prepare the complexes *cis*-$Mo(CO)_4(PCy_2H)_2$ (**1**), and *cis*-$W(CO)_4(PCy_2H)_2$ (**2**) in good yields, as described in Equation 2.1 below.

$$cis\text{-}M(CO)_4(NHC_5H_{10})_2 + 2PCy_2H \longrightarrow cis\text{-}M(CO)_4(PCy_2H)_2 + 2NHC_5H_{10} \quad (2.1)$$

1: M = Mo (71%)
2: M = W (68%)

Both **1** and **2** showed a single resonance in the $^{31}P\{^1H\}$ nmr spectrum at 25.9 and 10.0 ppm respectively (J_{P-H} = 301.1 and 312.6 Hz, respectively; J_{W-P} = 214.5 Hz). Infrared spectra (Table 2.2) showed four ν_{CO} absorptions consistent with C_{2v} symmetry and a *cis* geometry for these complexes.

The heterobimetallic complexes **3-8** were prepared via the reactions outlined in Equations (2.2) and (2.3) below. This approach is known as the bridge-assisted method[6] of metal-metal bond formation and was

discussed in Chapter One.

$$cis\text{-}M(CO)_4(PCy_2H)_2 + 2n\text{-}BuLi \longrightarrow Li_2[M(CO)_4(PCy_2)_2] + 2n\text{-}BuH \quad (2.2)$$

$$M'Cl_2(PPh_3)_2 + Li_2[M(CO)_4(PCy_2)_2] \longrightarrow (CO)_4M(\mu\text{-}PCy_2)_2M'(PPh_3) + 2\ LiCl + PPh_3 \quad (2.3)$$

3: M = Mo M' = Ni (56%)
4: M = Mo M' = Pd (48%)
5: M = Mo M' = Pt (41%)
6: M = W M' = Ni (60%)
7: M = W M' = Pd (44%)
8: M = W M' = Pt (42%)

A red-orange solution of $Li_2[M(CO)_4(PCy_2)_2]$ in THF was added to a slurry of $M'Cl_2(PPh_3)_2$, also in THF, and in each reaction an immediate colour change was observed, even at 0°C. The reaction was assumed to be complete when the undissolved $M'Cl_2(PPh_3)_2$ complex was no longer present, resulting in a clear dark orange or red solution. All complexes were found to be extremely soluble in most organic solvents, including diethyl ether, toluene, and *n*-hexane, and could be recrystallized in moderate to good yields by cooling a saturated *n*-hexane solution to -20°C for 24-72 hours. The MoPd (**4**), MoPt (**5**), WPd (**7**), and WPt (**8**) complexes were found to be air stable in the solid state, however, when their solutions were exposed to air they rapidly turned brown from red or orange, indicating that decomposition had occurred. The MoNi (**3**) and WNi (**6**) complexes were found to be air-sensitive in both the solid state and in solution; however, both were found to be thermally stable and were actually isolated in higher yields than complexes **4**, **5**, **7**, and **8**. This was in marked contrast to the PPh_2-bridged complex $(CO)_4W(\mu\text{-}PPh_2)_2Ni(PPh_3)$ prepared by Geoffroy and co-workers[36], which was reported to be obtained impure, in low

yield, and too unstable for detailed study. In Geoffroy's experiments, the heterobimetallic complexes $(CO)_4W(\mu\text{-}PPh_2)_2Pt(PPh_3)$, $(CO)_4W(\mu\text{-}PPh_2)_2Pd(PPh_3)$, and the WNi complex named above were isolated by column chromatography on alumina, where the first fractions off the column contained the final product.

$^{31}P\{^1H\}$ nmr and infrared spectral data are in Tables 2.1 and 2.2. As with other phosphido-bridged complexes, the $^{31}P\{^1H\}$ nmr spectra are very useful in assigning molecular structures[37,38]. Details of this are explained in Section 2.5.

A sample $^{31}P\{^1H\}$ nmr spectrum is shown in Figure 2.1. The spectra were essentially the same for complexes **3-8**, except for satellites in the spectra of complexes containing spin 1/2 nuclei such as W or Pt with less than 100% natural abundance. In this work, each complex shows a downfield resonance (doublet), due to two bridging PCy_2 ligands, and another resonance (triplet) due to a single terminal PPh_3 ligand. The two sets of resonances are well separated by approximately 140-225 ppm depending on the complex. The large downfield shift of the bridging ligands is probably indicative of a metal-metal bond[39]. Although this is not conclusive, it has been shown[39] that for most $\mu\text{-}PR_2$ ligands bridging a metal-metal bond the phosphorous chemical shift is downfield, (δ +50 → 300 ppm) and for the same ligands not bridging a metal-metal bond the resonances are further upfield (δ +50 → -200 ppm). However, it has been suggested that exceptions do occur, and therefore this type of correlation should be made only for closely related series of compounds supported by X-ray crystallography, as in this work[30].

Figure 2.1: $^{31}P\{^{1}H\}$ nmr spectrum of $(CO)_4Mo(\mu\text{-}PCy_2)_2Pd(PPh_3)$.

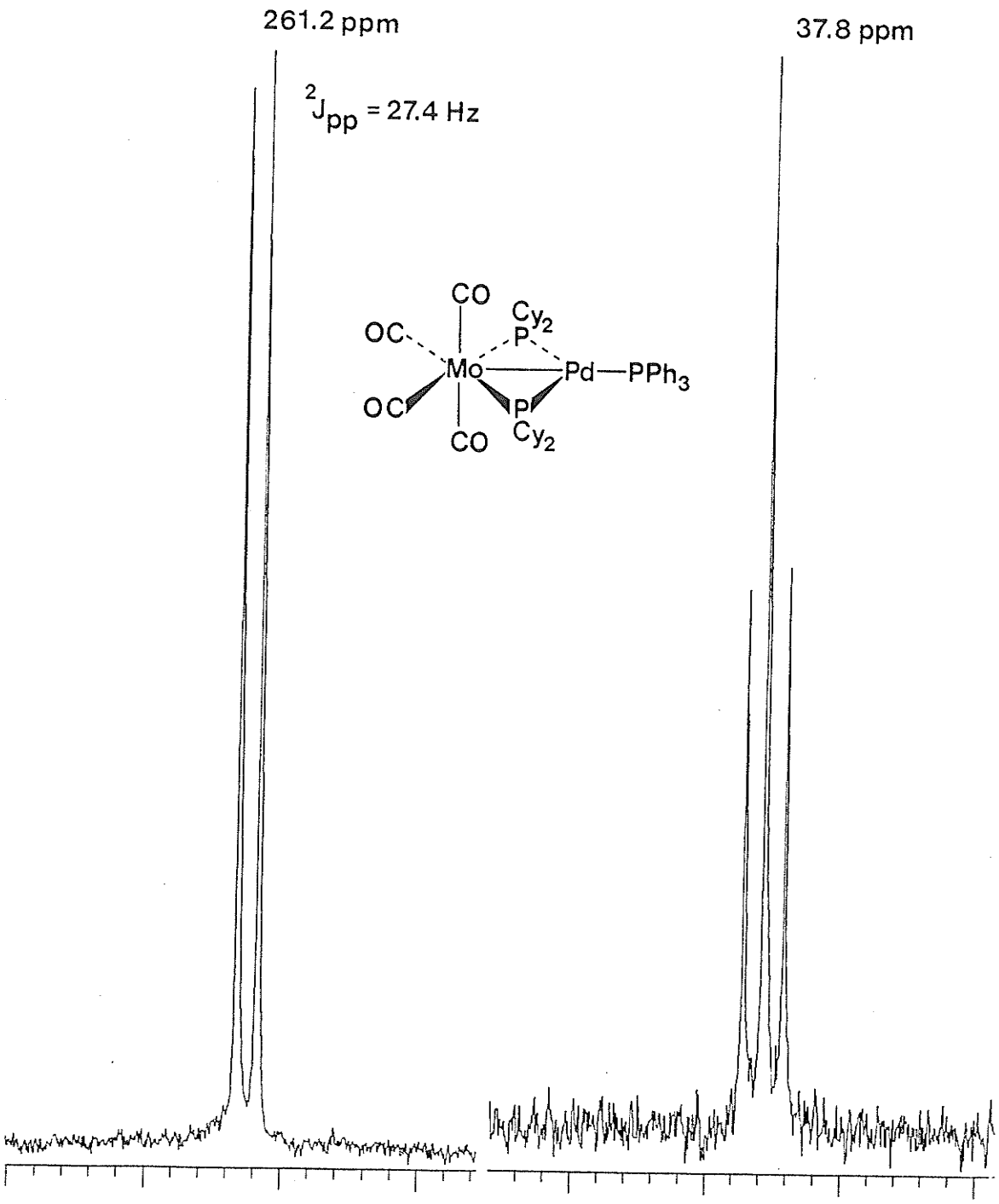
261.2 ppm
37.8 ppm
$^2J_{pp}$ = 27.4 Hz
CO
OC
Cy2
P
Mo
Pd—PPh3
OC
P
CO
Cy2

Table 2.1: $^{31}P\{^{1}H\}$ NMR Spectral Data[a]

Complex	$\delta(\mu\text{-}PCy_2)$[b]	$\delta(PPh_3)$	$^{2}J_{\mu P-P}$[c]	J_{M-P}
MoNi(**3**)	210.5d[d]	43.9t	34.0	
MoPd(**4**)	261.2d	37.8t	27.4	
MoPt(**5**)	259.6d	48.8t	60.0	2499.6 ($\mu\text{-}PCy_2$, M=Pt), 5238.6 (PPh_3, M=Pt)
WNi(**6**)	184.6d	42.3	27.8	151.0 ($\mu\text{-}PCy_2$, M=W)
WPd(**7**)	228.8d	35.4t	18.7	156.9 ($\mu\text{-}PCy_2$, M=W)
WPt(**8**)	228.5d	46.4t	49.4	140.5 ($\mu\text{-}PCy_2$, M=W), 2413.3 ($\mu\text{-}PCy_2$, M=Pt), 5121.2 (PPh_3, M=Pt)

[a]Recorded in CH_2Cl_2 solution. [b]Chemical shift units: ppm. [c]Coupling constant units: Hz. [d]Abbreviations: d = doublet, t = triplet.

The $^{31}P\{^{1}H\}$ nmr data also indicate that complexes **3-8** all have structures similar to that determined by X-ray diffraction for the MoPd complex **4** (Figure 2.4). Variations in chemical shifts within this series of complexes are presumably due to differences in electronic properties of the various metal centres. The Ni and Pt complexes' PPh_3 ligands shift to lower field compared to the Pd complexes, and there seems to be little difference between the W and Mo compounds, which may indicate that the presence of a second metal centre has little effect on the Ni, Pd, and Pt atoms. The bridging PCy_2 ligand shifts to higher field for the Ni complexes, whereas Pd and Pt complexes have similar shifts. In this case there is a shift of about 30 ppm to higher field for the W compounds as compared to Mo. It is difficult therefore, to draw any firm conclusions regarding chemical shifts in relation to electronic properties. The trends observed however, are consistent with those found for mononuclear compounds[40].

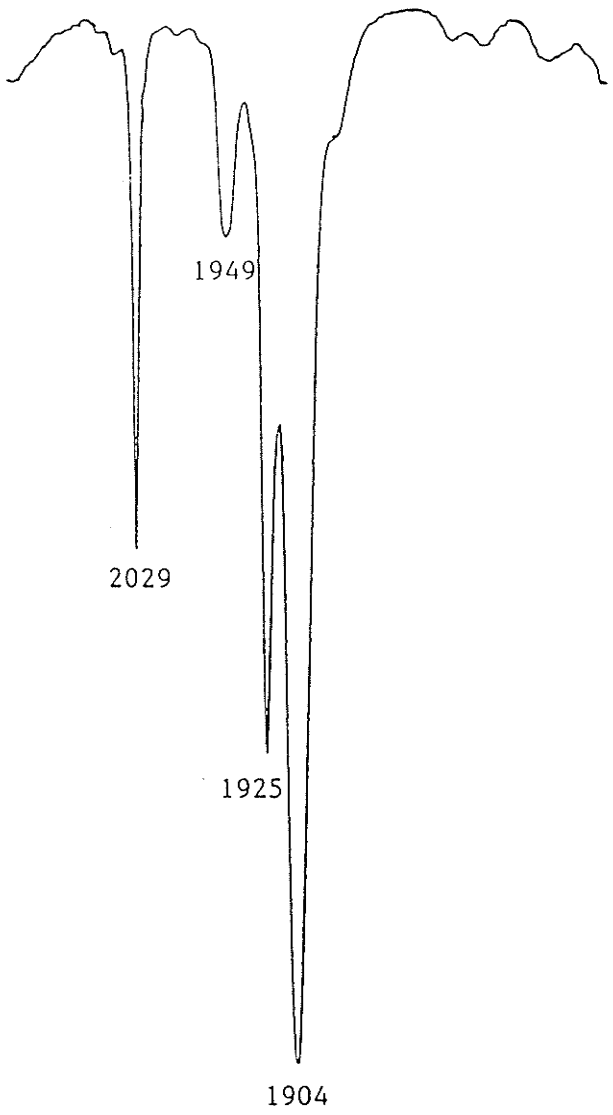

Figure 2.2: Infrared spectrum of complex 5, $(CO)_4Mo(\mu\text{-}PCy_2)_2Pt(PPh_3)$ in n-hexane. Peaks are labelled in units of cm^{-1}.

Table 2.2: Infrared Spectral Data

Complex	ν_{CO}[a], cm^{-1}
cis-$Mo(CO)_4(PCy_2H)_2$, **1**	2018(s)[b], 1923(s), 1903(vs), 1875(sh)
cis-$W(CO)_4(PCy_2H)_2$, **2**	2014(s), 1920(s), 1896(vs), 1872(m)
MoNi, **3**	2021(s), 1943(m,sh), 1928(s), 1910(vs,br)
MoPd, **4**	2025(s), 1955(m), 1947(m), 1919(vs)
MoPt, **5**	2029(s), 2949(m), 1925(m), 1904(s)
WNi, **6**	2015(s), 1935(m,sh), 1917(m), 1894(vs,br)
WPd, **7**	2024(s), 1949(s), 2940(m), 2910(vs)
WPt, **8**	2022(s), 1948(m), 1939(m), 1910(vs)

[a]All in hexane solutions. [b]Abbreviations: s = strong, v = very, br = broad, m = medium, sh = shoulder.

Infrared spectra of the heterobimetallic complexes **3** to **8** are very similar, all having approximately the same pattern as that shown in Figure 2.2. As is expected, each spectrum shows a four-band pattern for the terminal CO region, indicative of *cis*-$M(CO)_4L_2$, C_{2v} geometry. The four bands result from the four infrared-active CO stretching vibrations: $2a_1$, b_1, and b_2. The vibrations that correspond to these symmetry labels may be illustrated if the CO stretching motion is depicted as a vector[41], as in Figure 2.3 below.

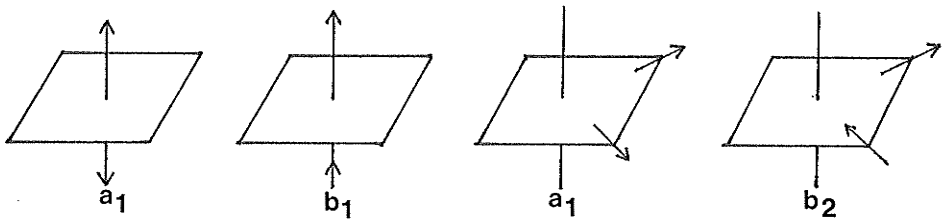

Figure 2.3: CO stretching motion of the *cis*-$ML_2(CO)_4$ unit.

In general, the number of infrared active ν_{CO} bands and their relative intensities depend on the local symmetry of the coordination sphere. The active vibrations are those which have a dipole moment change, therefore, the number of IR active bands cannot exceed but may be less than the number of CO groups in the complex[26]. The positions of the ν_{CO} absorptions are shifted to significantly higher values (10-40 cm^{-1}) compared to those of the precursor secondary phosphine complexes. This is indicative of a partial oxidation of the $M(CO)_4$ portion. Metal-CO π-backbonding is decreased because the electron density is transferred to the second metal centre instead of to the π^* orbitals of the CO ligand. A weaker M-CO bond results in higher stretching frequencies for coordinated CO's. This partial oxidation is interpreted as resulting from a M(0) → M'(II) dative metal-metal bond, detailed in Section 2.6.

2.4 Crystal and Molecular Structure of $(CO)_4Mo(\mu\text{-}PCy_2)_2Pd(PPh_3)$, (4)

A perspective view of **4** giving the atom numbering scheme is shown in Figure 2.4, and a representation of the inner coordination sphere of the molecule is shown, with some relevant parameters, in Figure 2.5. The unit cell (the repeating unit that makes up the crystal lattice)[42] contains four discrete molecules of **4**. Table 2.3 outlines other crystallographic data, collected and solved at the University of Windsor by D. W. Stephan and L. Gelmini.

Table 2.3: Summary of Crystal Data, Intensity Collection, and Structure Refinement for $(CO)_4Mo(\mu\text{-}PCy_2)_2Pd(PPh_3)$ (4)

formula	$MoPdP_3O_4C_{45}H_{59}$
solvent	*n*-hexane
crystal colour, form	red-orange, blocks
a, Å	21.474(4)
b, Å	10.573(1)
c, Å	22.954(4)
β, deg	117.53(1)
crystal system	monoclinic
space group	Cc
volume, $Å^3$	4621(1)
ρ(calc'd) g/cm^3	1.40
Z	4
crystal dimensions, mm	0.27 x 0.46 x 0.96
μ, abs. coeff., cm^{-1}	7.17
radiation, (λ, Å)	MoKα (0.71069)
temp, °C	24
scan speed, deg/min	2.0-5.0 (θ/2θ scan)
scan range, deg	1.0 below K_1 to 1.1 above K_2
background/scan time ratio	0.5
data collected	6570; 2θ of 4.5 to 50 (+h, +k, ±l)
unique data ($F_o^2 > 3\sigma F_o^2$)	3566
number of variables	370 (2 blocks)
R, %	3.41
R_w, %	3.75

The overall geometry of this binuclear complex is a combination of the individual coordination geometries of the Mo and Pd atoms. The Pd atom is bonded to the three phosphorous atoms with an average Pd-P distance of 2.278(8)Å. The largest deviation from the least squares plane formed by the Pd and three P atoms is 0.0676Å, and the P-Pd-P angles average 119.8(1)°. This is consistent with a trigonal-planar geometry about the Pd atom if we neglect the Mo-Pd interaction. The Mo atom is bonded to the two bridging P atoms (P1 and P2) and four carbonyl carbon atoms. The Mo-P distances are typical and average 2.536(1)Å. The Mo-C distances average 2.03(2)Å and also fall within the expected range. The C-Mo-C and P-Mo-C angles are consistent with a slightly distorted octahedral geometry, ranging from 83.6(3)° to

Figure 2.4: ORTEP of complex 4, showing the atom numbering scheme.

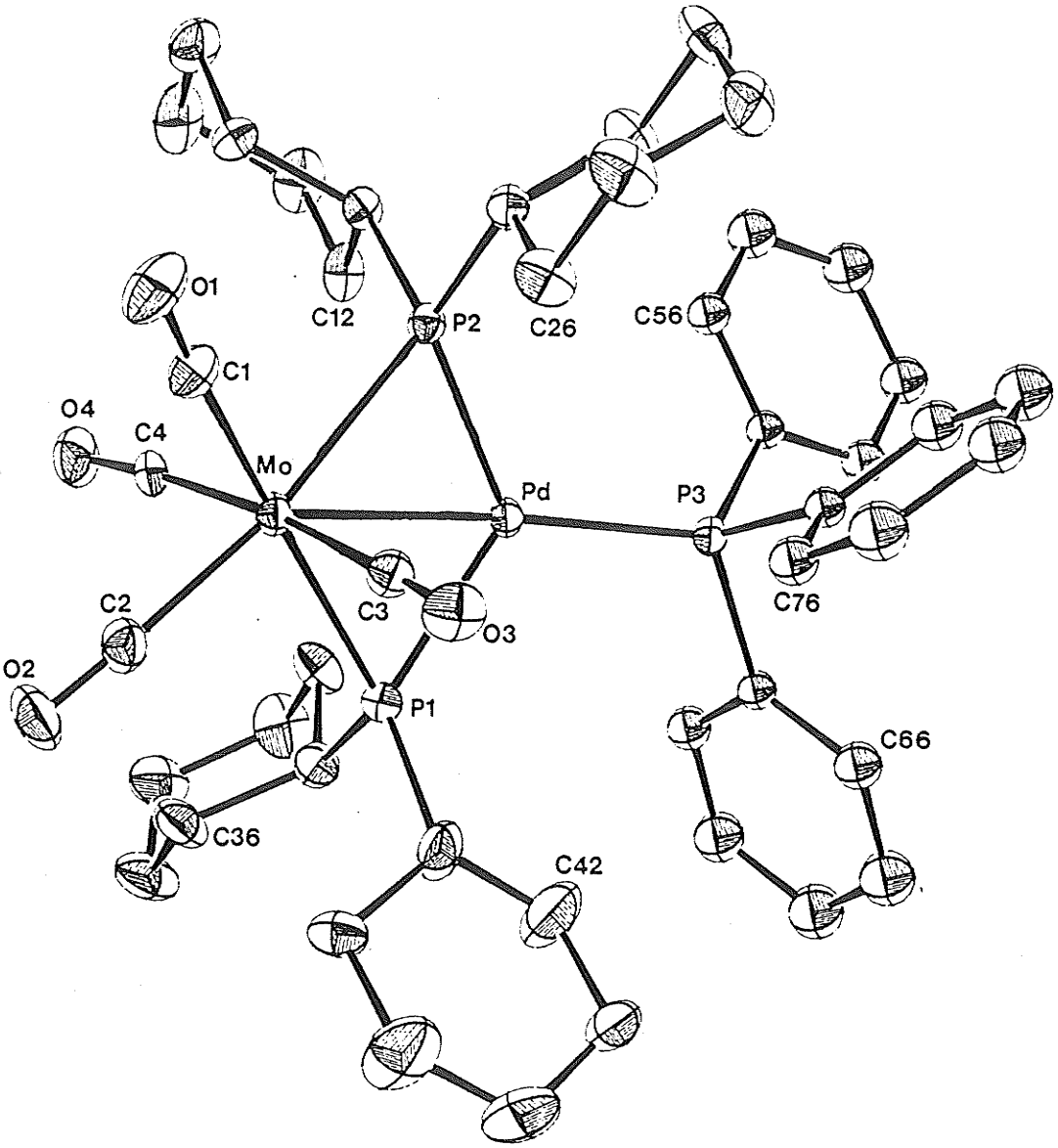
O1
C12
P2
C26
C56
C1
O4
C4
Mo
Pd
P3
C2
C3
O3
C76
O2
P1
C66
C36
C42

Figure 2.5: Representation of the inner coordination sphere of complex 4.

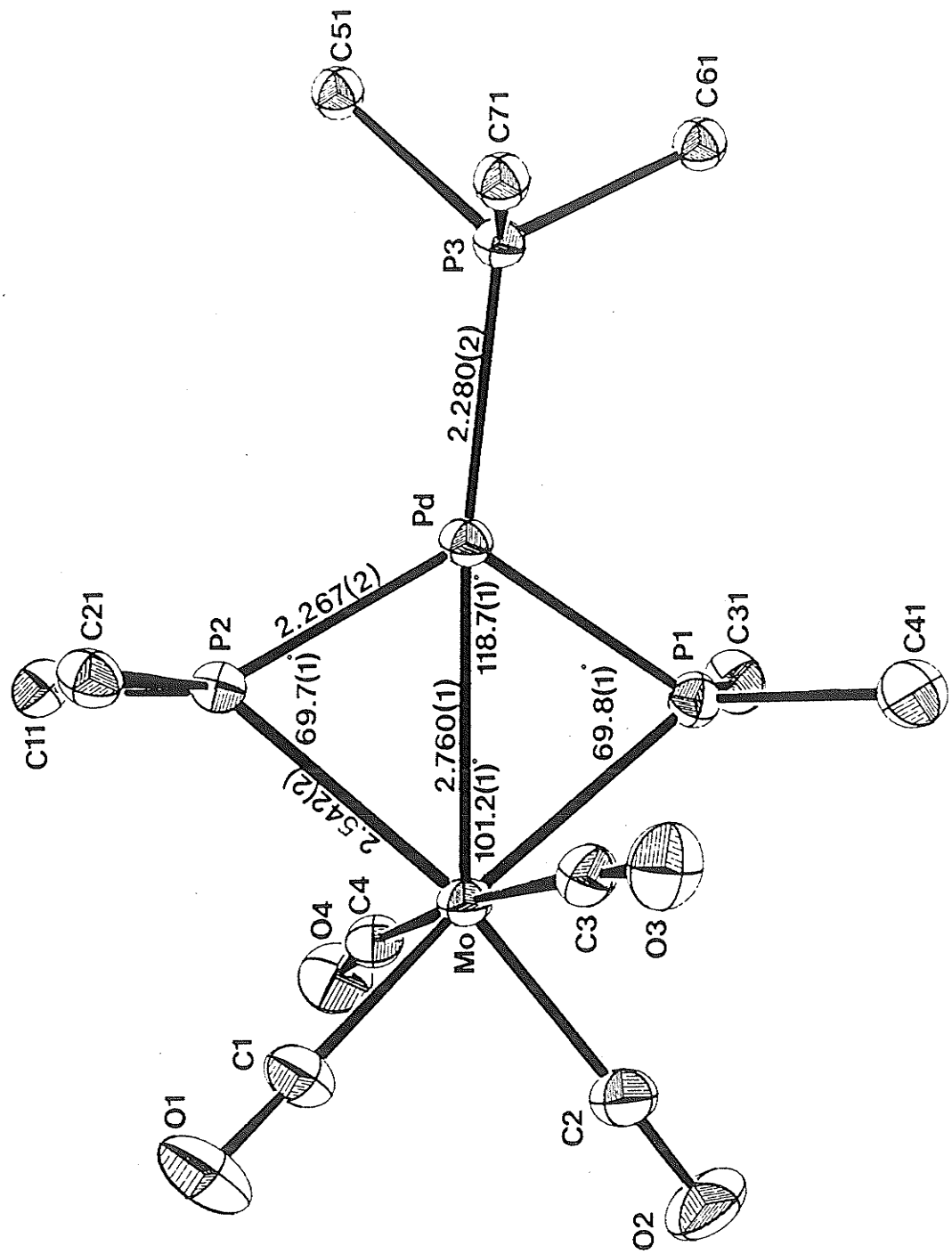
C51
C71
C61
P3
2.280(2)
Pd
2.267(2)
C21
P2
C11
69.7(1)°
118.7(1)°
P1
C31
C41
2.760(1)
69.8(1)°
2.542(2)
101.2(1)°
C4
O4
Mo
C3
O3
C1
O1
C2
O2

101.2(1)° about the Mo atom. Data are listed in Appendix 2.1.

The $Mo(\mu\text{-}PCy_2)_2Pd$ core is not planar. The dihedral angle between the P1-Mo-P2 and P1-Pd-P2 planes is 15.4°, giving the molecule a very slight butterfly distortion, as shown in Figure 2.6. The Mo-Pd distance of 2.760(1)Å is shorter than any yet determined[43]: $\{PdNMe_2CH_2C_6H_4\}_2\{\mu\text{-}Mo(CO)_3(\eta\text{-}C_5H_5)\}\mu\text{-}Cl]$, 2.832(1)Å and 2.788(1)Å; $[Pd(8\text{-methylquinoline-}C,N)PPhMe_2Mo(Co)_3(\eta\text{-}C_5H_5)]$, 3.059(1)Å; $[Pd_2Mo_2(\eta\text{-}C_5H_5)_2(\mu^2\text{-}CO)_2(PEt_3)_2]$, 2.827(1)Å and 2.865(1)Å. The most similar structure to **4** is that of $MoPd(\mu\text{-}Ph_2Ppy)_2(\mu\text{-}CO)(CO)_2Cl_2$ (py = pyridine)[44], where the Mo-Pd distance was found to be 2.817(1)Å, which is also longer than the 2.760(1)Å found for **4**. The Mo-Pd distance in **4** is equal to the sum of the covalent radii[45] of the Mo and Pd atoms; a covalent radius is equal to half the bond length between a molecule X-X in which two atoms X are singly-bonded to each other (Mo = 1.45Å, Pd = 1.31Å). Therefore this distance is not unusual or unexpected, does not indicate multiple bonding, and is consistent with a single bond between the metal atoms.

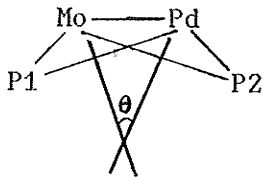

θ = 15.4°

Figure 2.6: Dihedral angle of the $M(\mu\text{-}PCy_2)_2M'$ core.

As illustrated in Figure 2.5, other bond distances and angles in the $Mo(\mu\text{-}PCy_2)_2Pd$ core are consistent with a Mo-Pd bond. For example, the Mo-P1-Pd and Mo-P2-Pd angles are constrained to 69.7(1)° and 69.8(1)° respectively, where we would expect angles of approximately 109° for tetrahedral phosphorous atoms. Similarly the P1-Mo-P2 angle

has opened up to 101.2(1)° from the 90° expected for an octahedral complex. The P1-Pd-P2 angle is 118.7(1)°, close to the 120° expected for a trigonal planar complex. Other workers[30,39c] have noted that although the metal-metal interaction may be described as occurring through bridging phosphorous orbitals, all data collected in this case indicate a closing of the Mo-Pd distance, and therefore would not be interpreted as being imposed by the phosphido ligands.

The diphenylphosphido-bridged complex $(CO)_4W(\mu\text{-}PPh_2)_2Pt(PPh_3)$ has also been characterized by an X-ray diffraction study[36], and, similar to complex **4**, has a group 6 metal and a group 10 metal bridged by phosphido ligands. A comparison with $(CO)_4Mo(\mu\text{-}PCy_2)_2Pd(PPh_3)$, **4**, illustrates the effect of replacing phenyl by bulky cyclohexyl groups as substituents on the bridging phosphorous atoms. The molecular structures of these two complexes are very similar, and the coordination geometries about the metal atoms are essentially identical. This is particularily true for the $M(\mu\text{-}PR_2)_2M'$ cores, in which the bond lengths and angles show little difference; for example, the W-Pt bond distance[36] is 2.764(1)Å and the Mo-Pd bond distance is 2.760(1)Å. The only major difference is the larger $M(\mu\text{-}PR_2)_2M'$ dihedral angle of 15.4° for **4** compared with 2.2° for $(CO)_4W(\mu\text{-}PPh_2)_2Pt(PPh_3)$. A comparison of structural data for the two compounds is shown in Table 2.4.

Table 2.4 Comparison of Structural Data for $(CO)_4W(\mu\text{-}PPh_2)_2Pt(PPh_3)$ and $(CO)_4Mo(\mu\text{-}PCy_2)_2Pd(PPh_3)$

Structural Feature	W-Pt	Mo-Pd
M-M Bond Distance	2.764(1)Å	2.760(1)Å
Dihedral Angle	2.2°	15.4°
M-P1-M' Angle	70.8(1)°	69.7(1)°
M-P2-M' Angle	70.6(1)°	69.8(1)°
P1-M-P2 Angle	100.8(1)°	101.2(1)°
P1-M'-P2 Angle	117.8(1)°	118.791)°
P1-M Distance	2.509(4)Å	2.530(1)Å
P2-M Distance	2.507(3)Å	2.542(2)Å
P1-M' Distance	2.249(3)Å	2.287(2)Å
P2-M' Distance	2.266(4)Å	2.267(2)Å

Bulky substituents on the $M(\mu\text{-}PR_2)_2M'$ ring might be expected to produce a more planar structure since this planarity would reduce steric interactions between adjacent R groups. Indeed, Jones[46] has found that for the complexes $[Fe(\mu\text{-}t\text{-}Bu_2P)Cl(PMe_3)]_2$, $Co_2(\mu\text{-}t\text{-}Bu_2P)_2Cl(PMe_3)_2$, and $[Ni(\mu\text{-}t\text{-}Bu_2P)(PMe_3)]_2$, bridged by the very bulky $t\text{-}Bu_2P$ ligand, the $M(\mu\text{-}t\text{-}Bu_2P)_2M$ core is essentially planar, as shown in Table 2.5 below.

Table 2.5: Dihedral Angles Between M-P1-M' and M-P2-M' for $M(\mu\text{-}PR_2)_2M'$ Complexes

Complex	Dihedral Angle	Reference
$[Fe(\mu\text{-}t\text{-}Bu_2P)Cl(PMe_3)]_2$	0°	46a
$Co_2(\mu\text{-}t\text{-}Bu_2P)_2Cl(PMe_3)_2$	0°	46b
$[Ni(\mu\text{-}t\text{-}Bu_2P)(PMe_3)]_2$	0°	46c
$[Rh(\mu\text{-}t\text{-}Bu_2P)(CO)(PMe_3)]_2$	0°	46d
$(CO)_4W(\mu\text{-}PPh_2)_2Re(CO)_3CH_3$	1.5°	47
$(CO)_4W(\mu\text{-}PPh_2)_2Ir(H)(CO)(PPh_3)$	7.8°	48
$[(CO)_3(C(OMe)Ph)W(\mu\text{-}PPh_2)_2Ir(H)(CO)PPh_3)]$	2.8°	48

However, **4** contains not only sterically demanding dicyclohexylphosphido-bridging ligands but also a relatively large ancillary triphenylphosphine ligand. The threefold symmetry of the

PPh_3 group superimposed on the $Mo(\mu\text{-}PCy_2)_2Pd$ core results in steric interactions between Cy3 and Cy4 (H32B - H62 = 2.352Å; H42B - C61 = 2.967Å), where Ph5 is edge on to the face of Cy1 (H12B - H56 = 2.376Å), and Ph7 is face to face with Cy2 (H26B - C76 = 3.035Å). We presume therefore that the observed dihedral angle in the $Mo(\mu\text{-}PCy_2)_2Pd$ core occurs simply to minimize these group interactions. This does not occur for $(CO)_4W(\mu\text{-}PPh_2)_2Pt(PPh_3)$ since the PPh_2 ligands are less bulky, and it does not occur for the μ-*t*-Bu_2P complexes mentioned since the terminal ligands are relatively small. It should be noted, however, that this type of bridging-terminal ligand interaction can be very important, for example, in the group 9 complexes $[M(\mu\text{-}PR_2)L_2]_2$, (M = Co, Rh, Ir), in which increasing the steric bulk of L increasingly favoured C>B>A (Figure 2.7)[49].

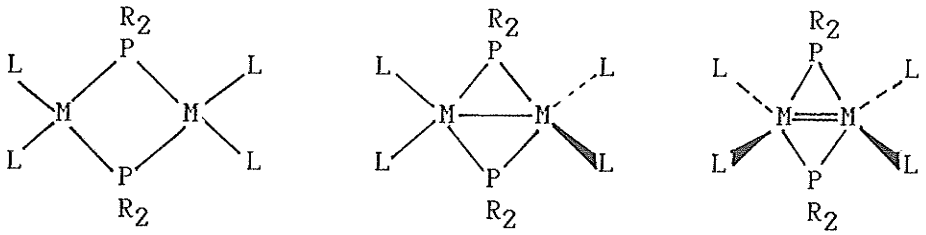

L = CO, PR_3, etc.

Figure 2.7: Effect of increasing the steric bulk of ligands, L.

2.5 Correlation of $^{31}P\{^{1}H\}$ NMR and X-ray Crystallography Data

As stated in Section 2.3, $^{31}P\{^{1}H\}$ nmr spectra are very useful in assigning molecular structures, and in this section $^{31}P\{^{1}H\}$ nmr data will be compared to X-ray crystallography data for several heterobimetallic complexes, including **4**.

The most obvious and most studied correlation between $^{31}P\{^{1}H\}$ nmr and crystallographic data is that between the chemical shift of the bridging phosphide ligand and the metal-metal bond distance. As stated in Section 2.3, a large downfield shift is expected for phosphide ligands that bridge a metal-metal bond, however, exceptions to this general rule do occur. Therefore, a generalization such as this can only be made for closely-related complexes supported by X-ray data. Table 2.6 gives examples of several complexes, their μ-PR_2 chemical shifts, and metal-metal bond distances.

Table 2.6: Chemical Shifts for Bridging Phosphido Ligands vs Metal-Metal Bond Distances

Complex	$\delta(\mu\text{-}PR_2)$	M-M Distance (Å)		Ref.
$(PPH_3)(CO)_3Ru(\mu\text{-}PPh_2)Co(CO)_3$	183.6(s)	2.7681(4)	Ru-Co	50a
$(CO)_4W(\mu\text{-}PPh_2)_2Ir(H)(COD)$	147.6(s)	2.893(1)	W-Ir	50b
$(CO)_4W(\mu\text{-}PPh_2)_2Re(CO)_3(CH_3)$	177.8(d)	3.015(1)	W-Re	47
$(CO)_4W(\mu\text{-}PPh_2)_2Pt\{CH_3O_2CC{=}CCO_2CH_3\}$	187.1(s)	2.764(1)	W-Pt	36
$(CO)_3Os(\mu\text{-}I)(\mu\text{-}PPh_2)Os(CO)_3$	48.0(s)	2.789(1)	Os-Os	50c
$[Co(\mu\text{-}t\text{-}Bu_2P)(PMe_3)N_2]_2$	214.95(d)	2.414(1)	Co-Co	50d
$Ni_2(\mu\text{-}t\text{-}Bu_2P)_2(CO)_2(PMe_3)$	268.90(d)	2.446(2)	Ni-Ni	50e
$(CO)_5Cr(\mu\text{-}t\text{-}Bu_2P)Rh(COD)$	215.0(s)	2.738(1)	Cr-Rh	46
$(CO)_4Mo(\mu\text{-}PCy_2)_2Pd(PPh_3)$	261.2(d)	2.760(1)	Mo-Pd	50f
$[Rh(\mu\text{-}t\text{-}Bu_2P)(CO)_2]_2$*	402.8(d)	2.7609(9)	Rh-Rh	50g
$[Rh(\mu\text{-}t\text{-}Bu_2P)(CO)_2]_2$†	402.8(d)	3.717(1)	Rh-Rh	50g

*tetrahedral core. †planar molecule

Especially notable in these examples are the complexes $(CO)_3Os(\mu\text{-}I)(\mu\text{-}PPh_2)Os(CO)_3$ with a $\mu\text{-}PPh_2$ chemical shift of 48.0 ppm, even though a metal-metal bond is present, and the planar complex $[Rh(\mu\text{-}t\text{-}Bu_2P)(CO)_2]_2$ with a $\mu\text{-}t\text{-}Bu_2P$ chemical shift of 402.8 ppm where no Rh-Rh bond is present.

Another correlation that seems to occur for phosphido-bridged complexes is that between $\mu\text{-}PR_2$ chemical shifts and M-P-M angles. Carty[39c] did establish a correlation between M-P-M angles and ^{31}P nmr chemical shifts for a series of related $Fe_2(\mu\text{-}PPh_2)(\mu\text{-}X)(CO)_6$ complexes and he also pointed out that the chemical shift value was, in this case, a very sensitive indicator of changes in bond angles. Geoffroy[30], on the other hand, structurally characterized several $(CO)_4W(\mu\text{-}PPh_2)_2ML_n$ complexes[36,48,51,52] and tried to correlate structural results to ^{31}P nmr chemical shift data for these compounds as in Table 2.7. However, no obvious correlation existed among the metal-metal distances, M-P-M angles, and ^{31}P nmr data. These results point out serious problems in relating chemical shift to M-P-M angles and metal-metal bonds except for closely related compounds.

Table 2.7: Structural Parameters and ^{31}P NMR Data for a Series of $(CO)_4W(\mu\text{-}PPh_2)_2ML_x$ and Related Compounds

Compound	M-M, A	M-P-M, deg	δ	Ref.
$(CO)_4W(\mu\text{-}PPh_2)_2Pt(PPh_3)$	2.764(1)	70.8(1), 70.6(1)	173.8	36
$(CO)_4W(\mu\text{-}PPh_2)_2Pt(CH_3CO_2C{\equiv}CCO_2CH_3)$	2.795(1)	72.4(1), 72.5(1)	187.1	36
$(CO)_4W(\mu\text{-}PPh_2)_2Ir(H)(COD)$	2.893(1)	74.2(2), 72.5(2)	157.6	51
$(CO)_4W(\mu\text{-}PPh_2)_2Ir(H)(CO)(PPh_3)$	2.8764(6)	72.7(1), 72.9(1)	132.8	48
$(CO)_3[C(OMe)Ph]W(\mu\text{-}PPh_2)_2Ir(H)(CO)(PPh_3)$	2.858(1)	73.0(1), 72.6(1)	119.3, 97.7	48
$(CO)_4W(\mu\text{-}PPh_2)_2ZrCp_2$	3.289(1)	79.3(8), 79.2(2)	156.6	36
$(CO)_4W(\mu\text{-}PPh_2)_2Re(CO)_3CH_3$	3.014(1)	76.1(1), 76.2(2)	177.8	52

If any conclusions can be made regarding $^{31}P\{^{1}H\}$ nmr, X-ray crystallographic data, and the presence or absence of a metal-metal bond, we would have to say that in order to reach an unambiguous conclusion X-ray crystallography must support ^{31}P nmr data.

2.6 The Metal-Metal Bond

From X-ray data described in Section 2.4 we can conclude that a bond does exist between the two metal atoms Mo and Pd. However, a description of that bond is needed to better understand the type of interaction between the two metal atoms.

To describe the metal-metal bond as a direct bond two conditions are necessary. First there must exist some sort of metal-metal interaction to give each metal a satisfactory electron count: 18 electrons for Mo, and 16 electronsfor Pd. Secondly, there are two anionic PCy_2 ligands in the complex, and therefore a total metal oxidation state of +2 must be accounted for. The three possible descriptions of the metal-metal bond are:

(a) the molecule could be described as having a direct covalent single bond between d^5 Mo(I) and d^9 Pd(I) centres,

(b) the metal-metal bond may be described as a polar donor-acceptor bond between d^6 Mo(0) and d^8 Pd(II), or

(c) the bond may be a polar donor-acceptor bond between the two metals in the opposite direction between d^4 Mo(II) and d^{10} Pt(0).

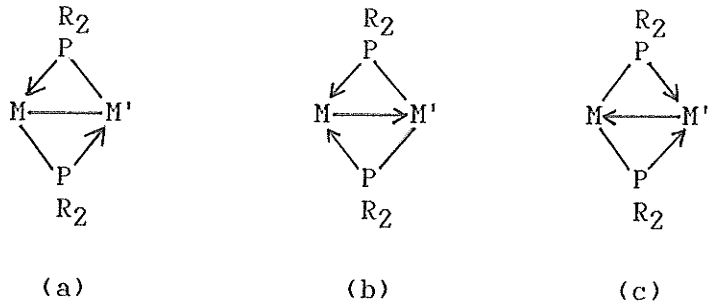

Figure 2.8 Descriptions of the metal-metal bond.

It is difficult to say which description best fits the molecule descibed here, since it is not known whether the interacting orbitals on each metal have the same energy as in (a), or whether the palladium or molybdenum orbitals lie at higher energy, as in (b) and (c). In Figure 2.8, (b) and (c) are illustrations of donor-acceptor bonds. On an orbital basis this simply means that the metal-localized orbitals that overlap to form the metal-metal bonding and antibonding orbitals are of different initial energies. Therefore the bonding molecular orbital will be closer in energy to one of the initial metal orbitals, and thus the electron density in that molecular orbital will be more localized on one metal than the other, as in Figure 2.9. A similar situation arises for the usual donor-acceptor mode of ligand-metal binding with electron density localized on the ligand. For heterometallic complexes, an important question concerns the strength of these donor-acceptor bonds and the particular chemistry that may result as a consequence of their presence[53].

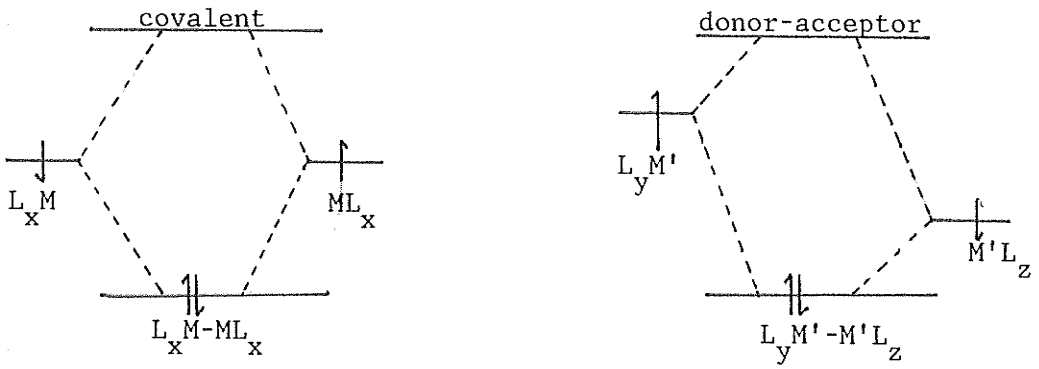

Figure 2.9: Molecular orbital descriptions of covalent and donor-acceptor bonds.

Given the information regarding CO stretching frequencies in Section 2.3 and the fact that the initial oxidation states of the metals were Mo(0) and Pd(II), formulation (b), the donor-acceptor bond from Mo(0) to Pd(II) seems the most reasonable explanation for the metal-metal bond.

2.4 Summary and Conclusions

In this chapter, the versatility of the bridge-assisted synthesis for phosphido-bridged heterobimetallic complexes has been demonstrated by its application to a series of dicyclohexylphosphido complexes that link Mo or W with Ni, Pd, and Pt. The substitution of cyclohexyl for phenyl groups adds stability, as evidenced by the ease of preparation and characterization of the nickel complexes, where in earlier syntheses related compounds were unisolable. This stability is probably due to a combination of increased basicity of the bridging phosphorous atoms and steric shielding by the cyclohexyl groups. We

also found that on stirring the Mo-Pd complex, **4**, under CO and H_2 that no reaction occurred. When **4** was reacted with dimethylacetylene dicarboxylate no identifiable products were observed in the $^{31}P\{^{1}H\}$ nmr spectrum. Therefore, although these complexes do appear interesting, the presence of two dicyclohexylphosphido-bridges makes them generally unreactive.

APPENDIX 2.1
SELECTED BOND DISTANCES AND ANGLES FOR
$(CO)_4Mo(\mu\text{-}PCy_2)_2Pd(PPh_3)$ (4)

Table 1: Distances (A)

Mo-Pd	2.760(1)	P3-C61	1.848(6)
Mo-P1	2.530(1)	P3-C71	1.819(6)
Mo-P2	2.542(2)	Mo-C1	2.00 (1)
Pd-P1	2.287(2)	Mo-C2	2.027(9)
Pd-P2	2.267(2)	Mo-C3	2.027(8)
Pd-P3	2.280(2)	Mo-C4	2.051(7)
P1-C31	1.85 (1)	C1-O1	1.14 (1)
P1-C41	1.85 (1)	C2-O2	1.12 (1)
P2-C11	1.859(7)	C3-O3	1.13 (1)
P2-C21	1.86 (1)	C4-O4	1.126(9)
P3-C51	1.839(5)		

Table 2: Angles (degrees)

P1-Pd-P2	118.7(1)	C2-Mo-C3	86.6(4)
P1-Mo-P2	101.2(1)	Mo-P1-C31	123.4(3)
P1-Mo-C3	84.7(3)	Mo-P2-C11	117.6(2)
P2-Mo-C2	170.3(2)	Pd-P1-C41	121.4(4)
C1-Mo-C2	89.9(4)	Pd-P3-C51	121.5(1)
C2-Mo-C3	90.8(3)	C51-P3-C61	100.4(2)
Mo-P1-Pd	69.7(1)	P2-Pd-P3	122.3(1)
Mo-P2-Pd	69.8(1)	P1-Mo-C2	87.7(3)
Pd-P1-C31	117.1(3)	P2-Mo-C1	82.0(3)
Pd-P2-C21	125.9(2)	P2-Mo-C4	91.7(3)
Pd-P3-C71	105.9(2)	C1-Mo-C4	94.6(4)
C61-P3-C71	105.1(3)	C3-Mo-C4	174.3(3)
P1-Pd-P3	118.5(1)	Mo-P1-C41	118.2(4)
P1-Mo-C1	170.9(3)	Mo-P2-C21	120.8(2)
P1-Mo-C4	93.8(3)	Pd-P2-C11	119.1(3)
P2-Mo-C3	94.0(2)	Pd-P3-C61	118.8(2)
C1-Mo-C3	86.6(4)	C51-P3-C71	103.3(2)

CHAPTER THREE

SINGLY-BRIDGED COMPLEXES OF Fe-Ir

3.1 Introduction

In this chapter, the chemistry of singly-bridged dicyclohexylphosphido complexes is investigated, in which the two metal centres involved are Fe and Ir. As was shown in Chapter Two, a doubly-bridged system was quite unreactive. No substitution reactions or oxidative-addition chemistry was found, and although donor-acceptor bonds such as those present in $(CO)_4M(\mu\text{-}PCy_2)_2M'(PPh_3)$ might be expected to be labile, when two bulky dicyclohexylphosphide bridges were present, the metal-metal bond was not perturbed. A single phosphido bridge on the other hand, should still impart stability to a heterobimetallic system, while allowing the two metal centres to be more accessible to chemical transformations.

The heterobimetallic complexes $(CO)_3(PPh_3)Fe(\mu\text{-}PCy_2)Ir(PPh_3)(CO)_2$ (**2**), and $(CO)_4Fe(\mu\text{-}PCy_2)Ir(COD)$ (**3**), shown below in Figure 3.1, are prepared via the bridge-assisted synthesis. Complex **2** is prepared by reacting $Li[Fe(CO)_4(PCy_2)]$ with Vaska's compound[54], *trans*-$IrCl(CO)(PPh_3)_2$. Square planar d^8 complexes, such as Vaska's compound, have a formal electron count of 16 and are therefore coordinatively unsaturated. These Ir(I) species are known to undergo oxidative

addition reactions with numerous addenda. For example, *trans*-$IrCl(CO)(PPh_3)_2$ reacts with HCl to give the oxidative-addition product $IrCl_2(H)(CO)(PPh_3)_2$. This Ir(III) complex has a formal electron count of 18 and is therefore coordinatively saturated, and has a full octahedral coordination sphere. It should prove interesting then, to study the effect a proximate iron atom will have on the reactivity of the iridium centre in a heterobimetallic complex.

Complex **3** is prepared by reacting $2Li[Fe(CO)_4(PCy_2)]$ and *trans,trans*-$[IrCl(COD)]_2$[55] (COD = 1,5-cyclooctadiene). This complex is also coordinatively unsaturated at the iridium centre, and therefore should undergo similar addition reactions. As well, 1,5-COD is usually displaced readily by other ligands such as CO and PR_3[19]. Thus the potential exists for both addition and substitution reactions to occur with the heterobimetallic complex **3**.

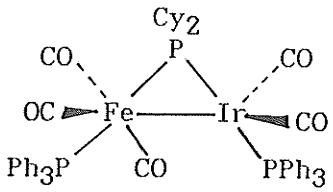

2

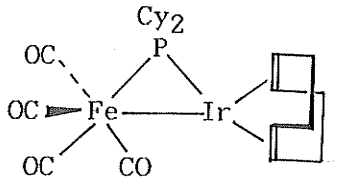

3

Figure 3.1: Complexes 2 and 3.

3.2 Experimental

i) General

Trans-$IrCl(CO)(PPh_3)_2$[54] and $[IrCl(COD)]_2$[55] were prepared according to literature procedures. *n*-BuLi, PPh_3, PEt_3, P*n*-Bu_3, P*i*-Pr_3, PMe_2Ph, $PMePh_2$, tetrafluoroboric acid-diethyl ether complex (HBF_4-etherate), $Fe_2(CO)_9$, 1,5-cyclooctadiene (1,5-COD), MeI, bis(diphenylphosphino)ethane (dppe) (Aldrich), $IrCl_3 \cdot 3H_2O$, PCy_3, PCy_2H, bis(diphenylphsophino)methane (dppm) (Strem), and dimethylacetamide (DMA) (Eastman), were purchased and used as received. PBz_3 was courtesy D. W. Stephan, University of Windsor. Dimethylacetamide hydrochloride (DMA•HCl) was prepared by bubbling HCl gas through a benzene solution of DMA which gave immediate formation of DMA•HCl as a white precipitate. The latter was washed with benzene, dried under vacuum, and stored under N_2 for later use. CH_2Cl_2 was dried by distillation from CaH_2 under N_2; tetrahydrofuran (THF), *n*-hexane, and toluene were dried by distillation from Na-benzophenone-ketyl under N_2; *n*-heptane and diethyl ether were dried over molecular sieves and degassed with N_2 prior to use. All reactions were conducted under an N_2 atmosphere using standard Schlenk[35] techniques, as explained in Section 2.2.

$^{31}P\{^1H\}$ nmr spectra were recorded at 36.4 MHz on a Brüker WH90 spectrometer at 300K with an external D_2O lock and at 121.5 MHz on a Brüker AM300 at 220K. Phosphorous chemical shifts were measured relative to external H_3PO_4 (85%) with positive shifts downfield. ^1H nmr spectra were obtained at 300 MHz on a Brüker AM300 at 300K and are

reported relative to Me_4Si. $^{13}C\{^1H\}$ nmr spectra were obtained at 74.5 MHz on a Bruker AM300 at 300K. Infrared spectra were recorded on a Perkin-Elmer 781 grating infrared spectrometer using CH_2Cl_2 or *n*-hexane solutions in NaCl solution cells. Gas chromatography and mass spectral data were collected on a Hewlett-Packard HP 5890 gas chromatograph linked to an HP 5970B mass selective detector. Samples were analyzed on a Hewlett- Packard fused silica capillary column of crosslinked 5% phenyl methyl silicone (25 m x 0.20 mm) operating at 70°C. Elemental analyses were performed by Canadian Microanalytical Service Ltd., New Westminster, British Columbia, Canada.

ii) Preparation of $Fe(CO)_4(PCy_2H)$ (1)

To a solution of $Fe_2(CO)_9$ (5.0 g, 13.75 mmoles) in toluene (50 mL) was added PCy_2H (2.84 mL, 13.75 mmoles). The orange-brown solution was stirred for 24 hours at 35°C, during which time all of the $Fe_2(CO)_9$ dissolved. The solvent was removed in vacuo to leave a brown oil which was dissolved in *n*-heptane (30 mL) and which was recrystallized by cooling the solution to -20°C for 12 hours. This yielded a brown crystalline solid, 4.14 g, 11.29 mmoles, 82%. Anal. calc'd. for $C_{16}H_{25}O_4PFe$: C, 52.47%; H, 6.37%. Found: C, 51.06%; H, 6.21%.

ii) Preparation of $(CO)_3(PPh_3)Fe(\mu\text{-}PCy_2)Ir(PPh_3)(CO)_2$ (2)

n-BuLi, (1.65 mL, 1.55M in hexanes, 2.56 mmoles) was added via syringe to a red-brown solution of $Fe(CO)_4(PCy_2H)$ (0.938 g, 2.56 mmoles) in THF (15 mL). This solution immediately turned dark brown. After stirring for 10 minutes, the solution was added dropwise to a yellow slurry of *trans*-$IrCl(CO)(PPh_3)_2$ (2.00 g, 2.56 mmoles) in THF (30 mL) at 23°C. After 20 minutes all of the *trans*-$IrCl(CO)(PPh_3)_2$ had dissolved and the resultant orange-brown solution was stirred for 24 hours at 23°C. The solvent was removed in vacuo and the remaining brown oily solid was washed with hexane (3 x 10 mL), and then extracted with CH_2Cl_2 (5 x 10 mL). The volume of CH_2Cl_2 solution was reduced to approximately 10 mL and the solution was cooled to -20°C for 18 hours, yielding orange microcrystals of **2**. (2.21 g, 1.98 mmoles, 75%). Anal. calc'd. for $C_{53}H_{52}FeIrO_5P_3$: C, 57.31%; H, 4.73%. Found: C, 57.24%; H, 4.63%.

iv) Preparation of $(CO)_4Fe(\mu\text{-}PCy_2)Ir(COD)$ (3)

n-BuLi, (0.51 mL, 1.6M in hexanes, 0.816 mmoles) was added via syringe to a red-brown solution of $Fe(CO)_4(PCy_2H)$ (0.300g, 0.816 mmoles) in THF (10 mL). The dark brown solution was stirred for 10 minutes, cooled to 0°C, then added dropwise to an orange solution of $[IrCl(COD)]_2$ (0.274 g, 0.408 mmoles) in THF (10 mL) at 0°C. The solution immediately turned an intense red-brown colour. After stirring at 0°C for four hours the solvent was removed in vacuo, and a

red-brown oily solid resulted. Complex **3** was unstable at 0°C in the solid state and in solution, and was therefore prepared and used in situ.

v) General Reactions of Complex 2

a) Reaction of 2 with MeI or DMA·HCl

To partially dissolved solutions of **2** (0.100 g, 0.090 mmoles) in toluene (10 mL) were added equimolar amounts of either MeI or DMA·HCl. The solutions were stirred for 18 hours, with no change in the orange colour. $^{31}P\{^{1}H\}$ nmr indicated that no reactions had occurred.

b) Reaction of 2 with H_2

Complex **2**, (0.142 g, 0.128 mmoles) was partially dissolved in toluene (5 mL) and stirred under H_2 (one atmosphere) at 60°C for 20 minutes with no change in the orange solution. $^{31}P\{^{1}H\}$ nmr indicated that no reaction had occurred.

c) Reaction of 2 with CO

Complex **2**, (0.200g, 0.180 mmoles) was partially dissolved in toluene (5 mL) and stirred under CO (one atmosphere) for two hours without change in the orange solution. $^{31}P\{^{1}H\}$ nmr indicated that no reaction had occurred.

d) Preparation of $(CO)_3(PPh_3)Fe(\mu\text{-}PCy_2)Ir(PPh_3)(CO)(t\text{-}BuCN)$ (4)

Complex **2**, (0.190 g, 0.171 mmoles) was partially dissolved in toluene (5 mL) and *t*-BuCN (0.019 mL, 0.171 mmoles) was added. After stirring at 60°C for 20 minutes a clear orange solution resulted. $^{31}P\{^1H\}$ nmr indicated that *t*-BuCN had replaced CO on Ir to the extent of 50%, however, the product proved unisolable due to persistent contamination by **2**.

e) Preparation of $[(CO)_2(PPh_3)(H)Fe(\mu\text{-}PCy_2)Ir(PPh_3)(CO)_2]^+ BF_4^-$ (5)

Complex **2**, (0.120 g, 0.108 mmoles) was partially dissolved in THF (5 mL) and HBF_4-etherate (0.025 mL, 0.108 mmoles) was added. After stirring at 23°C for 18 hours the volume of the solution was reduced to ca. 3 mL and then cooled to -20°C for 48 hours to yield light yellow **5** (0.044 g, 35%)

vi) Phosphine Substitution Reactions

a) Preparation of $(CO)(PPh_3)Fe(\mu\text{-}PCy_2)Ir(PR_3)(CO)_2$ [R = Et (6), *n*-Bu (7), *i*-Pr (10), Bz (11)] and $(CO)_3(PPh_2Me)Fe(\mu\text{-}PCy_2)Ir(PPh_2Me)(CO)_2$, (12)

To a partially dissolved solution of **2** (0.150 g, 0.135 mmoles) in toluene (10 mL) was added twice the equimolar amount of phosphine. After stirring for approximately 15 minutes all of complex **1** dissolved,

resulting in orange solutions. All reactions mixtures were stirred for 12 hours at 23°C, and the toluene removed in vacuo. The remaining orange oil was then washed with diethyl ether (2 x 3 mL) to leave the product as a yellow or yellow-orange powder. The yields and elemental analysis data are summarized in Table 3.1.

b) Preparation of $(CO)_3(PMe_2Ph)Fe(\mu\text{-}PCy_2)Ir(PPh_3)(CO)_2$, (8), and $(CO)_3(PPh_3)Fe(\mu\text{-}PCy_2)Ir(PCy_3)(CO)_2$, (9)

To a partially dissolved solution of **2** (0.150 g, 0.135 mmoles) in toluene (10 mL) was added twice the equimolar amount of either PMe_2Ph or PCy_3. After stirring for approximately 15 minutes complex **1** dissolved completely, leaving an orange solution of **8** or an orange-red solution of **9**. The reaction mixtures were stirred at 23°C for 12 hours, and the toluene was removed in vacuo. The minimum amount of diethyl ether was added to dissolve the remaining orange oil, and the ether solutions were cooled to -20°C for 24 hours, precipitating orange-yellow microcrystals of **8**, and orange microcrystals of **9**

Table 3.1: Yields and Elemental Analyses Results for Phosphine Substitution Products of $(CO)_3(PPh_3)Fe(\mu\text{-}PCy_2)Ir(PPh_3)(CO)_2$

Phosphine	Yield			Elemental Analysis			
	grams	%	formula	calculated		found	
				%C	%H	%C	%H
PEt_3, **6**	0.143	57	$C_{41}H_{52}FeIrO_5P_3$	50.96	5.43	51.27	5.53
$Pn\text{-}Bu_3$, **7**	0.150	63	$C_{47}H_{64}FeIrO_5P_3$	53.74	6.15		
PMe_2Ph, **8**	0.072	55	$C_{43}H_{48}FeIrO_5P_3$	52.36	4.92		
PCy_3, **9**	0.079	68	$C_{53}H_{70}FeIrO_5P_3$	56.40	6.26	55.43	6.52
$Pi\text{-}Pr_3$, **10**	0.081	61	$C_{44}H_{58}FeIrO_5P_3$	52.41	5.81	52.43	5.63
PBz_3, **11**	0.132	58	$C_{56}H_{61}FeIrO_5P_3$	58.19	5.08	56.39	4.92
PPh_2Me, **12**	0.116	63	$C_{43}H_{48}FeIrO_5P_3$	52.35	4.91	51.11	4.75

vii) Preparation of $(PPh_3)(CO)_3Fe(\mu\text{-}PCy_2)Ir(CO)(PPh_3)$ (13)

When a solution of **2** (0.200 g, 0.180 mmoles) in toluene (10 mL) was refluxed for one hour, CO loss from Ir occurred to the extent of 50% according to $^{31}P\{^1H\}$ nmr. Further heating of the orange-red solution resulted in decomposition to a brown coloured solution. The product was not isolable due to persistent contamination by **2**.

viii) Preparation of $(PPh_3)(CO)_3Fe(\mu\text{-}PCy_2)Ir(CO)(PCy_3)$ (14)

Complex **2** (0.200 g, 0.180 mmoles)was partially dissolved in toluene (10 mL) and PCy_3 (0.100 g, 0.360 mmoles) was added. After refluxing for one hour and removing the toluene in vacuo the remaining red oil was dissolved in diethyl ether. After cooling the solution at -20°C for 48 hours, solid product precipitated from solution but resulted in unsatisfactory elemental analysis, probably due to phsophine contamination.

ix) Preparation of $(CO)_4Fe(\mu\text{-}PCy_2)Ir(CO)_3$ (15)

A solution of **3** (0.200 g, 0.300 mmoles) in toluene (10 mL) was stirred under CO (one atmosphere) for one hour. The toluene was removed in vacuo and the residue dried in vacuo for four hours to remove 1,5-COD. *n*-Hexane (2 mL) was added to dissolve the product,

and after cooling to -20°C for 48 hours red **15** was collected, (0.096 g, 50%).

x) Preparation of $(CO)_4Fe(\mu\text{-}PCy_2)Ir(PCy_3)(CO)_2$ (16)

To a red-brown solution of **3** (0.136 g, 0.204 mmoles) in toluene (10 mL) was added PCy_3 (0.057 g, 0.204 mmoles) at 23°C. The solution was stirred at 23°C under CO (one atmosphere) for two hours, during which time no colour change was observed. The toluene was removed in vacuo and the brown residue dried in vacuo for four hours to remove 1,5- COD. The residue was then dissolved in *n*-hexane (3 mL) and cooled to -20°C for 48 hours to yield red-brown **16** (0.098 g, 56%).

xi) Preparation of $(CO)_3(PEt_3)Fe(\mu\text{-}PCy_2)Ir(PEt_3)(CO)_2$ (17)

To a THF (10 mL) solution of **3** (0.217 g, 0.327 mmoles) was added PEt_3 (0.097 mL, 0.654 mmoles). The dark red-brown solution was stirred for three hours at 50°C, without a change in colour. The THF was removed in vacuo, and the red-brown oil was dried in vacuo for two hours to remove 1,5-COD. Toluene (4 mL) was added to dissolve the oil, and after cooling to -20°C for 24 hours brown microcrystals of **17** precipitated (0.128 g, 48%).

xii) Preparation of $(CO)_3Fe(\mu\text{-}PCy_2)(\mu\text{-}dppe)Ir(CO)(COD)$ (18a) and $(CO)_3Fe(\mu\text{-}PCy_2)(\mu\text{-}dppe)Ir(CO)_2$ (18b)

To a THF (5 mL) solution of **3** (0.109 g, 0.164 mmoles) was added dppe (0.065 g, 0.164 mmoles). The red-brown solution was stirred for 18 hours at 23°C without colour change. $^{31}P\{^1H\}$ nmr indicated an approximate 3:2 ratio of complex **18b** to complex **18a**. On warming this solution to 50°C for three hours, $^{31}P\{^1H\}$ nmr indicated complete conversion to **18b**. The THF was removed in vacuo, and the resultant red-brown oil was dried in vacuo for four hours to remove 1,5-COD. Toluene (4 mL) was added to dissolve the solid, and after cooling to -20°C for 24 hours yielded red-brown **18b** (0.083 g, 52%).

xiii) Preparation of $(CO)_3Fe(\mu\text{-}PCy_2)(\mu\text{-}dppm)Ir(CO)_2$ (19a, b, and c)

To a THF (10 mL) solution of **3** (0.217 g, 0.327 mmoles) was added dppm (0.126 g, 0.327 mmoles). The red-brown solution was stirred at 50°C for three hours during which time there was no colour change in the solution. The THF was removed in vacuo and the red-brown oily residue was dried in vacuo for four hours to remove 1,5-COD. $^{31}P\{^1H\}$ nmr showed the formation of three products, **19a**, **b**, and **c**.

xiv) Preparation of $(CO)_4Fe(\mu\text{-}PCy_2)Ir(THF)_x$ (20)

A solution of **3** (0.200 g, 0.300 mmoles) in THF (10 mL) was stirred under H_2 (one atmosphere) for one hour. The THF was removed in vacuo and the residue dried in vacuo for four hours to remove 1,5-COD. *n*-Hexane (2 mL) was added to dissolve the brown oily solid, which did not precipitate product from solution after cooling to -20°C for one week.

xv) Hydrogenation of Styrene by Complex 1

To a brown solution of complex **1** (0.027 g, 0.040 mmoles) in THF (10 mL) was added styrene (1.10 mL, 1.0 g, 9.62 mmoles). This solution was maintained under H_2 (one atmosphere) at 23°C. 20 μL of the reaction solution was removed and diluted in 2 mL THF, and 5 μL of this solution was analyzed by GC-MS. The dilution and injection procedure was begun at time zero, and repeated approximately every 15 minutes for one hour, and then every hour for the following three hours, and finally at eight hours.

3.3 Synthesis and Characterization of Complexes 1 and 2

In 1978 Treichel and coworkers[56] reacted $Fe_2(CO)_9$ and several monodentate primary and secondary phosphines to yield monosubstituted

$Fe(CO)_4(PR_3)$ and $Fe(CO)_4(PR_2H)$. We have used this method to prepare $Fe(CO)_4(PCy_2H)$ in 82% yield, as did Geoffroy[23] to prepare $Fe(CO)_4(PPh_2H)$. The product is red-brown in colour, and is air-stable for short periods of time both as a solid and in solution. Equation 3.1 below outlines the general synthetic procedure.

$$Fe_2(CO)_9 + PCy_2H \xrightarrow[60°C]{\text{toluene}} Fe(CO)_4(PCy_2H) + Fe(CO)_5 \qquad (3.1)$$

Compound **1** shows a single resonance in the $^{31}P\{^1H\}$ nmr spectrum at δ54.63 ppm (J_{P-H} = 344.3 Hz). The infrared spectrum shows four ν_{CO} absorptions, consistent with C_{2v} symmetry, as expained in Section 2.3.

Complex **2** was prepared using the bridge-assisted method[6] of synthesis as outlined in Equations 3.2 and 3.3 below.

$$Fe(CO)_4(PCy_2H) + n\text{-BuLi} \longrightarrow Li[Fe(CO)_4(PCy_2)] + n\text{-BuH} \qquad (3.2)$$

$$Li[Fe(CO)_4(PCy_2)] + trans\text{-}IrCl(CO)(PPh_3)_2 \longrightarrow (CO)_3(PPh_3)Fe(\mu\text{-}PCy_2)Ir(PPh_3)(CO)_2 + LiCl \qquad (3.3)$$

A brown solution of $Li[Fe(CO)_4(PCy_2)]$ was added to a yellow slurry of *trans*-$IrCl(CO)(PPh_3)_2$ in THF. The reaction was assumed to be complete when all of the undissolved *trans*-$IrCl(CO)(PPh_3)_2$ had dissolved, resulting in an orange-brown solution. The product was found to be only partially soluble in most solvents, although more polar CH_2Cl_2 was the most suitable solvent for recrystallization in good yield, 75%. Complex **2** is air stable in the solid state and also

in solution for a very short time period, decomposing to a brown coloured solution within five minutes. Geoffroy[23] has prepared a similar complex, $(CO)_3(PPh_3)Fe(\mu\text{-}PPh_2)Ir(PPh_3)(CO)_2$ by the same method, and after column chromatography on alumina reported a yield of 37%.

The $^{31}P\{^1H\}$ nmr and infrared spectral data for complex **2** are shown in Tables 3.2 and 3.3 respectively. Figure 3.2 shows the $^{31}P\{^1H\}$ nmr spectrum for complex **2**. All resonances are well separated; the downfield doublet of doublets at δ148.9 ppm is due to the bridging PCy_2 ligand, the doublet at δ74.31 ppm is due to the PPh_3 ligand on Fe, and the doublet at δ10.72 ppm is due to PPh_3 on Ir. The position of the resonances of the PPh_3 ligands is based on data presented by Geoffroy[23] for $(CO)_3(PPh_3)Fe(\mu\text{-}PPh_2)Ir(PPh_3)(CO)_2$ for which the μ-PPh_2 resonance occured at δ114.1 ppm, that for PPh_3 on Fe at δ74.2 ppm, and that for PPh_3 on Ir at δ14.0 ppm. It is also supported by results presented in Chapter Four for $(CO)_3(PPh_3)Fe(\mu\text{-}PCy_2)Rh(PPh_3)(CO)$ (*vide infra*), where the resonance for the PPh_3 on Rh is easily identifiable as occurring upfield at δ24.6 ppm as a doublet of doublets due to phosphine coupling to the phosphide and Rh. Phosphine atoms on Fe are commonly found in the δ50-80 ppm range[57] in ^{31}P nmr spectra. As was explained in Chapter Two, the downfield shift of the μ-PCy_2 ligand is probably an indication of a metal-metal bond. The large coupling constant of 178 Hz for PPh_3(Ir) coupled to μ-PCy_2 suggests that the ligands have a *trans* geometry, since according to established correlations[58], those compounds with coupling constants ($^2J_{P-P}$) between P atoms in the range 140-225 Hz would be expected to have a *trans* arrangement of phosphorous ligands, whereas those with coupling constants in the range of 9-25 Hz should have a *cis* arrangement.

Figure 3.2: $^{31}P\{^{1}H\}$ nmr spectrum of complex 2, $(CO)_3(PPh_3)Fe(\mu\text{-}PCy_2)Ir(PPh_3)(CO)_2$.

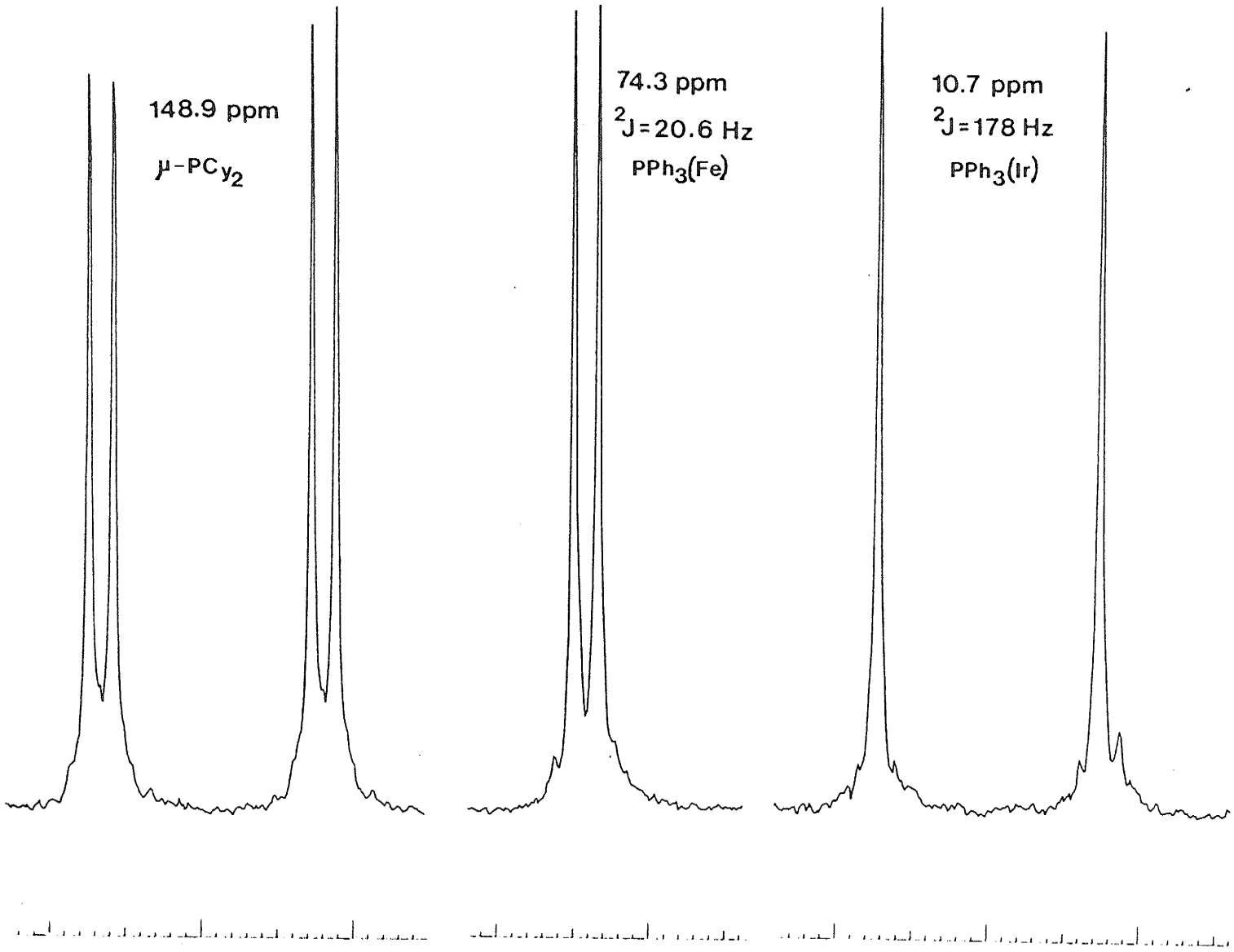
148.9 ppm
μ-PCy2
74.3 ppm
2J=20.6 Hz
PPh3(Fe)
10.7 ppm
2J=178 Hz
PPh3(Ir)

The infrared spectrum of compound **2** is shown in Figure 3.3. It is difficult to distinguish CO stretching bands belonging to carbonyls on Fe from those belonging to carbonyls on Ir, though general assignments can be made by referring to Figure 3.4 below.

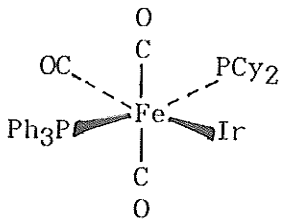

C_{2v} symmetry

3 ν_{CO} bands: $2a_1 + b_2$

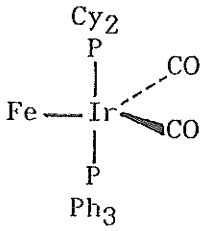

C_{2v} symmetry

2 ν_{CO} bands: $a_1 + b_2$

Figure 3.4: Assignments of the carbonyl stretching bands for the infrared spectrum of complex 2.

The number of bands in the infrared spectrum and their intensity depends largely on the symmetry about the metal to which the carbonyls are attached. Therefore, because each metal atom has approximate C_{2v} symmetry, as depicted in Figure 3.4, five carbonyl stretching bands are expected and observed. The intensities of these bands are not easily predicted, however, it is known that the more symmetric vibrations have smaller extinction coefficients, and therefore bands due to symmetric vibrations are less intense than those due to asymmetric vibrations.[41]

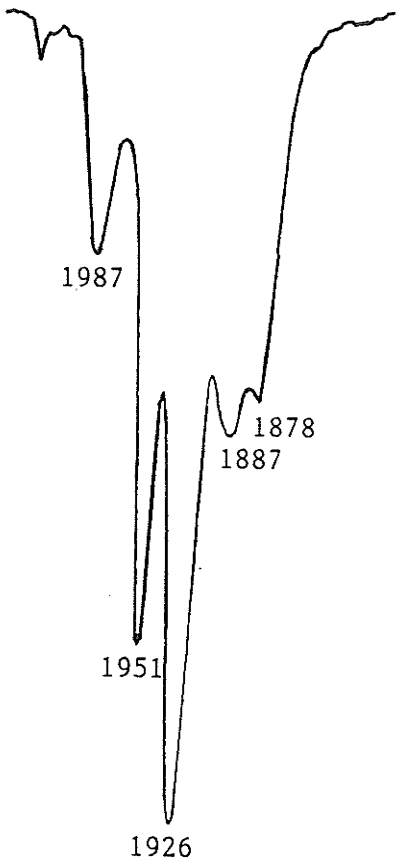

Figure 3.3: Infrared spectrum of complex 3, $(CO)_3(PPh_3)Fe(\mu\text{-}PCy_2)Ir(PPh_3)(CO)_2$.

3.4 General Reactions of 2

In order to study the basic reactivity of complex **2**, several different types of reactions were performed. Since complex **2** is similar in structure to $(CO)_3(PPh_3)Fe(\mu\text{-}PPh_2)Ir(PPh_3)(CO)_2$[23], which was found to have a metal-metal bond by X-ray crystallography, it may be assumed that this type of metal-metal interaction also exists in **2**. A formal electron count would suggest that a donor-acceptor bond exists between d^8 Fe(0) and d^8 Ir(I), so that both metals can be considered to be coordinatively saturated with 18 electrons. Therefore, any addition reactions that do occur must be at the expense of the metal-metal bond. Simple addition reactions were attempted by reacting **2** with CO or *t*-BuCN. CO does not add at either metal centre, supporting the idea that coordinative saturation exists at both metals. Furthermore, addition of CO across the metal-metal bond does not occur. Although *t*-BuCN does substitute for one CO ligand on Ir to the extent of 50%, *t*-BuCN does not add to either metal or across the metal-metal bond.

Oxidative-addition reactions with molecules such at MeI, H_2, and HCl were also undertaken to test the reactivity of the Ir centre. We observed that complex **2** does not undergo oxidative addition reactions with MeI, H_2, or HCl. This was shown by $^{31}P\{^1H\}$ nmr, in which no change in the spectrum of **2** was observed.

Finally, protonation of the complex was attempted by reacting **2** with acids such as HCl and HBF_4. No reaction was observed with HCl, but HBF_4 afforded a hydride complex, **5**. This is probably due to the fact that HBF_4 is a much stronger acid than HCl. The hydride complex **5** was

characterized by $^{31}P\{^{1}H\}$ and ^{1}H nmr. The ^{31}P nmr spectrum of **5** indicates that all phosphorous atoms in the molecule are coupled to each other. An overlapping doublet of doublets at δ148.91 ppm due to μ-PCy_2 shows *cis* coupling to both of the terminal phosphines. The three bond coupling constant between PPh_3(Fe) and PPh_3(Ir) is 9.6 Hz. The ^{1}H nmr shows a doublet of doublets at δ-11.2 ppm. Since protonation of a bimetallic complex could occur at either metal centre or at the metal-metal bond, a selective decoupling experiment was devised to identify unambiguously the site of protonation. The μ-PCy_2 resonance was decoupled first, yielding a doublet for the ^{1}H spectrum. This doublet was attributed to coupling of 12.7 Hz between the hydride and a terminal phosphorous atom. The PPh_3(Fe) resonance was decoupled next, and did not change the ^{1}H spectrum, indicating that the hydride was not bonded to Fe. Finally, the PPh_3(Ir) resonance was decoupled, yielding a doublet with a coupling constant of 19.0 Hz, due to coupling between the bridging phosphorous atom and the hydride. The results of the selective decoupling experiment are shown in Figure 3.5. The presence of a sharp band at 2072 cm^{-1} in the infrared spectrum of complex **5** is also consistent with a terminal metal hydride compound. The proposed structure of **5** is shown in Figure 3.6.

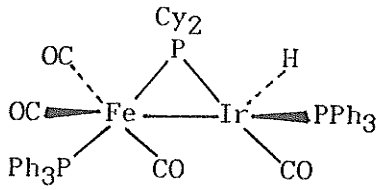

Figure 3.6: Proposed Structure of Complex 5.

Figure 3.5: Results of selectively decoupling ^{1}H from ^{31}P in complex 5, $[(CO)_3(PPh_3)Fe(\mu\text{-}PCy_2)Ir(PPh_3)(CO)(H)]^{+}[BF_4]^{-}$. Spectrum a) full undecoupled spectrum, b) decoupled from ^{31}P at δ165.61 ppm, c) decoupled from ^{31}P at δ51.49 ppm, d) decoupled from ^{31}P at δ5.72 ppm.

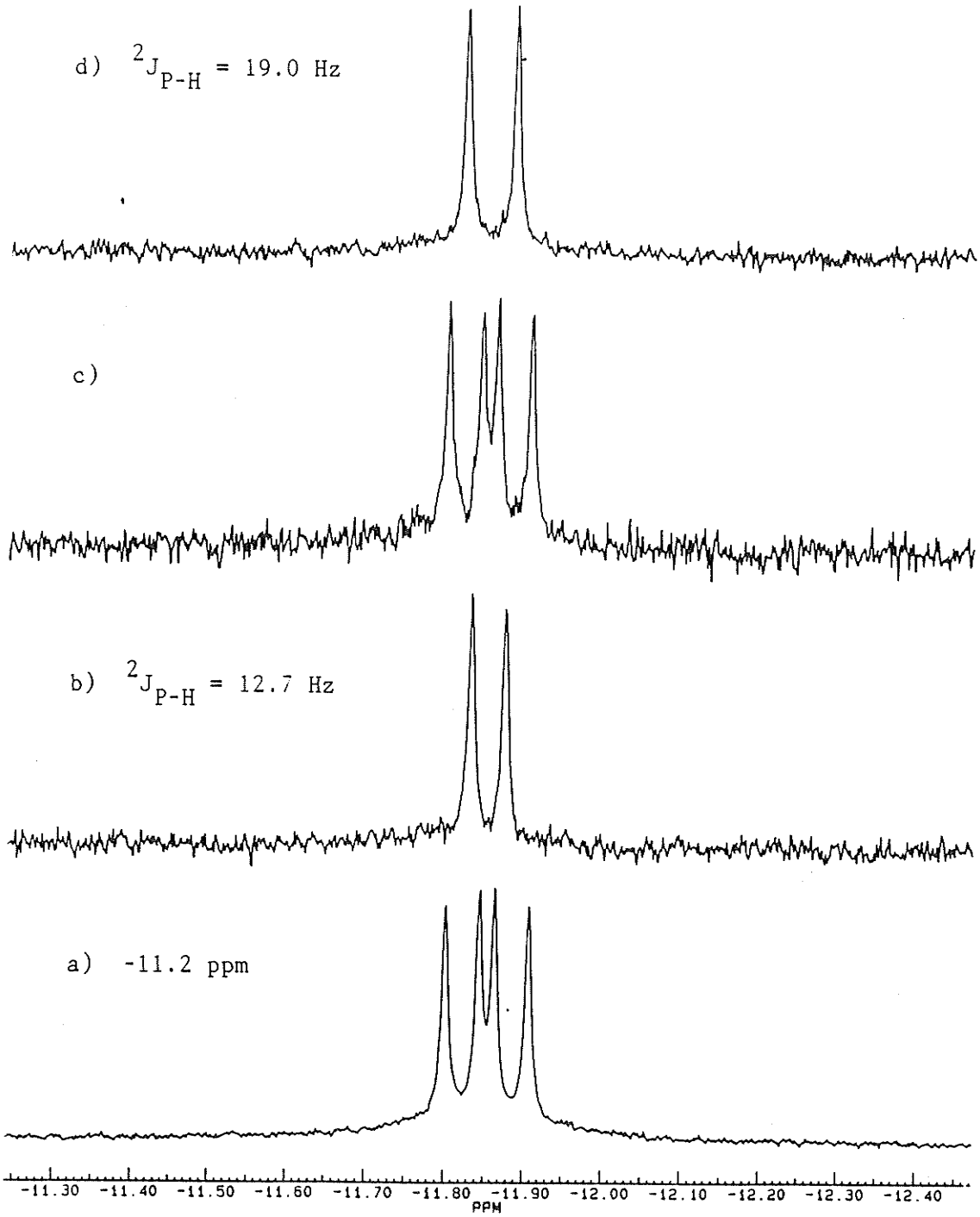
d) $^2J_{P-H}$ = 19.0 Hz
c)
b) $^2J_{P-H}$ = 12.7 Hz
a) -11.2 ppm
-11.30 -11.40 -11.50 -11.60 -11.70 -11.80 -11.90 -12.00 -12.10 -12.20 -12.30 -12.40
PPM

It is interesting to compare these results with those found by Geoffroy[23], who reported a series of reactions of CO and H_2 with $(CO)_3(PPh_3)Fe(\mu\text{-}PCy_2)Ir(PPh_3)(CO)_2$. For example, on maintaining a CO atmosphere over $(CO)_3(PPh_3)Fe(\mu\text{-}PPh_2)(PPh_3)(CO)_2$ he claims that the $(CO)_6$ complex shown below in Equation 3.4 is formed where addition of CO has caused the loss of the donor-acceptor metal-metal bond.

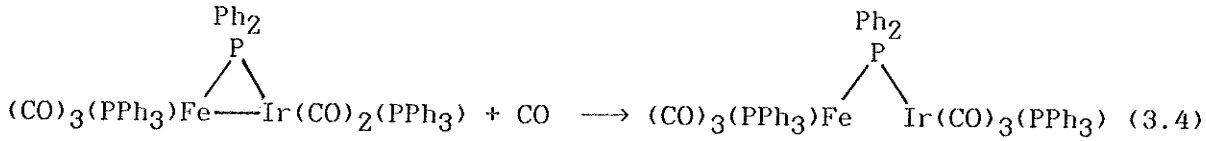

(3.4)

Similarly, on reaction with H_2 the metal-metal bond is lost, as in Equation 3.5.

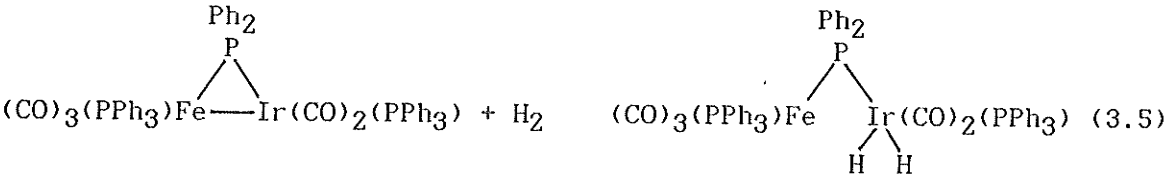

(3.5)

For complex **2** cleavage of the metal-metal bond does not occur in any addition reactions. Since the only difference between $(CO)_3(PPh_3)Fe(\mu\text{-}PPh_2)Ir(PPh_3)(CO)_2$ and complex **2** is the nature of the phosphide bridge, it can be concluded that the increased basicity and steric bulk of the $\mu\text{-}PCy_2$ ligand imparts some type of stability to the metal-metal bond, making the complex unreactive to substitution and oxidative-addition.

Since compound **2** is unreactive toward addition of ligands to displace the metal-metal bond, and since the Ir(I) atom appears to be

inert towards oxidative-addition, we therefore decided to attempt the thermal displacement of CO from Ir in order to generate coordinative unsaturation at that metal. When complex **2** is refluxed in a toluene solution for one hour a 1:1 mixture of complex **2** and complex **13** is produced. $^{31}P\{^{1}H\}$ nmr shows that for **13** the PPh_3 on Ir is now *cis* to the μ-PCy_2 unit, the $^{2}J_{\mu P-PPh_3}$ coupling constant having been reduced to 18.8 Hz from 178.2 Hz. This data is consistent with that of Geoffroy[23] and would lead us to believe that CO has been removed, resulting in a *cis* disposition of the phosphorous atom on Ir, as in Figure 3.7. This coordinatively unsaturated complex would be useful in further reactivity studies, however **13** could not be isolated in pure form, due to persistent contamination by **2**.

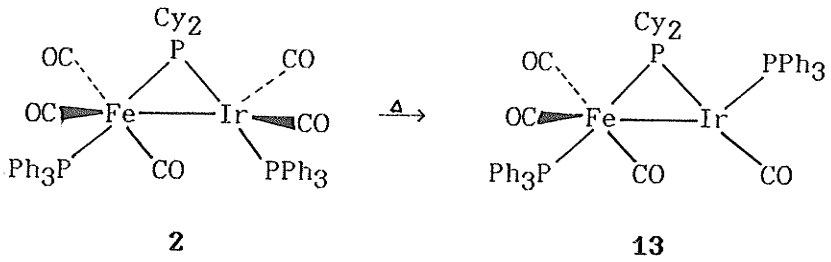

2 **13**

Figure 3.7: Coversion of 2 to 13

Table 3.2: $^{31}P\{^{1}H\}$ NMR Data[a] for Complex 2 and Derivatives

Complex	$\delta(\mu\text{-}PCy_2)$[b]	$\delta(P_{Fe})$	$\delta(P_{Ir})$	$^{2}J_{\mu P\text{-}P_{Fe}}$[c]	$^{2}J_{\mu P\text{-}P_{Ir}}$
1		54.63s[d]			
2	148.90dd	74.31d	10.72d	20.6	178.2
4	132.70dd	78.92d	14.99d	18.2	208.2
5	165.61dd	51.49dd	5.72dd	42.5	11.0
					9.6[e]
6	149.75dd	78.64d	-5.67d	17.3	164.7
7	150.10dd	78.51d	-13.64d	17.1	165.5
8	145.11dd	37.54d	9.45d	19.1	177.9
9	143.71dd	77.69d	23.31d	16.8	163.5
10	143.89dd	77.96d	31.60d	16.8	163.3
11	152.17dd	78.90d	-8.15d	16.5	174.2
12	148.91dd	58.02d	-13.59d	18.6	173.4
13	135.82dd	75.49d	22.12d	25.1	18.8
14	120.52dd	76.18d	39.40d	17.2	14.1

[a]Recorded as toluene solutions. [b]Chemical shift units: ppm. [c]Coupling constant units: Hz. [d]Abbreviations: s = singlet, d = doublet. [e] $^{3}J_{P_{Fe}\text{-}P_{Ir}}$

Table 3.3: Infrared Spectral Data for Complex 2 and Derivatives

Complex	ν_{CO} (cm^{-1})[a]
1[b]	2051(s),[c] 1979(s), 1943(s,br), 1910(w)
2	1987(m), 1951(s), 1926(s,br), 1887(w), 1878(w)
5	2072(m), 2039(s), 2020(s), 1992(sh), 1979(s,br)
6	1979(m), 1943(s), 1914(s,br), 1888(s), 1871(sh)
7	1978(w), 1944(s), 1917(s,br), 1891(sh), 1875(sh)
8	1986(w), 1948(s), 1921(s,br), 1879(sh)
9	1983(m), 1945(s), 1918(s,br), 1884(s)
10	1985(m), 1947(s), 1922(s,br), 1885(s)
11	1985(m), 1950(s), 1925(vs), 1888(m,br)
12	1983(m), 1948(s), 1921(s,br), 1894(sh), 1875(sh)
14	1961(m), 1930(s,br), 1886(s,br), 1811(m,br)

[a]Recorded in CH_2Cl_2 solutions unless otherwise specified.
[b]Recorded in *n*-hexane solution.
[c]Abbreviations: w = weak, m = medium, s = strong, br = broad, sh = shoulder.

3.5 Phosphine Substitution Reactions

Complex **2**, as was shown in Section 3.4, is inert to substitution of the Fe-Ir dative bond and oxidative addition at the Ir centre. We therefore chose to study phosphine substitution reactions of **2** for two reasons. Firstly, by substituting other phosphines for PPh_3 we could determine whether this variation affects only the substituted metal or whether the complex acts as a bimetallic entity in which this perturbation affects both metals. Secondly, by substituting for PPh_3 by more bulky phosphines the possibility exists for the generation of coordinative unsaturation at one of the metal centres due to steric restrictions. Infrared spectroscopy should provide a good indication of the electronic effects, that is, whether both metals or only one is affected by the substitution. $^{31}P\{^1H\}$ nmr can be used to monitor the sites of reaction. A coordination shift of 15-30 ppm should occur on going from the free to the coordinated phosphine, thus indicating that substitution has taken place.

Complex **2** reacts with several phosphines in a 2:1 ratio to produce phosphine substitution products. When reactions were performed at a 1:1 molar ratio mixtures resulted, in which only half of the starting material reacted with the phosphine ligand. This is probably due to a solution equilibrium between **2** and the substitution product. A 100% excess of PR_3 was added to drive the reaction to the formation of product. The $^{31}P\{^1H\}$ nmr spectra were very similar to that of complex **2** shown in Figure 3.2. Substitution patterns were followed by noting the change in chemical shifts of the phosphines on Fe and Ir, where a

chemical shift change of 10-20 ppm for the phosphine on a particular metal indicated that substitution had occurred at that metal.

One would expect more basic PR_3 groups to easily substitute for PPh_3, especially when the cone angles of the incoming phosphines are smaller than that of PPh_3, since this would also reduce any steric congestion in the coordination sphere. The phosphines PEt_3, P*n*-Bu_3, PCy_3, P*i*-Pr_3, and PBz_3 all substituted cleanly for PPh_3 on Ir to form complexes **6**, **7**, **9**, **10**, and **11**, respectively. Data in Table 3.4 show that all of these phosphines are more basic than PPh_3, although PBz_3 has approximately the same basicity as PPh_3. For the most part substitution for PPh_3 by PR_3 occurred at Ir, probably due to reduced steric hindrance at Ir as compared to Fe. There were exceptions to this observation, noted below.

Exceptions to substitution at Ir occur for the complexes **8** and **12**, in which PMe_2Ph and PPh_2Me respectively have substituted for PPh_3. Complex **8** is the only compound for which substitution has occurred exclusively at Fe. PMe_2Ph has the smallest cone angle, at 122°, and therefore substitution at Fe is probably not unexpected. The fact that the other phosphines used in this series, all more basic than PPh_3, substitute at Ir is probably due to less overall steric congestion at Ir as compared to Fe.

Complex **12** is anomalous in this series of substitution reactions because substitution occurs at both metals rather than just one. This may be because PPh_2Me is only slightly less bulky than PPh_3, and is of approximately the same basicity. All of the substitution products are a result of both steric and electronic properties, and both must be considered in order to explain the site of substitution.

Table 3.4: Electronic Parameters, Cone Angles[31], and Phosphorous Chemical Shifts of the Various Phosphines Used in this Study.

PR_3	ν^a (cm^{-1})	cone angle, θ, (degrees)	δPR_3 (ppm)[59]
PPh_3	2068.9	145	-6.6
PEt_3	2061.7	132	-20.0
P*n*-Bu_3	2060.3	132	-32.3
PMe_2Ph	2065.3	122	-46.0
PCy_3	2056.4	170	+7.0
P*i*-Pr_3	2059.2	160	+19.3
PBz_3	2066.4	165	-12.9
PPh_2Me	2067.0	136	-28.0

[a]Electronic Parameter: the A_1 carbonyl mode of $Ni(CO)_3L$ in CH_2Cl_2.

An interesting point to note regarding the infrared spectra of the substitution products is that, regardless of which metal centre undergoes the phosphine substitution reaction, all of the CO stretching bands shift to lower wavenumbers by approximately the same amount. This would indicate that the molecule is behaving more like a single entity rather than two separate metal centres. An explanation for this behaviour may be that the change in electron density, due to the substitution of more basic phosphines for PPh_3, is dispersed over both metals, affecting the entire molecule. A sample IR spectrum of $(CO)_3(PPh_3)Fe(\mu\text{-}PCy_2)Ir(PEt_3)(CO)_2$ is shown in Figure 3.8, where it can be seen that the first three bands retain their general pattern and the last two weak bands have become more weak. For other substitution products such as those containing PPh_2Me, PCy_3, and P*i*-Pr_3 these last two bands may overlap.

Finally, it should be noted that although two moles of phosphine are added to drive the reaction to completion, only one final product is ever obtained. Multiple substitution is seen only for the PPh_2Me product, but not for any other phosphine. We do not see cleavage of the metal-metal bond, which may occur, although it was shown to be

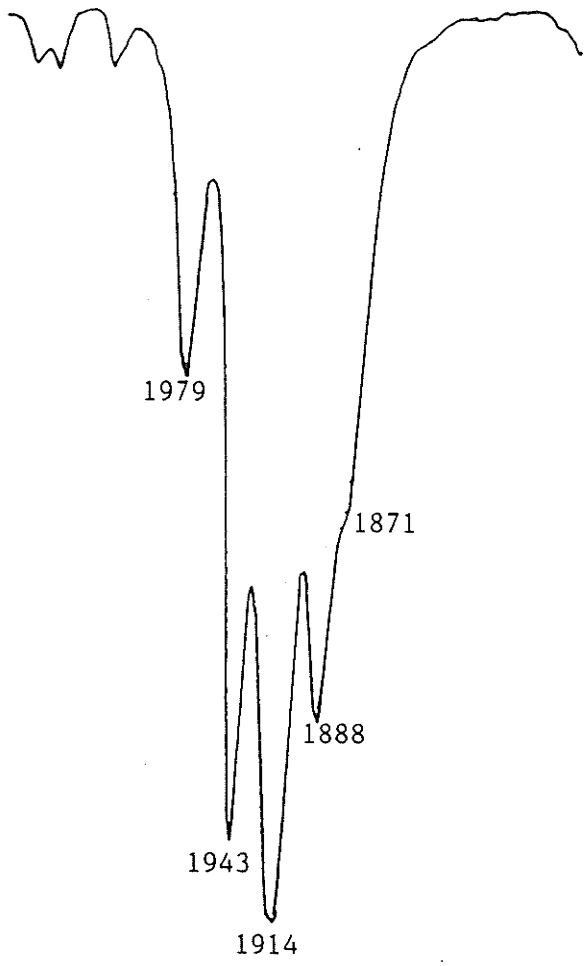

Figure 3.8: Infrared spectrum of complex 6, $(CO)_3(PPh_3)Fe(\mu\text{-}PCy_2)Ir(PEt_3)(CO)_2$ in CH_2Cl_2. Peaks are labelled in units of cm^{-1}.

unlikely from other addition reactions already performed. There is also no evidence of phosphine exchange at room temperature on the ^{31}P nmr time scale, since all $^{31}P\{^{1}H\}$ nmr spectra recorded showed well resolved peaks.

Unfortunately, none of the phosphine substitution products prepared thus far are coordinatively unsaturated, and therefore the same problem with unreactivity that existed for complex **2** is likely to occur with these compounds. However, $(CO)_3(PPh_3)Fe(\mu\text{-}PCy_2)Ir(PCy_3)(CO)_2$, **7**, contains the very bulky PCy_3 ligand, which has a cone angle of 170°, at Ir. It might be possible to eliminate CO thermally to produce a complex which is coordinatively unsaturated at Ir, and which would be stabilized by the large PCy_3 and μ-PCy_2 ligands. Conversion of **7** to the coordinatively unsaturated complex **14** was afforded by heating **7** to drive off CO. Since it proved difficult to isolate **7** free of phosphine contamination, **14** was prepared by reacting **2** with two equivalents of PCy_3 and heating this mixture. The $^{31}P\{^{1}H\}$ nmr spectrum of **14** showed a *cis* arrangement for the μ-PCy_2 and PCy_3 groups, indicating that CO had been lost. Isolation of pure material was difficult and complex **14** therefore could not be used for large scale reaction studies.

3.6 Preparation and Characterization of $(CO)_4Fe(\mu\text{-}PCy_2)Ir(COD)$ (3)

We have shown that the generation of coordinatively unsaturated complexes via **2** from Vaska's compound, although possible, is relatively impractical. Complex **3** is coordinatively unsaturated at

Ir, and 1,5-COD is easily displaced by PR_3 and CO. This complex is therefore more likely to undergo reactions than was complex **2**.

Complex **3** was prepared in the usual manner, by reacting $2Li[Fe(CO)_4(PCy_2)]$ with $[IrCl(COD)]_2$ at 0°C, resulting in an intense red-brown oil which decomposed above 0°C in both the solid state and in solution. It was therefore prepared and used in situ in reactions with various reagents (*vide infra*). $^{31}P\{^1H\}$ nmr showed only one product, indicating that complex **3** had been prepared in quantitative yield. Equations 3.6 and 3.7 outline the synthesis of complex **3**.

$$2\ Fe(CO)_4(PCy_2) + 2\ n\text{-BuLi} \longrightarrow 2\ Li[Fe(CO)_4(PCy_2)] + 2\ n\text{-BuH} \quad (3.6)$$

$$2\ Li[Fe(CO)_4(PCy_2)] + [IrCl(COD)]_2 \longrightarrow 2\ (CO)_4Fe(\mu\text{-}PCy_2)Ir(COD) + 2\ LiCl \quad (3.7)$$

$^{31}P\{^1H\}$ nmr and infrared spectral data for complex **3** are shown in Tables 3.5 and 3.6 respectively. The $^{31}P\{^1H\}$ nmr spectrum of **3** at 220K shows one single resonance at δ201.39 ppm due to the μ-PCy_2 ligand. As explained in Section 2.3, this downfield shift is probably indicative of the presence of a metal-metal bond between Fe and Ir. The chemical shift value for the bridging ligand is not unexpected in comparison to $(MeCp)(CO)_2Mn(\mu\text{-}t\text{-}Bu_2P)Ir(COD)$[21], with a chemical shift of δ184.9 ppm for the bridging ligand. The infrared spectrum of **3** shows bands assignable to terminal CO's only. We would expect, with C_{2v} symmetry at the Fe atom, to see four bands in the infrared spectrum, but instead six bands are seen. This could possibly be due to the formation of different isomers in solution at room temperature,

though the $^{31}P\{^{1}H\}$ nmr spectrum at 220K gives no evidence of this. Jones[10] also observed additional ν_{CO} bands for $(MeCp)(CO)_2Mn(\mu\text{-}t\text{-}Bu_2P)M(COD)$ (M = Ir, Rh), where three ν_{CO} bands for each complex were observed, when only two CO molecules were present. This was explained by Jones as the formation of isomers with and without semi-bridging carbonyls. However, Geoffroy[50b] did observe the expected number of bands for the complexes $(CO)_4M(\mu\text{-}PPh_2)_2Ir(H)(COD)$ (M = W, Mo, Cr), and for $(CO)_3Fe(\mu\text{-}PPh_2)Ir(Cl)(COD)$, four and three bands, respectively.

Table 3.5: $^{31}P\{^{1}H\}$ NMR Data[a] for Complex 3 and Derivatives.

Complex	$\delta(\mu\text{-}PCy_2)$[b]	$\delta(P_{Fe})$	$\delta(P_{Ir})$	$^2J_{\mu P-P_{Fe}}$[c]	$^2J_{\mu P-P_{Ir}}$	$^2J_{P_{Fe}-P_{Ir}}$
3	201.39s[d]					
15	160.75s					
16	125.74d		22.97d		170.0	
17	151.92dd	60.8d	-4.24d	12.2	163.4	
18a	28.50dd	87.13d	22.42d	40.1	8.5	
18b	148.02dd	69.83d	1.14d	25.5	175.0	
19a	167.31dd	73.39dd	25.60dd	29.4	204.1	87.2
19b	186.35dd	62.15dd	-3.27dd	26.3	171.3	67.7
19c	139.39	54.50	8.80	not resolved		
20	130.06s					

[a]Recorded as toluene solutions. [b]Chemical shift units: ppm. [c]Coupling constant units: Hz. [d]Abbreviations: s = singlet, d = doublet.

Table 3.6: Infrared spectral Data for Complex 3 and Derivatives.

Complex	ν_{CO} (cm^{-1})[a]
3	2012(s)[b], 2000(s), 1982(s), 1962(w), 1939(w), 1920(w)
15	2082(w), 2037(s), 2012(s), 1998(s), 1967(w), 1940(w), 1919(w), 1849(w), 1824(w)
16	2047(w), 1998(m), 1957(s), 1943(s,br), 1889(sh)
17	2078(sh), 2053(sh), 2036(sh), 2013(s), 2000(s), 1980(m), 1961(sh), 1941(sh)

[a]Recorded as *n*-hexane solutions. [b]Abbreviations: s = strong, m = medium, w = weak, br = broad, sh = shoulder.

3.7 Preparation and Characterization of Substitution Products of Complex 3

Complex **3** was prepared specifically because it can be synthesized by a direct route, resulting in a molecule that is coordinatively unsaturated at the Ir centre, and because it contains a 1,5-COD ligand on Ir which is generally labile. When complex **3** is reacted with various reagents, reactions can occur a) at the coordinatively unsaturated Ir centre, b) to displace the 1,5-COD ligand, or c) at the metal-metal bond. $^{31}P\{^{1}H\}$ nmr and infrared spectral data for complex **3** and derivatives of **3** are in Tables 3.5 and 3.6 respectively.

Complex **3** was stirred as a toluene solution under one atmosphere CO for 30 minutes, whereupon the solution changed colour from intense red-brown to red. The $^{31}P\{^{1}H\}$ nmr spectrum of complex **15** under N_2 showed a single peak at δ160.75 ppm, indicating that the metal-metal bond was retained. When the ^{31}P nmr spectrum of **15** under one atmosphere of CO is recorded no other peaks are observed, indicating that the metal-metal bond is retained under excess CO. $^{13}C\{^{1}H\}$ nmr under N_2 indicates that free 1,5-COD is present in solution, and we conclude that at room temperature under one atmosphere CO the 1,5-COD ligand is replaced by three CO's. The infrared spectrum of **15** shows ν_{CO} bands due to terminal CO's (2082 to 1919 cm^{-1}) and bands at 1849 and 1824 cm^{-1}, which may be due to semi-bridging or terminal CO's. Comparing infrared spectra of **3** and its CO adduct **15** indicates that the band at 1982 for **3** is no longer present in **15**; instead new bands appear at 1967, 1849, and 1824 cm^{-1}. The proposed structure of this

complex is shown in Figure 3.9.

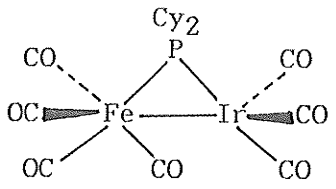

Figure 3.9: Proposed structure of complex 15.

We also attempted to displace 1,5-COD by PCy_3 and CO in hopes of preparing a coordinatively unsaturated compound. When an equimolar amount of PCy_3 is stirred with **3** under one atmosphere CO, a slight colour change from red-brown to orange-brown is observed. $^{31}P\{^1H\}$ nmr shows two doublets at δ125.74 ppm and δ22.97 ppm due to μ-PCy_2 and PCy_3 ligands respectively, when the spectrum is recorded under N_2. The coupling constant of 170.1 Hz between the bridging phosphide and terminal phosphine indicates *trans* geometry. If the 1,5-COD ligand is displaced, then the expected structure of **16** would be that shown in Figure 3.10. If complex 16 is maintained under a CO atmosphere and the $^{31}P\{^1H\}$ nmr spectrum recorded, peaks due to complex **16** and complex **15** are observed. There are no peaks attributable to a complex where the metal-metal interaction has been lost due to additional substitution by CO, and there are no other resonances due to othre PCy_3-substituted species. Therefore, we can conclude that **16** is coordinatively saturated at Ir, as in Figure 3.10.

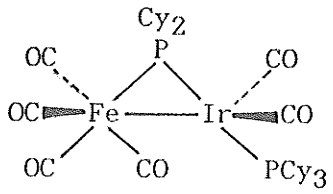

Figure 3.10: Structure of Complex 16.

The 1,5-COD ligand can also be replaced by uni- and bidnetate phosphines to form complexes comparable to compound **2** and its phosphine-substituted derivatives. Complex **17**, $(CO)_3(PEt_3)Fe(\mu\text{-}PCy_2)Ir(PEt_3)(CO)_2$, is synthesized by reacting **3** with two molar equivalents of PEt_3 at 60°C. Displacement of 1,5-COD occurs, followed by rearrangement of the phosphine ligands. The $^{31}P\{^1H\}$ nmr spectrum of **17** has a similar pattern to that of complex **2**; a doublet of doublets at δ159.9 ppm due to $\mu\text{-}PCy_2$, a doublet at δ60.8 ppm due to $PEt_3(Fe)$, and a doublet at δ-4.2 ppm due to $PEt_3(Ir)$. The $^2J_{\mu P-P_{Ir}}$ coupling constant of 163.4 Hz indicates *trans* geometry. A *trans* coupling constant between the bridging phosphide and the terminal phosphine on Ir would also indicate that **17** is coordinatively saturated, since for the coordinatively unsaturated complexes **13** and **14** the phosphine on Ir shifted to a *cis* position on loss of CO. Additional CO molecules may be present in the form of unreacted starting material, $Fe(CO)_4(PCy_2H)$, and therefore the formation of the coordinatively saturated complex **17**, $(CO)_4Fe(\mu\text{-}PCy_2)Ir(PCy_3)(CO)_2$, while not desired, is also not unexpected.

The $^{31}P\{^1H\}$ nmr spectrum of **17** is comparable to that of complex **6**, $(CO)_3(PPh_3)Fe(\mu\text{-}PCy_2)Ir(PEt_3)(CO)_2$. The chemical shifts for the

bridging phosphides differ by two ppm, δ151.9 ppm for **17**, and δ149.7 ppm for **6**. Similarly, the difference in chemical shifts for PEt_3(Ir) is 1.5 ppm; δ-4.2 ppm for **17** and δ-5.7 ppm for **6**. We can conclude then, solely on the basis of $^{31}P\{^1H\}$ nmr data, that the structure of complex **17** is similar to that of the related complex **6**.

The infrared spectrum of complex **17** also has a very similar form to that of complex **6**. Five bands at 2003, 1958, 1943, 1912, and 1886 cm^{-1} due to terminal CO's would indicate that **17** is coordinatively saturated. With the exception of the first, the positions of all of the bands for **17** are also simialr to those for **6**. The proposed structure of complex **17** is shown in Figure 3.11 below.

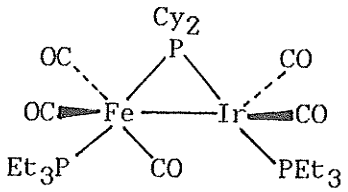

Figure 3.11: Proposed structure of complex 17, $(CO)_3(PEt_3)Fe(\mu\text{-}PCy_2)Ir(PEt_3)(CO)_2$.

When complex **3** was stirred at room temperature with one molar equivalent of the bidentate phosphine dppe, two compounds were formed. $^{31}P\{^1H\}$ nmr data indicated that the dppe moeity was in a bridging mode between the two metal atoms, not chelated solely to the Ir atom. Complex **18a**, with $^{31}P\{^1H\}$ nmr chemical shifts of δ28.5 ppm (doublet of doublets) for the bridging phosphide, δ87.1 ppm (doublet) due to the phosphine at Fe, and δ22.4 ppm (doublet) due to the phosphine at Ir,

does not have a metal-metal interaction. This is the first time that loss of the metal-metal bond has been observed for any Fe-Ir complex in this system, and we believed complex **18a** to be the intermediate complex shown in Figure 3.12, en route to the formation of complex **18b**. The *cis* coupling constant between the bridging phosphide and the phosphine on Ir indicated that another ligand must be present on the Ir atom; we formulate complex **18a** as $(CO)_3Fe(\mu\text{-}PCy_2)(\mu\text{-}dppe)Ir(CO)(COD)$.

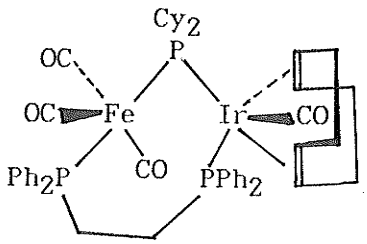

Figure 3.12: Structure of complex 18a, the only Fe-Ir complex in this study where cleavage of the metal-metal bond has occurred.

Complex **18b** was then generated by heating the solution of **3** and dppe to 60°C for three hours. $^{31}P\{^1H\}$ nmr indicates that only complex **18b**, $(CO)_3Fe(\mu\text{-}PCy_2)(\mu\text{-}dppe)Ir(CO)_2$ has been formed. The $^{31}P\{^1H\}$ nmr spectrum of 18b is similar to that of complex **2** and its phosphorous substitution derivatives: a doublet of doublets at δ148.0 ppm due to $\mu\text{-}PCy_2$, a doublet at δ69.8 ppm due to phosphine on Fe, and a doublet at δ1.1 ppm due to phosphine on Ir. There is no evidence of a complex containing a chelating bidentate phosphine ligand; dppe bridges both metal atoms. The *trans* coupling constant of 175 Hz between bridging phosphide and phosphine on Ir would seem to indicate that coordinative

saturation exists at the Ir centre. The additional CO ligand again has probably come from $Fe(CO)_4(PCy_2H)$.

The $^{31}P\{^1H\}$ nmr spectrum for **18b** can be compared to that of complex **12**, $(CO)_3(PPh_2Me)Fe(\mu\text{-}PCy_2)Ir(PPh_2Me)(CO)_2$. The chemical shifts of $\mu\text{-}PCy_2$ are approximately the same for both compounds, which may indicate that the bridging phosphide has approximately the same environment in both complexes. However, in complex **12** the phosphine on Fe resonates at slightly higher field (δ58.0 ppm) than that of **18b** (δ69.8 ppm), similar to the phosphine on Ir: δ-13.6 ppm for **12**, δ-1.1 ppm for **18b**. These differences may arise because of a ring effect that exists for the bridging dppe ligand. The similarity in the $^{31}P\{^1H\}$ nmr spectra of the complexes would therefore indicate a similarity between their structures.

Infrared spectral data for **18b** indicate that five CO molecules are present, since five ν_{CO} bands arise. The shape of the spectrum and ν_{CO} band positions are very similar to those of complex **12**, with the exception of the band at highest energy, which is approximately 20 cm^{-1} higher than the highest energy band for **12**. This observation also occurred for complex **17** compared to complex **6**. The proposed structure of compound **18b** is shown in Figure 3.13.

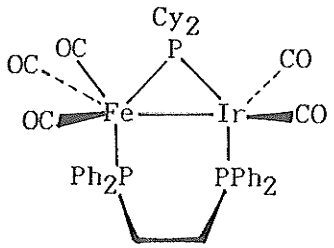

Figure 3.13: Proposed strucutre of complex 18b, $(CO)_3Fe(\mu\text{-}PCy_2)(\mu\text{-dppe})Ir(CO)_2$.

Finally, complex **3** was also reacted with the more constrained bindentate phosphine dppm, resulting in the fomration of three complexes, **19a**, **b**, and **c**, shown in Figure 3.14. The $^{31}P\{^{1}H\}$ nmr spectrum indicates that in all three complexes dppm is bridging the two metal atoms, not chelating to one or the other, similar to the situations for complexes **18a** and **18b**. Heating the mixture to 60°C for three hours does not drive the reaction to the formation of one product. The $^{31}P\{^{1}H\}$ nmr spectrum of this system indicates that complex **19a** probably still has 1,5-COD ligated to Ir. Direct comparison of ^{31}P nmr data for **19a** and complex **12** indicates a large difference in both chemical shift for the phosphine ligands on Ir and the $^{2}J_{\mu P-P_{Ir}}$ coupling constants: for **12**, a chemical shift of δ-13.6 ppm as compared to δ25.6 ppm for **19a**, and $^{2}J_{\mu P-P_{Ir}}$ coupling constants of 173 Hz for **12**, 204 Hz for **19a**.

Compound **19a** is probably the precursor for compound **19b**. In **19a**, dppm has displaced CO on Fe and added at Ir. Complex **19b** shows substitution of two CO molecules for 1,5-COD at Ir. The $^{31}P\{^{1}H\}$ nmr spectrum of **19b** as compared to that of **12** is very similar, both in chemical shifts of the phosphines and in phosphide-phosphine coupling constants. However, the chemical shifts for the bridging phosphides differ by almost 40 ppm: δ186.4 ppm for **19b**, δ148.9 ppm for **12**. This large shift difference is probably due to the ring constraint of dppm, which was not seen to the same extent for **18b** when dppe was the bridging ligand. Complexes **18b** and **19b** have very similar $^{31}P\{^{1}H\}$ nmr spectra, and the formulation of **19b** as a coordinatively saturated compound is not unreasonable.

The $^{31}P\{^{1}H\}$ nmr spectrum of **19c** is not fully resolved, even at

220K. The formulation of **19c** is tentatively proposed as $(CO)_3Fe(\mu\text{-}PCy_2)(\mu\text{-dppm})Ir(CO)$, shown in Figure 3.14, since the chemical shift for the phosphine on Fe is similar to that of **12**. However, the phosphine on Ir has shifted further downfield in comparison to **12**, indicating that this centre may be coordinatively unsaturated.

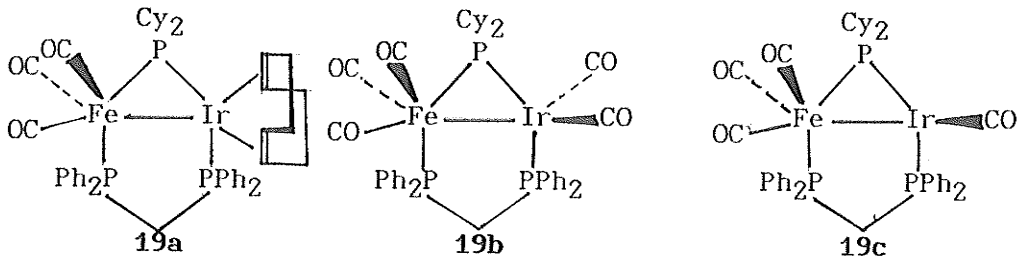

Figure 3.14: Proposed structures of complexes 19a, b, and c.

3.8 Preparation and Characterization of $(CO)_4Fe(\mu\text{-}PCy_2)Ir(THF)_x$ (20). Hydrogenation of Styrene by Complex 3.

It has been shown by Osborn[60] that in coordinating solvents such as acetone, ethanol, or THF, the complexes $[M(COD)L_2]ClO_4$ (M = Rh, Ir; L = tertiary phosphine) react with H_2 to give the isolable complexes $[MH_2L_2S_2]ClO_4$ (S = solvent). Crabtree[61] has also shown that in CH_2Cl_2 the complexes $[Ir(COD)L_2]PF_6$ (L = PPh_2Me, PPh_3) in the presence of a suitable substrate alkene under H_2 at 0°C become highly active catalysts for alkene hydrogenation. Complex **3** is similar to these complexes, and in order to determine if **3** is useful as a hydrogenation catalyst, it was reacted with one atmosphere H_2 in THF, a polar

coordinating solvent. $^{31}P\{^{1}H\}$ nmr shows one singlet at δ130.06 ppm, whether the sample is maintained under H_2 or N_2. $^{13}C\{^{1}H\}$ nmr does not show any resonances due to 1,5-COD, but sharp peaks at δ68.0 ppm and δ25.7 ppm do arise, attributed to coordinated THF. ^{1}H nmr shows no evidence for a metal hydride. However, all peaks in the ^{1}H nmr spectrum are extremely broad and unresolved, which may indicate that some type of fluxionality exists in complex **20**.

We assumed from nmr evidence that when complex **3** was reacted with H_2, 1,5-COD was hydrogenated to cyclooctane. Since we did not observe any high field resonances in the ^{1}H spectrum, even at 220K, we also assumed that THF had filled the open coordination sites on Ir. The ability of complex **3** to hydrogenate other molecules was tested by maintaining complex **3** under one atmosphere H_2 with one gram of styrene. Samples of the reaction solution were removed at specific time periods and subjected to GC-MS analysis to monitor the results. The peaks due to styrene and resultant ethyl benzene were integrated; results of this experiment are shown in Figure 3.15.

Complex **3** does catalyze the hydrogenation of styrene to ethyl benzene under one atmosphere H_2 at 23°C. Turnover numbers are of the ortder of 5.5 hr^{-1}. The turnover number is defined as the number of moles of product per mole of catalyst per hour[62]. For example, at 150 minutes, 55 x 10^{-2} mmoles ethyl benzene were produced. This is equal to 0.22 mmoles ethyl benzene produced per hour; dividing by mmoles of **3** (0.04) gives the turnover number of 5.5 h^{-1}. After three hours the amount of ethyl benzene produced failed to increase, presumably due to deactivation of the catalyst.

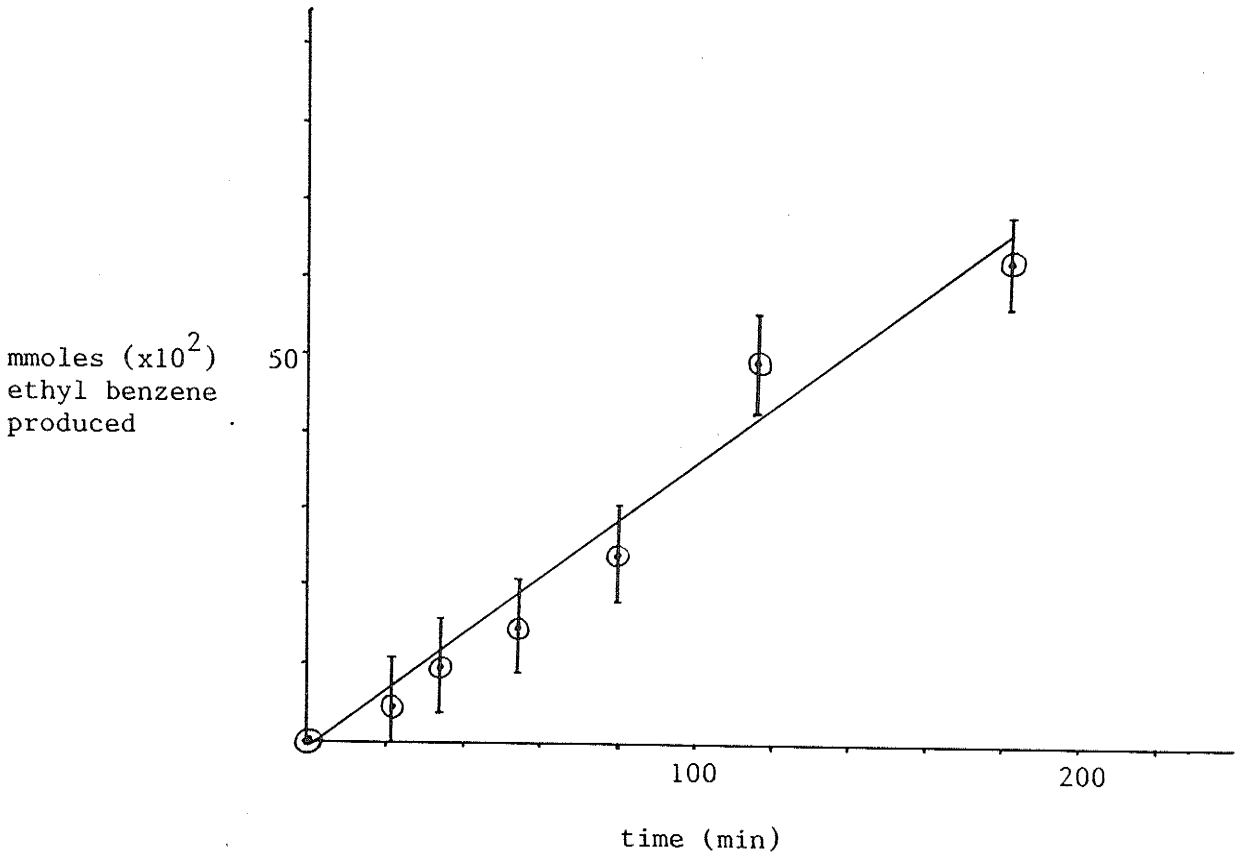

Figure 3.5: Least-squares plot of mmoles ethyl benzene produced over time in the hydrogenation of styrene by $(CO)_4Fe(u\text{-}PCy_2)Ir(COD)$.

3.9 Summary and Conclusions

In this chapter, the synthesis and reactivity of two singly-bridged complexes were investigated: $(CO)_3(PPh_3)Fe(\mu\text{-}PCy_2)Ir(PPh_3)(CO)_2$, complex **2**, and $(CO)_4Fe(\mu\text{-}PCy_2)Ir(COD)$, complex **3**. Complex **2** did not undergo oxidative-addition, nor did it undergo addition reactions with molecules such as CO or *t*-BuCN. However, by using a strong acid, HBF_4-etherate, the Ir centre was protonated. By reacting complex **2** with various phosphines to form substitution products, it was shown that the entire $(CO)_3(PPh_3)Fe(\mu\text{-}PCy_2)Ir(PPh_3)(CO)_2$ molecule was affected by substitution, rather than affecting only the site of substitution. The added phosphine generally displaced PPh_3 on Ir due to higher basicities of the incoming phosphines and fewer steric restrictions at Ir. However, there were exceptions, in the cases of PPh_2Me, which displaced PPh_3 on both Fe and Ir, and PMe_2Ph, which displaced PPh_3 on Fe only.

The unreactivity of complex **2** was believed to be due to the coordinative saturation that existed at both metals centres. Attempts to remove CO or to prepare a coordinatively unsaturated complex by reacting **2** with a bulky phosphine and heating the mixture resulted in side products and contamination by phosphine. Therefore, in order to alleviate problems with contaminants, the coordinatively unsaturated complex **3** was prepared by a direct route. In reactions with CO, or PCy_3 and CO, the 1,5-COD ligand was easily displaced at room temperature and under one atmosphere CO without formation of side products. Therefore it may prove to be relaitvely straightforward to

thermally displace CO from either of these two complexes, to generate coordinative unsaturation at Ir.

When complex **3** was reacted with H_2, one product resulted, which we believed to be $(CO)_4Fe(\mu\text{-}PCy_2)Ir(THF)_x$, **20**, from nmr evidence. Since **20** hydrogenated 1,5-COD to cyclooctane, we attempted the catalytic hydrogenation of styrene, and found turnover numbers to be of the order of 5.5 hr^{-1}. While this number is low, it does show that a bimetallic Fe-Ir system is capable of catalytic hydrogenation.

CHAPTER FOUR

SINGLY-BRIDGED COMPLEXES OF Fe-Rh

4.1 Introduction

The reactivity of singly-bridged dicyclohexylphosphido complexes is greater than that of doubly-bridged species, as we observed in Chapter Three. Coordinative unsaturation at Ir in the complex $(CO)_4Fe(\mu\text{-}PCy_2)Ir(COD)$ facilitated the hydrogenation of styrene to ethyl benzene. However, the Fe-Ir system was a relatively poor catalyst in comparison to mononuclear Rh catalysts such as $RhCl(PPh_3)_4$[63] and $[Rh(COD)(PR_3)_2]ClO_4$[60]. Since Rh is a less basic metal than Ir, it is more likely to be coordinatively unsaturated and therefore is more likely to undergo oxidative-addition and general addition reactions.

In this chapter, we take the same approach as in Chapter Three to synthesize coordinatively unsaturated Fe-Rh compounds. Complex **1**, $(CO)_3(PPh_3)Fe(\mu\text{-}PCy_2)Rh(PPh_3)(CO)$, shown in Figure 4.1, is prepared by reacting *trans*-$RhCl(CO)(PPh_3)_2$[64] with $Li[Fe(CO)_4(PCy_2)]$ using the bridge-assisted approach. Complex **2**, $(CO)_4Fe(\mu\text{-}PCy_2)Rh(COD)$, shown in Figure 4.17, is prepared by reacting $[RhCl(COD)$[65] with $2Li[Fe(CO)_4(PCy_2)]$ at -10°C. Both of these complexes, due to their coordinative unsaturation at Rh, should readily react with molecules

such as CO, PR_3, and H_2. Complex 2 should prove to be especially reactive, since 1,5-COD is easily displaced by incoming ligands. It should again prove interesting to investigate the effect the Fe atom has on the chemical reactivity of Rh.

4.2 Experimental

i) General

$Fe(CO)_4(PCy_2H)$[66], $RhCl(CO)(PPh_3)_2$[64], and $[RhCl(COD)]_2$[65] were prepared by literature methods. $Fe_2(CO)_9$, *t*-BuCN, MeI, PEt_3, 1,5-cyclooctadiene (COD), *n*-BuLi, PPh_3 (Aldrich), PCy_2H, $RhCl_3 \cdot 3H_2O$ (Strem) were purchased and used as received. Tetrahydrofuran (THF) and toluene were dried by distillation from Na-benzophenone ketyl under N_2. DMA·HCl was prepared by bubbling HCl through a benzene solution of dimethylacetamide (Eastman) under N_2 and washing the white precipitate with benzene. All reactions were conducted under an atmosphere of N_2 by standard Schlenk[35] techniques described in Section 2.3.

$^{31}P\{^1H\}$ nmr spectra were obtained at 121.5 Mhz on a Brüker AM300 spectrometer from 220-300K. Phosphorous chemical shifts were measured relative to H_3PO_4 with positive shifts downfield. Infrared spectra were recorded on a Perkin-Elmer 781 grating spectrometer. Elemental analyses were performed by Canadian Microanalytical Serivce Ltd., New Westminster, British Columbia, Canada.

ii) Preparation of $(CO)_3(PPh_3)Fe(\mu\text{-}PCy_2)Rh(PPh_3)(CO)$ (1)

n-BuLi (0.935 mL, 1.45 mmoles of 1.55 M solution in hexanes) was added via syringe to a brown solution of $Fe(CO)_4(PCy_2H)$ (0.530g, 1.45 mmoles) in THF (10 mL). This solution was stirred for 10 minutes then added dropwise to a yellow slurry of *trans*-$RhCl(CO)(PPh_3)_2$ (1.00g, 1.45 mmoles) in THF (10 mL) at 23°C. The resultant orange-brown solution was stirred for 24 hours at room temperature, then taken to dryness in vacuo. The remaining solid was extracted with toluene (4 x 5 mL), and the extractions were combined, reduced in volume to 10 mL, and cooled to -20°C for 24 hours to yield orange micorcrystals of product (0.94 g, 65%). Anal. calc'd. for $C_{52}H_{52}O_4P_3FeRh$: C, 62.87%; H, 5.29%. Found: C, 62.60%; H, 5.29%.

iii) Preparation of $(CO)_4Fe(\mu\text{-}PCy_2)Rh(COD)$ (2)

To a brown solution of $Fe(CO)_4(PCy_2H)$ (0.89 g, 0.243 mmoles) in THF (5 mL) was added *n*-BuLi (0.15 mL, 0.243 mmoles of 1.6M in hexanes). The solution turned dark brown on addition and was stirred at room temperature for 10 minutes. The solution was then cooled to -10°C and added dropwise to an orange solution of $[RhCl(COD)]_2$ (0.60 g, 0.122 mmoles) in 5 mL THF at -10°C. An immediate colour change from orange to very intense orange-brown was observed. Stirring was continued for three hours at -10°C, then the solution was taken to dryness in vacuo to leave a brown-black oil. Due to decomposition of the product above

-10°C in the solid state and in solution, complex **2** was prepared and used in situ.

iv) Reactions of $(CO)_3(PPh_3)Fe(\mu\text{-}PCy_2)Rh(PPh_3)(CO)$

a) Reaction of 1 with CO (Complexes 3a, 3b)

Complex **1** (0.050 g, 0.050 mmoles) was dissolved in toluene/ toluene-d_8 (1:1) (5 mL) and stirred under CO (one atmosphere) for 30 minutes. The solution darkened slightly from orange to orange-red. The $^{31}P\{^1H\}$ nmr spectrum was then recorded under CO atmosphere.

b) Reaction of 1 with PEt_3 (Complexes 4a-4d)

Complex 1 (0.050 g, 0.050 mmoles) was dissolved in toluene/ toluene-d_8 (1:1) (5 mL) and PEt_3 (0.0070 mL, 0.050 mmoles) was added. After stirring for 30 minutes the solution remained orange. The $^{31}P\{^1H\}$ nmr spectrum was then recorded.

c) Reaction of 1 with *t*-BuCN (Complexes 5a-5d)

Complex **1** (0.055 g, 0.055 mmoles) was dissolved in toluene/ toluene-d_8 (1:1) (5 mL) and *t*-BuCN (0.006 mL, 0.055 mmoles) was added. After 30 minutes no colour change in the solution was observed and the $^{31}P\{^1H\}$ nmr spectrum was then recorded.

d) Preparation of $(CO)_3(PPh_3)Fe(\mu\text{-}PCy_2)Rh(PPh_3)(H)_2$ (6)

Complex **1**, (0.050 g, 0.050 mmoles) was dissolved in toluene/ toluene-d_8 (1:1) (5 mL) and stirred under H_2 (one atmosphere) for 30 minutes. The solution darkened slightly from orange to orange-red. The $^{31}P\{^1H\}$ nmr spectrum was then recorded under H_2 atmosphere.

e) Preparation of $[(CO)_3(PPh_3)Fe(\mu\text{-}PCy_2)Rh(PPh_3)(Me)]^+[I]^-$ (7)

Complex **1** (0.050 g, 0.050 mmoles) was dissolved in toluene/ toluene-d_8 (1:1) (5 mL) and MeI (0.0030 mL, 0.050 mmoles) was added. After stirring for 10 minutes a red fluffy precipitate formed. The red solution was filtered into an nmr tube and the $^{31}P\{^1H\}$ nmr spectrum was recorded.

f) Preparation of $(CO)_4Fe(\mu\text{-}PCy_2)Rh(PPh_3)(H)(Cl)$ (8)

Complex **1** (0.050 g, 0.050 mmoles) was dissolved in toluene/ toluene-d_8 (1:1) (5 mL) and DMA•HCl (0.006 g, 0.050 mmoles) was added. After stirring for 30 minutes no colour change in the solution was observed and the $^{31}P\{^1H\}$ nmr spectrum was recorded.

v) Reactions of $(CO)_4Fe(\mu\text{-}PCy_2)Rh(COD)$

a) Reaction of 2 with CO

Complex 2, (0.150 g, 0.40 mmoles)was stirred under CO (one atmosphere) in toluene/toluene-d_8 (1:1) (5 mL) for 30 minutes, during which time the solution changed colour from very intense brown to red-brown. N_2 replaced CO and the $^{31}P\{^1H\}$ nmr spectrum was recorded.

b) Preparation of $(CO)_4Fe(\mu\text{-}PCy_2)Rh(PR_3)(CO)_2$ [R = Et (9), Cy (10)]

A toluene/toluene-d_8 (1:1) (4 mL) solution of **2** (0.100g, 0.264 mmoles) and one molar equivalent PR_3 were stirred under CO (one atmosphere) for 30 minutes. The solutions changed colour to orange-brown for PEt_3 and orange-red for PCy_3 within five minutes. After stirring for five hours the volume of the solution was reduced to approximately 3 mL and cooled to -20°C for 48 hours. This yielded orange microcrystals of **9** and orange-red microcrystals of **10**.

c) Reaction of 2 with H_2 (Complexes 11a-11c)

Complex 2, (0.150 g, 0.40 mmoles) was stirred under H_2 (one atmosphere) in toluene/toluene-d_8 (1:1) (5 mL) for 30 minutes, during which time the solution changed colour from very intense brown to red-brown. N_2 replaced H_2 and the $^{31}P\{^1H\}$ nmr spectrum was recorded.

4.3 Preparation and Characterization of $(CO)_3(PPh_3)Fe(\mu\text{-}PCy_2)Rh(PPh_3(CO)$, (1)

Complex **1** was prepared via the bridge-assisted method outlined in Chapter One and detailed below in Equation 4.1.

$$Li[Fe(CO)_4(PCy_2)] + \textit{trans}\text{-}RhCl(CO)(PPh_3)_2 \longrightarrow (CO)_3(PPh_3)Fe(\mu\text{-}PCy_2)Rh(PPh_3)(CO) + LiCl \qquad (4.1)$$

$Li[Fe(CO)_4(PCy_2)]$ was reacted with *trans*-$RhCl(CO)(PPh_3)_2$ in THF, and the reaction was assumed to be complete when all of the *trans*-$RhCl(CO)(PPh_3)_2$ had dissolved. Recrystallization from toluene yielded **1** as orange microcrystals in 65% yield. Complex **1** was found to be soluble in solvents such as toluene and CH_2Cl_2, but insoluble in most other organic solvents. It is air stable for short periods of time in the solid state, and decomposes rapidly in solution when exposed to air.

Complex **1** has been fully characterized by a single crystal X-ray diffraction study that showed the structure to be that in Figure 4.1. The $^{31}P\{^1H\}$ nmr spectrum of **1** (Figure 4.2) is fully consistent with the structure determined by X-ray diffraction. The doublet of doublets of doublets at δ167.2 ppm is attributed to the μ-PCy_2 ligand, which couples to both PPh_3(Fe) and PPh_3(Rh), as well as to the Rh atom. The downfield shift of this resonance is probably due to the presence of a metal-metal bond, and this is supported by X-ray crystallography. The doublet at δ78.0 ppm due to PPh_3(Fe) coupled to

Figure 4.2: $^{31}P\{^{1}H\}$ nmr spectrum of complex 1, $(CO)_3(PPh_3)Fe(\mu\text{-}PCy_2)Rh(PPh_3)(CO)$.

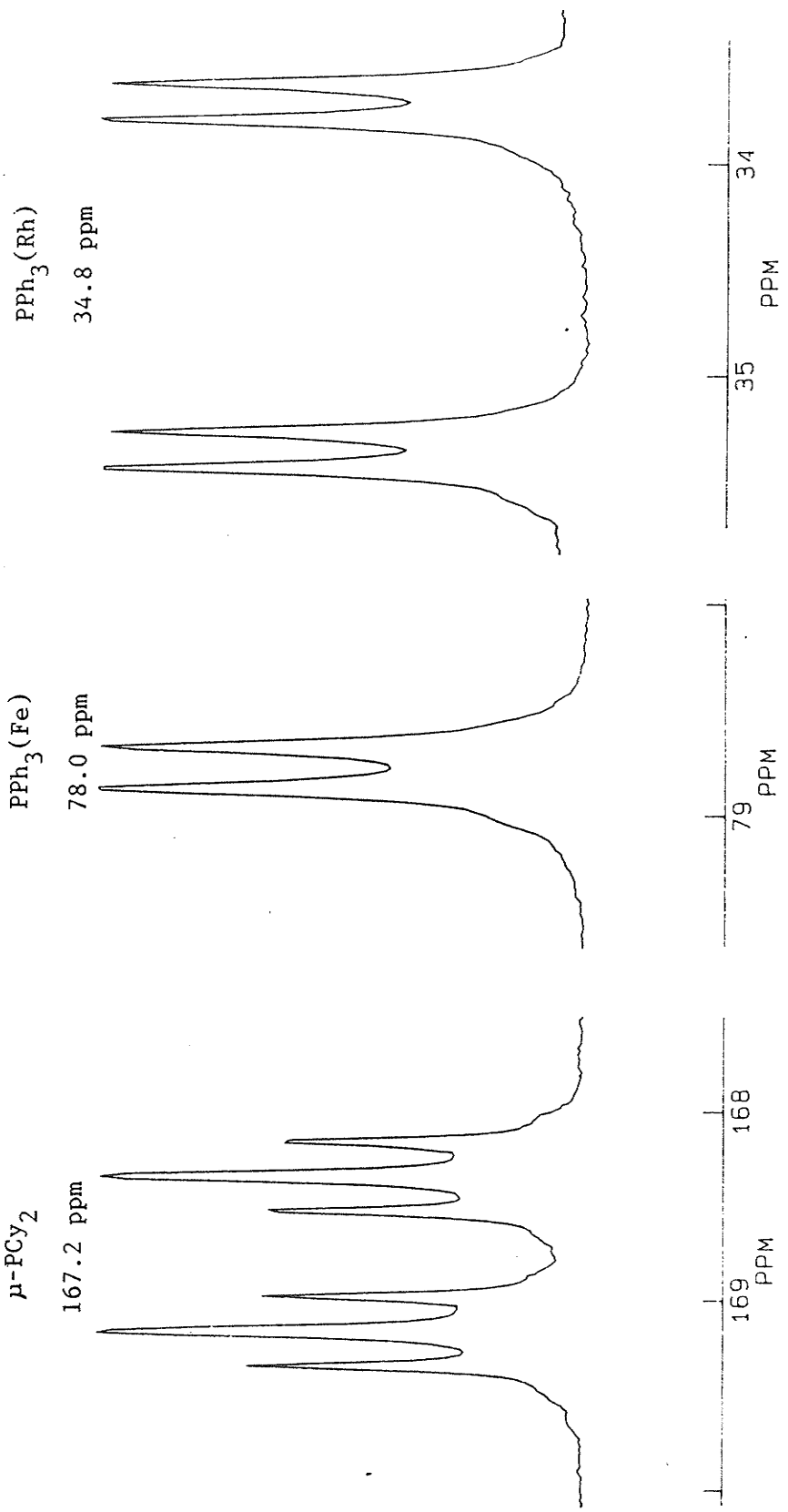
μ-PCy_2
167.2 ppm
PPh_3(Fe)
78.0 ppm
PPh_3(Rh)
34.8 ppm
169
168
PPM
79
PPM
35
34
PPM

μ-PCy_2 is in the expected region for phosphine ligands bonded to Fe^{57}, as was discussed in Chapter Three, and the doublet of doublets at δ34.8 ppm is assigned to PPh_3(Rh) coupled to μ-PCy_2 and Rh. The *cis* coupling between μ-PCy_2 and PPh_3(Rh) of 19.4 Hz is also consistent with the determined structure. $^{31}P\{^1H\}$ nmr data appear in Table 4.3.

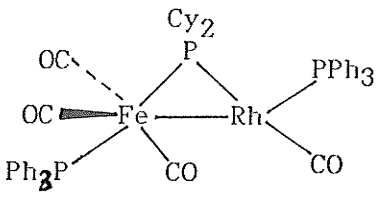

Figure 4.1: Structure of complex 1, $(CO)_3(PPh_3)Fe(\mu\text{-}PCy_2)Rh(PPh_3)(CO)$.

Table 4.1: Infrared Spectral Data for Complex 1

Complex	ν_{CO} (cm^{-1})[a]
1 (nujol)	1991(s), 1950(s), 1896(s), 1842(s)
1 (hexane)	2038(w), 1980(s), 1950(s), 1900(w)

[a]Abbreviations: s = strong, m = medium, w = weak.

The solid state IR spectrum shows the presence of a semi-bridging carbonyl, discussed in Section 4.5. In *n*-hexane solution all the ν_{CO} stretching bands have shifted to considerably higher wavenumbers so that the semi-bridging unit is no longer present. The presence of the semi-bridging carbonyl may in part be due to crystal packing forces which are not present when the molecule is in solution. Figure 4.3 shows both the solid state and solution spectra for comparison.

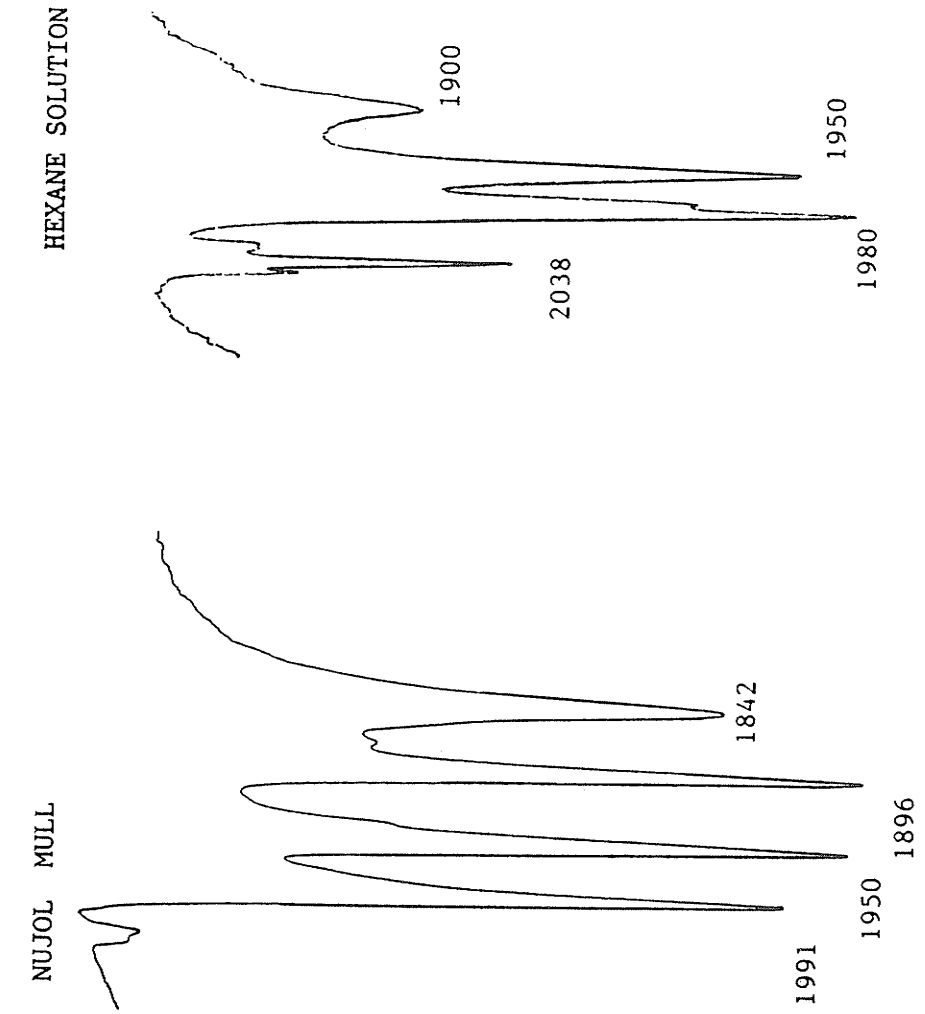

Figure 4.3: Infrared spectra of complex 1 in a) nujol, and b) n-hexane. Peaks are labelled in units of cm^{-1}.

4.4 X-Ray Crystal Structure of $(CO)_3(PPh_3)Fe(\mu\text{-}PCy_2)Rh(PPh_3)(CO)$ (1)

Orange crystals of **1** were grown by cooling a toluene solution to -20°C for 72 hours. A perspective view of **1** giving the atom numbering scheme is shown in Figure 4.4, and a representation of the inner coordination sphere of the molecule is shown, with relevant bond distances and angles, in Figure 4.5. The unit cell contains four discrete molecules of **1**. Table 4.2 gives other crystallographic parameters and data, collected and solved at the University of Windsor by D. W. Stephan.

Table 4.2: Summary of Crystal Data, Intensity Collection, and Structure Refinement for $(CO)_3(PPh_3)Fe(\mu\text{-}PCy_2)Rh(PPh_3)(CO)$ (1).

formula	$C_{52}H_{52}FeO_4P_3Rh$
crystal colour, form	orange blocks
a, Å	23.746(3)
b, Å	10.414(2)
c, Å	19.823(3)
β, degrees	100.91(1)
crystal system	monoclinic
space group	$P2_{1/c}$
volume, Å^3	4813(1)
ρ (calc'd), g/cm^3	1.37
Z	4
crystal dimensions, mm	0.63 x 0.48 x 0.44
μ, absorption coefficient, cm^{-1}	7.17
radiation (λ, Å)	MoKα (0.71069)
temperature, °C	24
scan speed, deg/min	2.0-5.0 (θ-2θ scan)
scan range, deg	1.0 below $K\alpha_1$, 1.0 above $K\alpha_2$
background/scan time ratio	0.5
data collected	6810
unique data ($F_o^2 > 3\sigma F_o^2$)	5041
number of variables	244
R, %	6.85
R_W, %	7.74

Figure 4.4: ORTEP of complex 1, showing the atom numbering scheme.

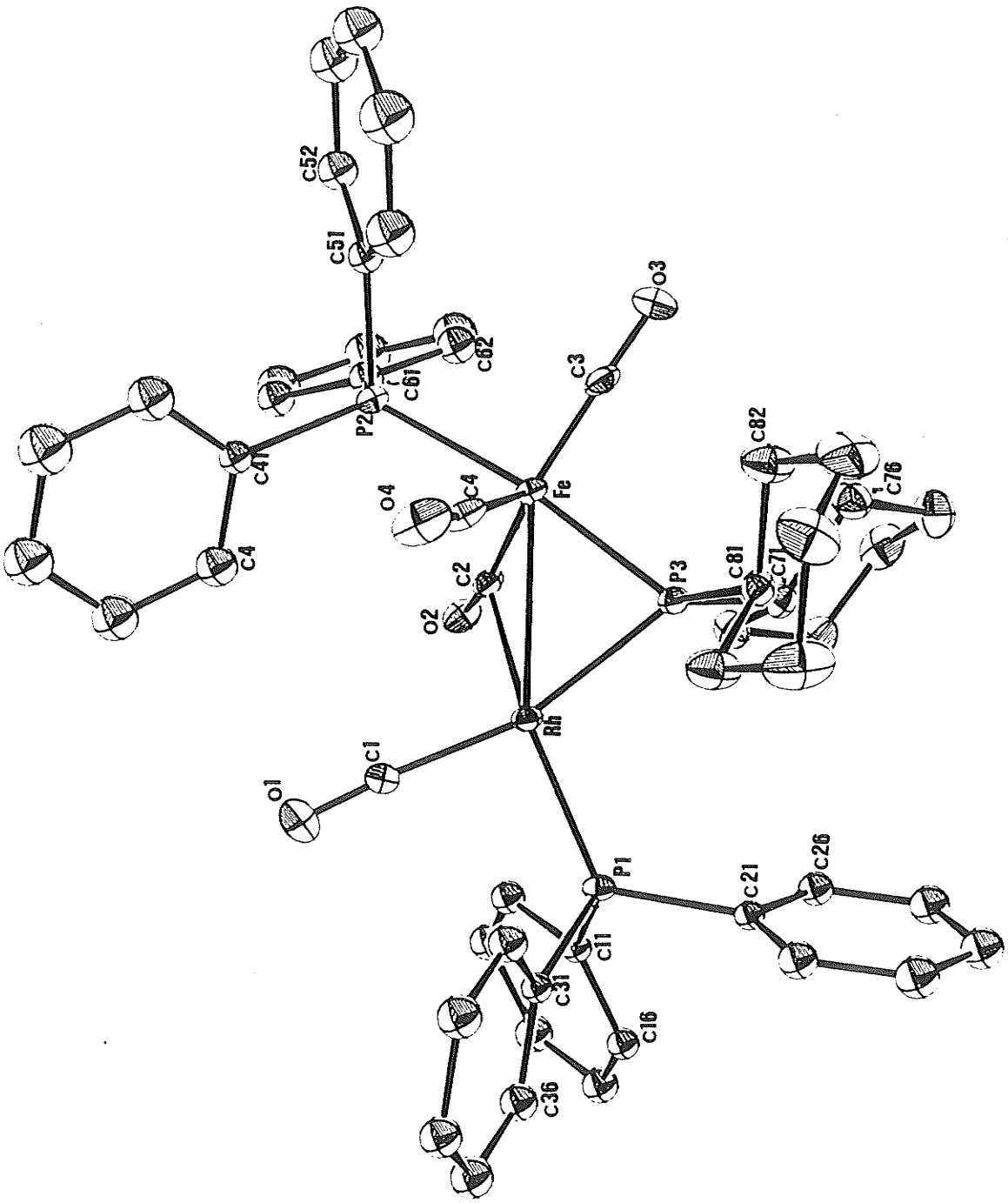
C52
C51
C62
C61
P2
C41
C4
O3
C3
O4
C4
Fe
C82
C76
C2
O2
P3
C81
C71
Rh
C1
O1
P1
C21
C26
C11
C31
C16
C36

Figure 4.5: Representation of the inner coordination sphere of complex 1.

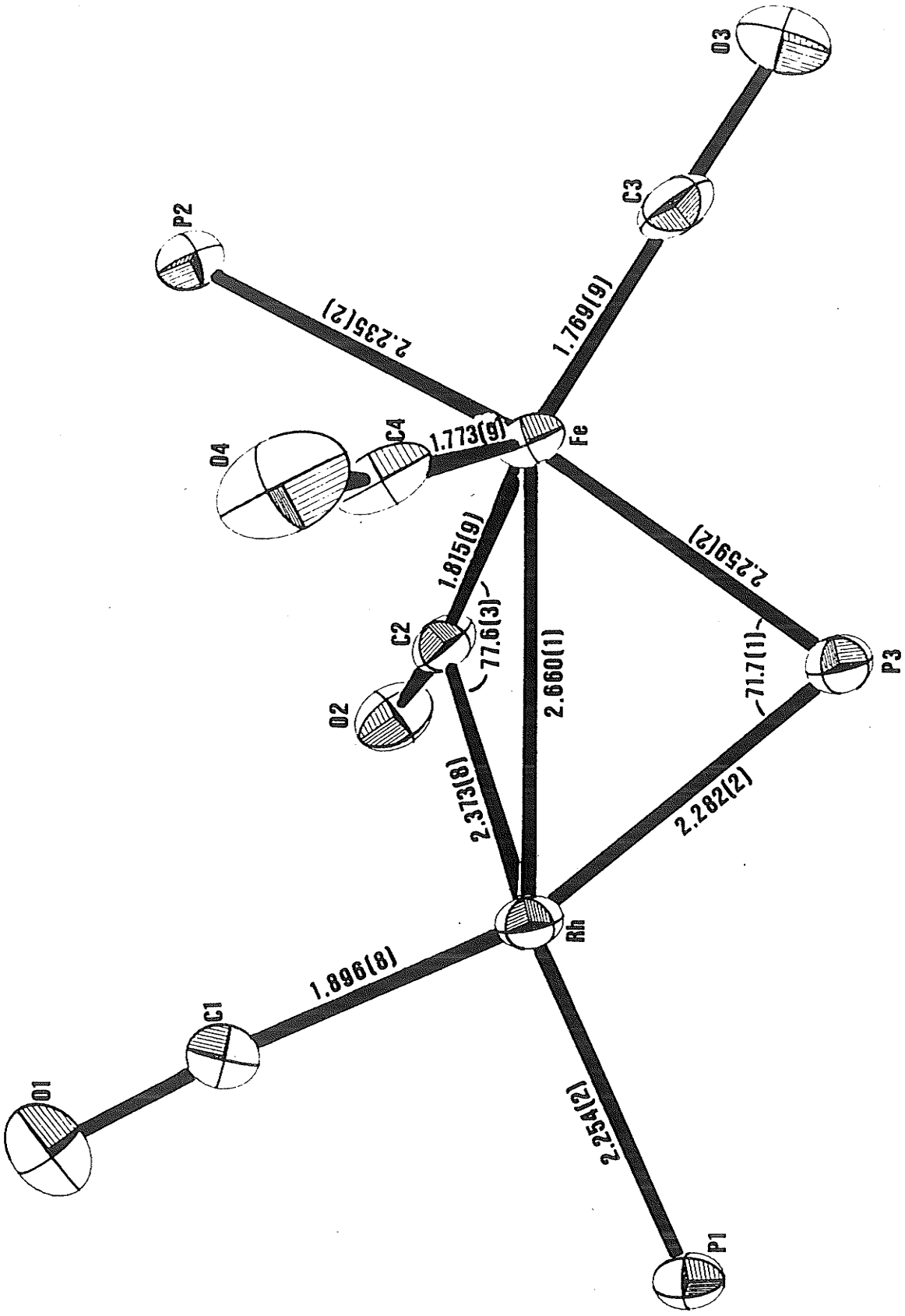
O3
C3
P2
2.235(2)
1.769(9)
O4
C4
1.773(9)
Fe
1.815(9)
2.259(2)
C2
77.6(3)
O2
2.660(1)
71.7(1)
P3
2.373(8)
2.282(2)
Rh
1.896(8)
C1
O1
2.254(2)
P1

In this heterobimetallic complex the metals Fe and Rh are bridged by a dicyclohexylphosphide unit. The Rh atom is further coordinated to a PPh_3 ligand, one CO, and the Fe metal centre. THe angles P3-Rh-P1, P1-Rh-C1, and C1-Rh-Fe are all within the range for square planar geometry, but the Fe-Rh-P3 angle of 53.7(1)° gives the Rh atom a distorted square planar geometry. The Fe atom is coordinated to the μ-PCy_2 ligand, one PPh_3 ligand, and three CO ligands, giving it a trigonal bipyramidal geometry. The Fe-P distances are typical, averaging to 2.247(2)Å; Fe-C distances average to 1.852(9)Å, and also fall within the expected range. Selected bond distances and angles are listed in Appendix 4.1.

The Fe-Rh bond length is 2.660(1)Å, consistent with a metal-metal bond. Known Fe-Rh bond distances range from 2.568 to 2.615Å[67], and 2.660(1) is slightly more than the sum of the covalent radii of the atoms: Fe = 1.20Å; Rh = 1.35Å; sum = 2.55Å. The complex can be formulated as having a donor-acceptor bond between d^8 Fe(0) and d^8 Rh(I) centres, with Fe functioning as a two electron donor to Rh, and the phosphido ligand functioning as a uninegative ligand to balance the +1 charge at Rh. Electron counting schemes would then provide Fe with 18 electrons and Rh with 16 electrons. The principles behind these assignments were discussed in Chapter Two, in which the complex $(CO)_4Mo(\mu\text{-}PCy_2)Pd(PPh_3)$ was investigated.

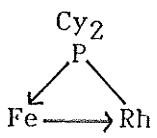

Figure 4.6: The Fe-Rh donor-acceptor bond.

The Rh centre, with a formal 16 electron count, is coordinatively unsaturated. In the solid state it would appear that the empty coordiantion site is filled by C2 in the form of a semi-bridging carbonyl between Fe and Rh. The Fe-C2 distance of 1.815(9)Å is somewhat longer than expected in comparison to the other Fe-C distances. The Rh-C2 distance of 2.373(8)Å is only 0.5Å longer than the Rh-C1 distance, which indicates that some interaction may be taking place. Evidence for this is shown in the solid state infrared spectrum of complex **1**, where the ν_{CO} band at 1842 cm^{-1} would be due to the semi-bridging carbonyl group. In *n*-hexane solution, this band is not present, and instead another band appears at 2035 cm^{-1}. There are two possible explanations for the semi-bridging carbonyl, which is present in the solid state and absent in solution. The semi-bridging carbonyl may be filling the empty coordination site at Rh, or it may be due to crystal packing forces present in the solid state but not in solution. The semi-bridging carbonyl is discused more thoroughly in Section 4.5.

It is difficult to compare the structure of **1** with the structure of the coordinatively saturated molecule $(CO)_3(PPh_3)Fe(\mu\text{-}PPh_2)Ir(PPh_3)(CO)_2$ solved by Geoffroy[23]. The Fe atom in the Fe-Ir complex is also trigonal bipyramidal, as is the Ir atom. In fact the Fe-Ir distance of 2.960Å is longer than expected, though some metal-metal interaction does occur. The complexes $(CO)_3(PEt_3)Fe(\mu\text{-}PPh_2)Rh(PEt_3)(CO)$ and $(CO)_3(PPh_3)Fe(\mu\text{-}PPh_2)Rh(PPh_3)(CO)$ were also prepared by Geoffroy[23], but were not structurally characterized.

4.5 The Semi-Bridging Carbonyl

Unsymmetrical or semi-bridging carbonyl units can be loosely defined by the case where the two metal-carbon distances vary by more than 0.25Å. The following section puts forward a simple and useful way to explain the occurrence of semi-bridging carbonyl groups. These ideas by no means represent a final dogma, but serve only as guidelines by which to understand the anomalous CO group.

The first example of a semi-bridging carbonyl was reported in 1961 by Hock and Mills[68] of the compound shown below in Figure 4.7.

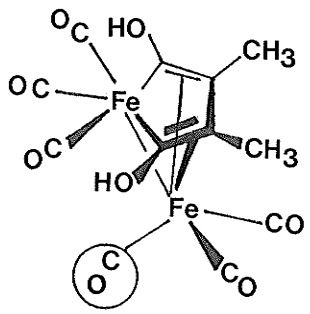

Figure 4.7: $C_4(CH_3)_2(OH)_2Fe_2(CO)_6$, the first reported example of a complex with a semi-bridging carbonyl.

They believed the carbonyl group circled above was unusual in two respects: 1) the Fe-C-O angle was only 168°, and 2) the distance from the carbon atom to the other iron atom was only 2.48Å, considerably less than that expected for nonbonded contact.

In the case of complex **1** the same features are seen, where the Fe-C2- O2 angle is 167.2(7)°, and the Rh-C2 distance is only 2.373(8)Å.

Cotton[69] and Wilkinson propose a series of steps as a rationalization for this phenomenon, and they are outlined below.

1) The number of valence shell electrons on each metal atom is counted neglecting the metal-metal bond and treating the anomalous CO group as a normal terminal CO group. The Fe atom in complex **1** then has the complete set of 18 valence shell electrons, whereas if we count the Rh as Rh(I), it has only 14 valence shell electrons.

2) Since the structure of compound **1** indicates the presence of an Fe-Rh single bond, two electrons from the 18-electron Fe atom are used to form a donor bond (explained in Section 2.6) to the 14 electron Rh atom.

3) The formation of the Fe→Rh bond gives a highly polar electron distribution, violating Pauling's electroneutrality principle, since there are adjacent atoms of opposite formal charges, +1 and -1.

4) This charge imbalance is resolved by the anomalous CO group, which uses one of its π^* orbitals to accept electron density from the Rh atom while still strongly π-bonded to the Fe atom. The nature of the bonding interaction is shown below in Figure 4.8.

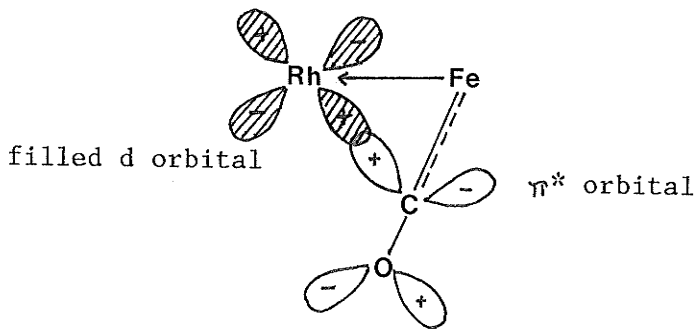

Figure 4.8: Sketch showing how electron density from a filled *d* orbital on Rh can be partially transferred into one of the π^* orbitals of a CO group that is principally bonded to the adjacent Fe atom.

4.6 Reactions of $(CO)_3(PPh_3)Fe(\mu\text{-}PCy_2)Rh(PPh_3)(CO)$

Reactions involving several different types of reagents will give a good indication of the reactivity features of a specific type of complex. As was seen in Chapter Three, the coordinatively saturated complex $(CO)_3(PPh_3)Fe(\mu\text{-}PCy_2)Ir(PPh_3)(CO)_2$ did not undergo addition reactions, but phosphine substitution occurred readily. Complex **1** is coordinatively unsaturated at the Rh centre and therefore it is much more likely to undergo oxidative-addition reactions. Also, addition of molecules such as CO will occur to fill the empty coordination site at Rh, or even to replace the Fe→Rh bond to saturate the Rh centre. Oxidative-addition is also more likely to occur at Rh as compared to Ir, since Rh is a second row element, less basic than Ir, and is equally stable in both the +1 and +3 oxidation states. Finally, substitution reactions may also occur to displace PPh_3 or CO on either metal atom. $^{31}P\{^1H\}$ nmr data for all products formed appear in Table 4.3.

i) Reaction of 1 with CO to form Complexes 3a and 3b

The addition of CO to the coordinatively unsaturated complex **1** is a logical starting point in studying the reactivity of **1**. Addition of one molecule of CO may occur at the Rh centre to fill the coordination sphere, or two molecules of CO may add to displace the metal-metal bond.

Table 4.3: $^{31}P\{^{1}H\}$ NMR Spectral Data[a] for Complex 1 and Derivatives

Complex	$\delta(PCy_2)$[b]	$\delta(P_{Fe})$	$\delta(P_{Rh})$	$^{2}J_{\mu P-P_{Fe}}$[c]	$^{2}J_{\mu P-P_{Rh}}$	$J_{\mu P-P_{Rh}}$	$J_{P_{Rh}-Rh}$	$J_{P_{Rh}-P_{Rh}}$
1	167.2ddd[d]	78.0d	34.8dd	23.1	19.4	103.3	200.5	
3a	196.6ddd	77.4d	36.0dd	21.9	187.1	80.1	100.8	
3b	189.8dd		38.8dd		199.3	82.6	103.3	
4a	183.9ddd		30.2ddd(PPh_3)		14.6	104.4	199.1(PPh_3)	29.1
			8.0ddd(PEt_3)		212.1		134.9(PEt_3)	
4b	177.4dd		31.5dd		212.7	98.4	136.1	
4c	162.2dd		18.3dd		214.8	94.8	136.8	
4d	156.9ddd	80.4d	21.2dd	20.0	210.9	94.8	134.9	
5a	191.9dd		40.0dd		194.4	83.8	105.7	
5b	180.3dd		30.1dd		209.3	94.8	139.4	
5c	165.9ddd	79.5d	35.3dd	18.3	220.6	87.5	104.7	
5d	146.0dd	76.6d		23.8		104.5		
6	196.6ddd	77.4d	32.0dd	20.6	187.1	117.8	135.7	
7	186.1ddd	75.2d	28.1dd	20.7	206.5	100.8	73.4	
8	188.0dd		36.9dd		198.0	82.6	104.1	

[a]Recorded as toluene solutions at 220K. [b]Chemical shift units: ppm.
[c]Coupling constant units: Hz. [d]Abbreviations: d = doublet.

When a toluene solution of complex **1** is stirred for 30 minutes under one atmosphere CO, two products are formed, shown below in Figure 4.9. In both cases CO has added at the Rh centre, causing rearrangement of PPh_3 to the *trans* position, according to $^{31}P\{^1H\}$ nmr.

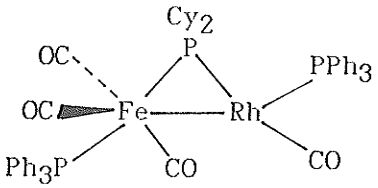

1

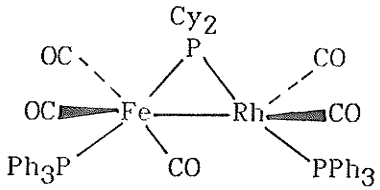

3a

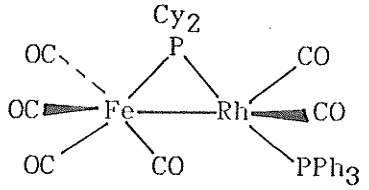

3b

Figure 4.9: The formation of complexes 3a and 3b.

Product **3a** is the CO adduct of complex **1**, a complex similar in structure to $(CO)_3(PPh_3)Fe(\mu\text{-}PCy_2)Ir(PPh_3)(CO)_2$, discussed in Chapter Three. Product **3b** on the other hand, is the result of both CO addition at Rh as well as CO substitution for PPh_3 at Fe. $^{31}P\{^1H\}$ nmr at room temperature gives a well resolved spectrum for **3b**, a doublet of doublets at δ189.9 ppm due to $\mu\text{-}PCy_2$ coupling to PPh_3(Rh) and Rh, and a doublet of doublets at δ38.8 ppm due to PPh_3(Rh) coupling to $\mu\text{-}PCy_2$ and Rh. However, exchange occurs at Rh in complex **3a** at room temperature, resulting in broad, unresolved resonances for $\mu\text{-}PCy_2$ and PPh_3(Rh). As the temperature is cooled to 240K, the peaks resolve to

the expected doublet of doublets of doublets at δ196.6 ppm due to μ-PCy_2 coupling to PPh_3(Fe), PPh_3(Rh), and Rh, a doublet due to PPh_3(Fe) arises at δ77.4 ppm, and a doublet of doublets due to PPh_3(Rh) arises at δ36.0 ppm due to coupling to μ-PCy_2 and Rh. If the CO atmosphere is removed, complexes **3a** and **3b** revert to complex **1**. Figure 4.10 shows the variable temperature $^{31}P\{^1H\}$ nmr spectra for this system from 240-300K.

Addition of CO at Rh is not unexpected, due to the coordinative unsaturation that exists there. For the complexes $(CO)_3(PR_3)Fe(\mu\text{-}PPh_2)Rh(PR_3)(CO)$ (R = Ph, Et)[23] addition of CO at Rh also occurred, and these reactions were also reversible. However, Geoffroy[23] did not report a substitution reaction of CO for PPh_3 occurring at Fe. Substitution may occur in order to reduce steric crowding at Fe due to interactions between PPh_3(Fe) and the μ-PCy_2 ligand. Substitution of CO for PPh_3 at Fe might relieve this strain. Since we did not observe substitution for PPh_3(Fe) by CO for $(CO)_3(PPh_3)Fe(\mu\text{-}PCy_2)Ir(PPh_3)(CO)_2$, the presence of the Rh atom may also have some effect on reactions at Fe. This is not completely unexpected, since in the preparation of heterobimetallic compounds we hope to observe metal cooperativity. However, it is surprising since such reactions at Fe have not been observed in similar compounds.

ii) Reaction of 1 with PEt_3 to form Complexes 4a-4d

Reacting complex **1** with one molar equivalent of PEt_3 would presumably yield similar substitution products to those observed for

Figure 4.10: $^{31}P\{^{1}H\}$ variable temperature nmr spectra of complexes 3a and 3b, from 240K to 300K.

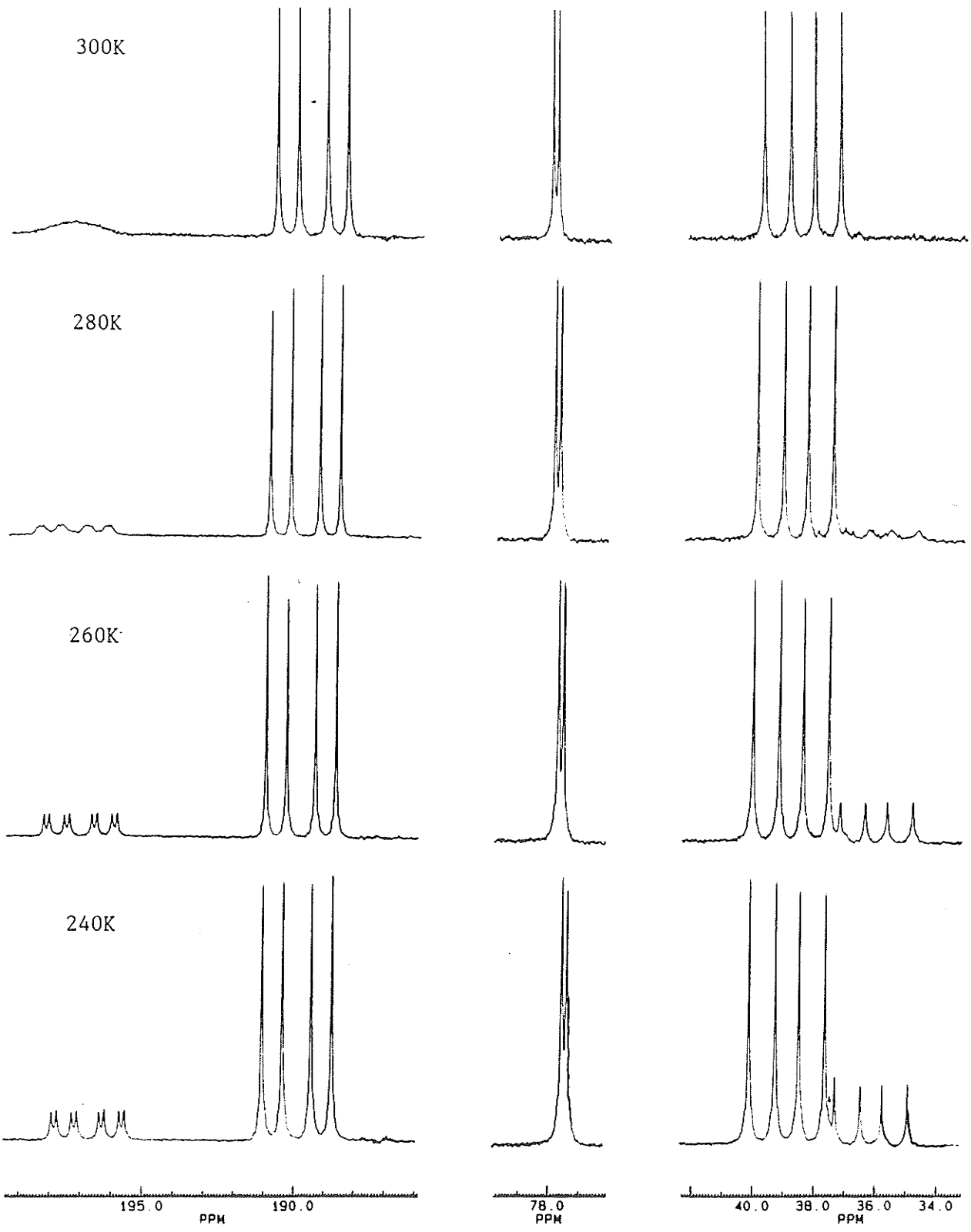
300K
280K
260K
240K
195.0
190.0
PPM
78.0
PPM
40.0
38.0
36.0
34.0
PPM

$(CO)_3(PPh_3)Fe(\mu\text{-}PCy_2)Ir(PPh_3)(CO)_2$. However, because **1** is coordinatively unsaturated at Rh, it is much more reactive and forms four products in reaction with an equimolar amount of PEt_3.

The low field portion of the $^{31}P\{^1H\}$ nmr spectrum of compounds **4a-4d** at 220K is shown in Figure 4.11. The five sets of resonances due to $\mu\text{-}PCy_2$ (including complex **1**) are well separated and we can clearly see that there is no major product, but that an approximately equal ratio of all five exists. Figure 4.12 shows the upfield portion of the $^{31}P\{^1H\}$ nmr spectrum at 220K. The resonances due to phosphine on Rh are not as distinct as resonances due to $\mu\text{-}PCy_2$, but unambiguous assignments of coupling constants can be made. The proposed structures of products **4a** to **4d** are shown in Figure 4.13.

The most straightforward reaction occurs for product **4d**, which is the simple substitution of PEt_3 for PPh_3(Rh). The $^{31}P\{^1H\}$ nmr spectrum for **4d** shows a doublet of doublets of doublets at δ156.9 ppm due to $\mu\text{-}PCy_2$, a doublet at δ80.4 ppm due to PPh_3(Fe), and a doublet of doublets at δ21.2 ppm due to PEt_3(Rh). The difference between the $^{31}\{^1H\}$ nmr spectrum of this compound and that of complex **1** is the *trans* coupling between $\mu\text{-}PCy_2$ and PEt_3(Rh) of 210.9 Hz, indicating that rearrangement has occurred.

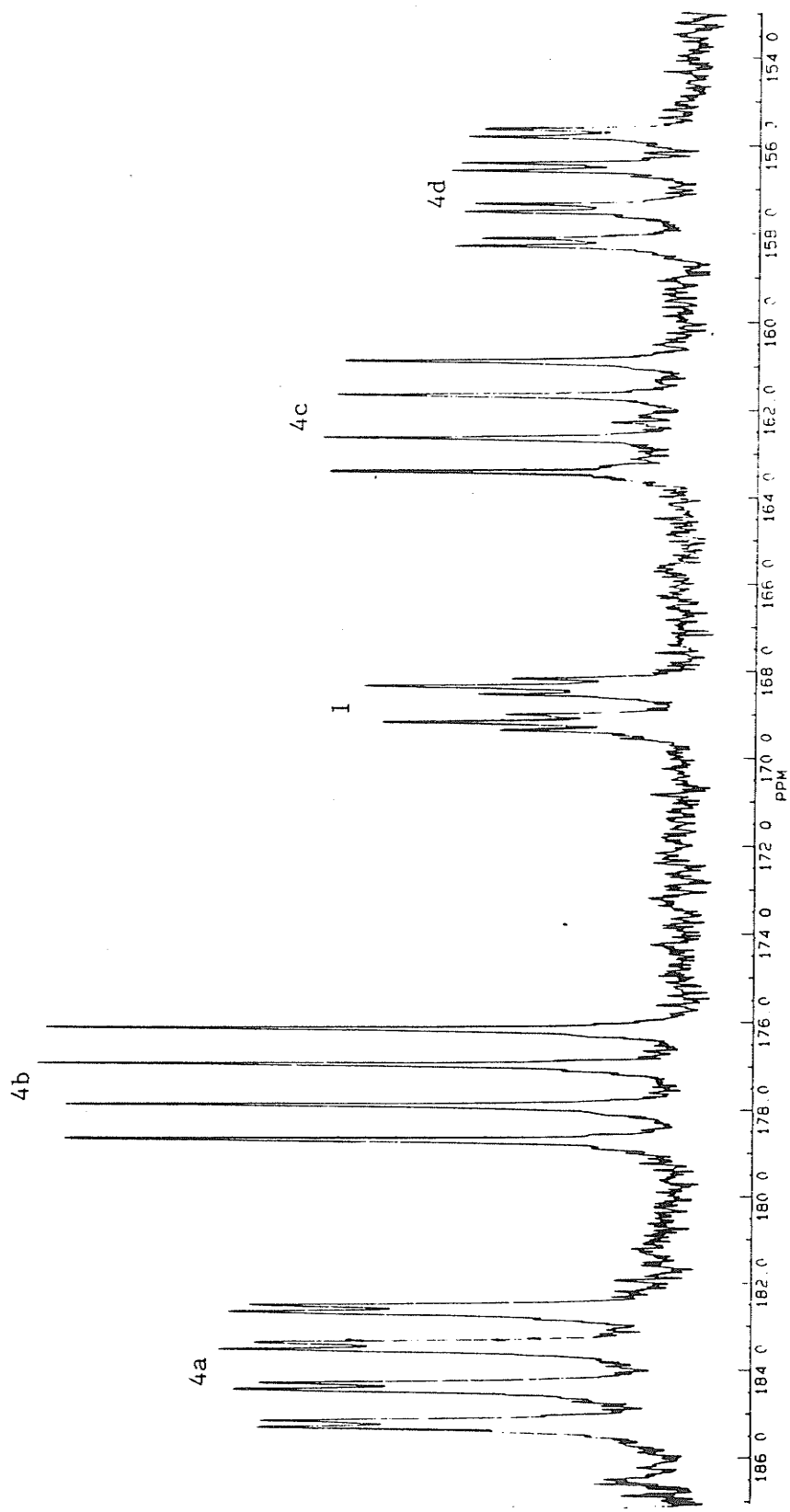

Figure 4.11: Low field portion of the $^{31}P\ ^{1}H$ nmr spectrum of complexes 4a-4d at 220K.

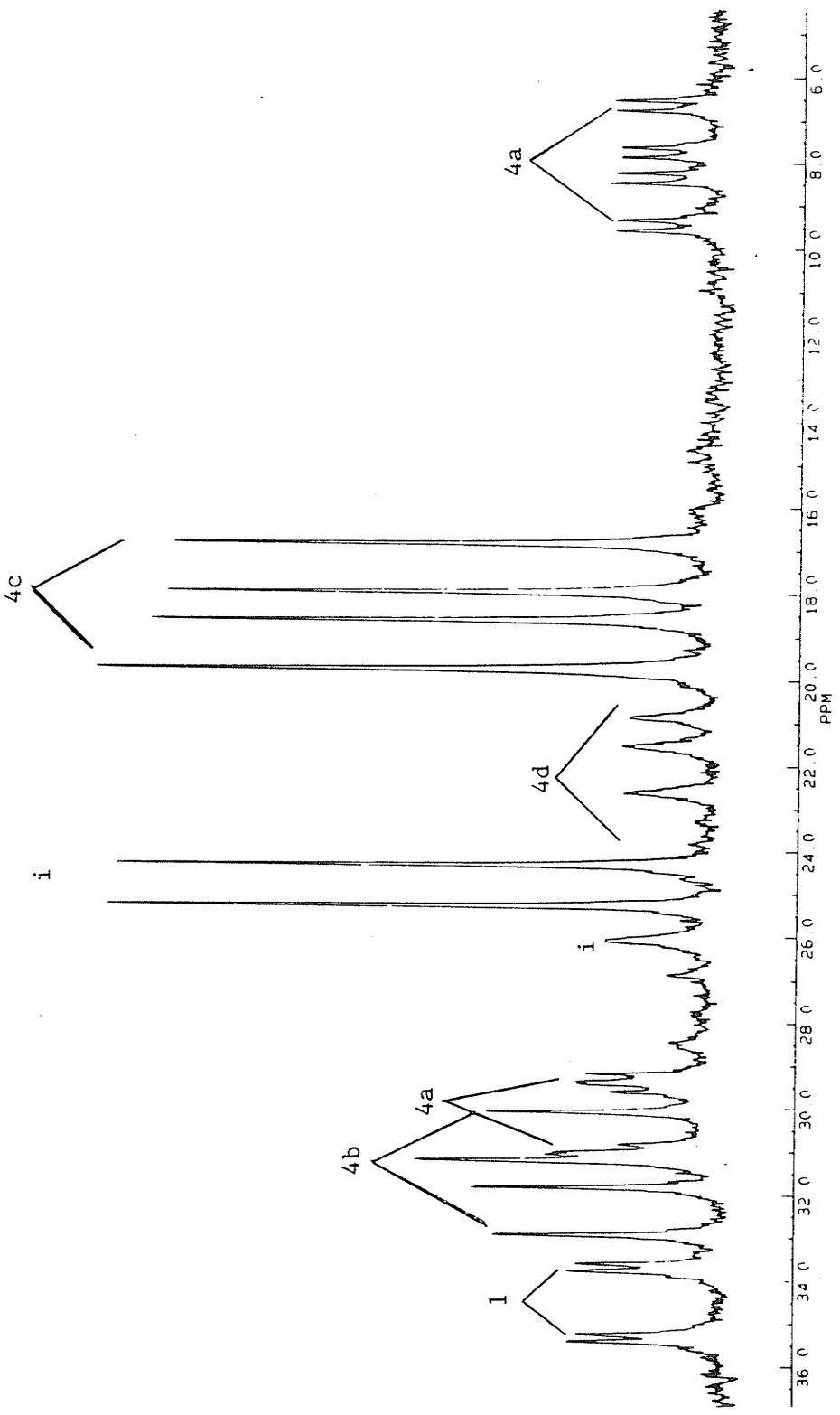

Figure 4.12: High field portion of the ^{31}P ^{1}H nmr spectrum of complexes 4a-4d at 220K. Peaks labelled with an i are impurities.

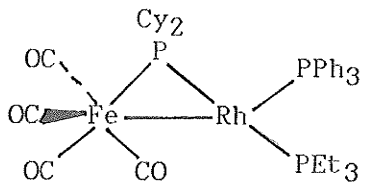

4a

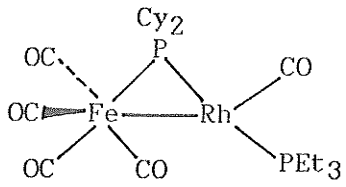

4c

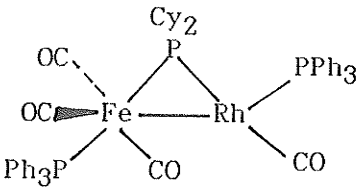

1

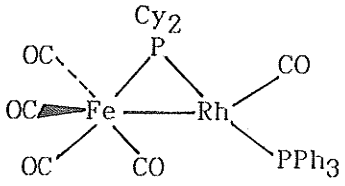

4b

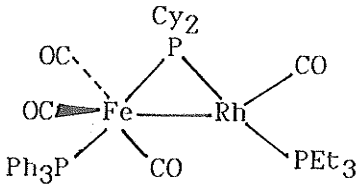

4d

Figure 4.13: Formation of complexes 4a-4d.

The $^{31}P\{^{1}H\}$ nmr spectrum of **4a** is interesting, since it shows a doublet of doublets of doublets at δ183.9 ppm, but no resonances in the PPh_3(Fe) region. This indicates that there must be two phosphines bonded to Rh, and indeed two doublets of doublets of doublets are observed at δ30.2 ppm and δ8.0 ppm due to PPh_3 and PEt_3 respectively. The $^{2}J_{_{PPh_3-PEt_3}}$ coupling constant of 212 Hz indicates that PEt_3 is in the *trans* position. We believe that PEt_3 has displaced CO on Rh, instead of substituting for PPh_3(Rh), and that the displaced CO ligand has migrated to Fe and further replaced PPh_3(Fe), giving **4a**.

Products **4b** and **4c** each contain only one phosphine ligand. The

$^{31}P\{^{1}H\}$ nmr spectrum of **4b** shows a doublet of doublets at δ177.4 ppm due to μ-PCy_2 and a doublet of doublets at δ31.5 ppm, presumably due to PPh_3(Rh). Product **4c** also shows a doublet of doublets at δ162.2 ppm due to μ-PCy_2, and a doublet of doublets at δ18.3 ppm due to PEt_3(Rh). Both show *trans* coupling between μ-PCy_2 and PR_3. In fact, all the coupling constants for **4b** and **4c** are within two hertz of each other, indicating that they have similar structures, as in Figure 4.13.

We can make several observations regarding the results of this substitution reaction. Firstly, we can differentiate between PPh_3 and PEt_3 on Rh by differences in their coordinated ^{31}P nmr chemical shifts. PPh_3 ligated to Rh appears between δ25-35 ppm, and PEt_3 ligated to Rh appears between δ5-25 ppm. These results are not unexpected due to the different basicities of the two phosphines. Secondly, in comparison to $(CO)_3(PPh_3)Fe(\mu\text{-}PCy_2)Ir(PPh_3)(CO)_2$, it is obvious that the coordinative unsaturation of **1** provides for several types of reaction pathways. Simple substitution of PEt_3 for PPh_3 is one of these, and product **4d** is expected on the basis of the phosphine substitution reactions reported in Chapter Three. Thirdly, product **4d** is the only product in which PPh_3 on Fe has been retained. Similar to product **3b**, CO has displaced PPh_3 on Fe in three of the four products; $^{31}P\{^{1}H\}$ nmr shows a single peak at δ-6.0 ppm due to free PPh_3. Additional CO molecules may be present in the form of $Fe(CO)_4(PCy_2H)$, as was seen in Chapter Three. We believe that the Fe portion of complex **1** may be behaving as a "CO sink", in which any CO molecules present in solution will ligate to Fe at the expense of phosphine.

iii) Reaction of 1 with *t*-BuCN to form Complexes 5a-5d

In the reaction of complex **1** with *t*-BuCN, we might expect to see products similar to those observed when **1** was reacted with CO, since CO and *t*-BuCN are isoelectronic molecules. However, on reacting **1** with one molar equivalent *t*-BuCN, products **5a** to **5d** are observed, and these are outlined below in Figure 4.14.

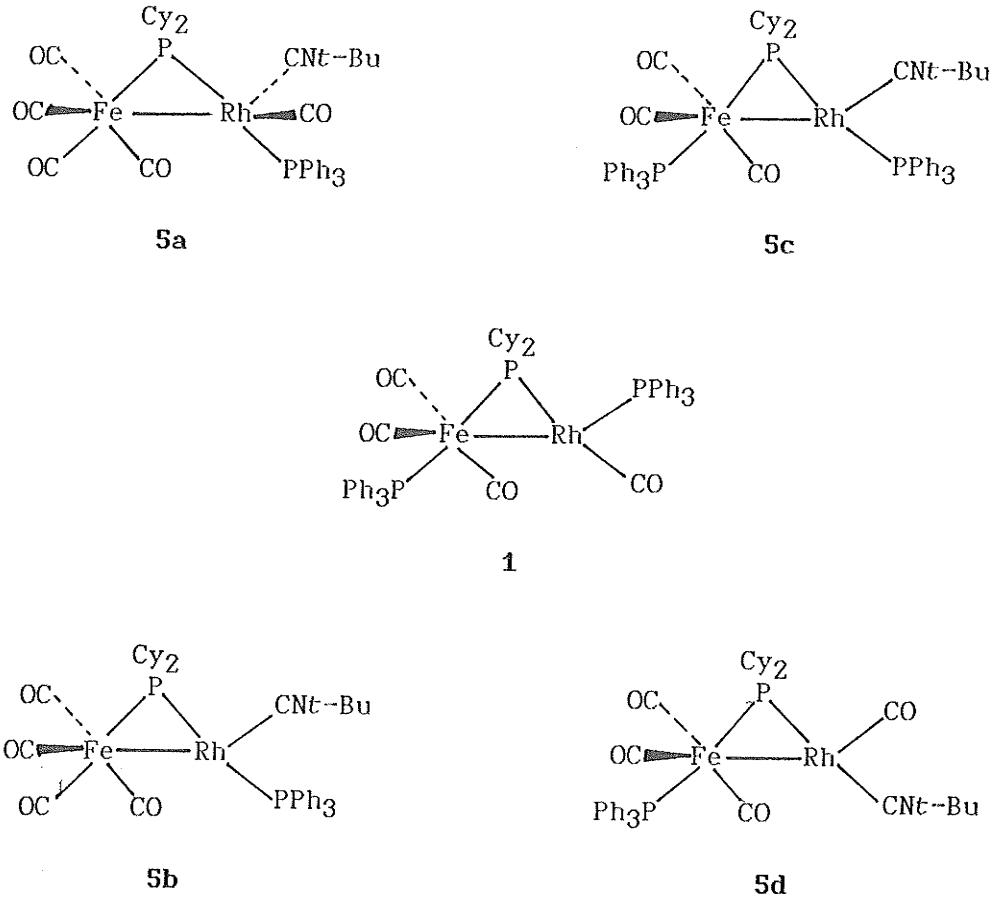

Figure 4.14: Formation of complexes 5a-5d.

Product **5c** is the result of substituiton of *t*-BuCN for CO at Rh. This complex is coordinatively unsaturated at Rh, and the $^{31}P\{^{1}H\}$ nmr spectrum shows the expected pattern: a doublet of doublets of doublets at δ165.9 ppm due to μ-PCy_2, a doublet at δ79.5 ppm due to PPh_3(Fe), and a doublet of doublets at δ35.3 ppm due to PPh_3(Rh). PPh_3 at Rh has *trans* geometry, presumably because *t*-BuCN is a more bulky ligand than CO.

Product **5d** is an anomaly in this series, since PPh_3(Rh) has been displaced by *t*-BuCN, while PPh_3(Fe) has been retained. The $^{31}P\{^{1}H\}$ nmr spectrum of this product shows a doublet of doublets at δ146.0 ppm due to μ-PCy_2, and a doublet at δ76.6 ppm due to PPh_3(Fe).

Products **5a** and **5b** are very similar. In **5a**, *t*-BuCN has added at Rh to form the coordinatively saturated product, while for **5b**, *t*-BuCN has added at Rh, causing loss of CO to form the coordinatively unsaturated product. The most obvious difference in the $^{31}P\{^{1}H\}$ nmr spectra of these two complexes is the differences in chemical shifts of the μ-PCy_2 ligands. For complex **5a** the resonance due to μ-PCy_2 occurs at δ191.9 ppm, and for complex **5b** the resonance due to μ-PCy_2 occurs at δ180.3 ppm. In both **5a** and **5b** PPh_3(Fe) has been replaced by CO, as we observed for complexes **4a-4c**.

We can make a direct comparison between prodcut **5a** and $(CO)_4Fe(\mu\text{-}PCy_2)Rh(PPh_3)(CO)_2$, **3b**, since both complexes are coordinatively saturated at Rh. The chemical shifts and coupling constants in the $^{31}P\{^{1}H\}$ nmr spectra of these two complexes differ by no more than two ppm or two hertz, respectively. These similarities arise because CO and *t*-BuCN are isoelectronic species, and as such, would not affect large differences in the $^{31}P\{^{1}\}$ nmr spectra of **3b** and **5a**.

iv) Oxidative-Addition Reactions of 1

It is well known that oxidative-addition reactions are more likely to occur at coordinatively unsaturated centres[26]. Therefore we expect that complex **1** will oxidatively-add molecules such as H_2, MeI, and HCl to form coordinatively saturated Rh(III) species.

When a toluene solution of **1** is stirred under one atmosphere H_2 for 30 minutes, two products are formed in an approximate 1:1 ratio. The first has been observed previously, complex **4b**, $(CO)_4Fe(\mu\text{-}PCy_2)Rh(PPh_3)(CO)$. The second complex is the oxidative-addition product **6**, $(CO)_3(PPh_3)Fe(\mu\text{-}PCy_2)Rh(PPh_3)(H)_2$. The $^{31}P\{^1H\}$ nmr spectrum of this complex shows the expected doublet of doublets of doublets at δ196.6 ppm due to $\mu\text{-}PCy_2$, a doublet at δ77.4 ppm due to PPh_3(Fe), and a doublet of doublets at δ32.0 ppm due to PPh_3(Rh). The PPh_3 ligand on Rh is *trans* to $\mu\text{-}PCy_2$. The proposed structure of complex **6** is shown in Figure 4.15.

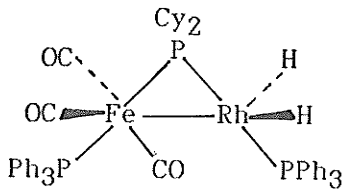

Figure 4.15: Proposed sturcture of complex 6, $(CO)_3(PPh_3)Fe(\mu\text{-}PCy_2)Rh(PPh_3)(H)_2$.

The $^{31}P\{^{1}H\}$ nmr spectrum of **6** bears close resemblance to that of compound **3a**, $(CO)_3(PPh_3)Fe(\mu\text{-}PCy_2)Rh(PPh_3)(CO)_2$, in that the chemical shifts of both the $\mu\text{-}PCy_2$ and the $PPh_3(Fe)$ ligands are equal, as are the $^{2}J_{\mu P-P_{Fe}}$ and $^{2}J_{\mu P-P_{Rh}}$ coupling constants. This similarity would seem to imply that the chemical shift of the $\mu\text{-}PCy_2$ ligand does not depend on the oxidation state of Rh. The $J_{\mu P-Rh}$ and J_{P-Rh} coupling constatns are approximately 25 Hz higher for complex **6** than for **3a**, and this difference is probably due to the change in oxidation state from Rh(I) in **3a** to Rh(III) in **6**.

Complex **1** also reacts with MeI to form product **4b** and the salt $[(CO)_3(PPh_3)Fe(\mu\text{-}PCy_2)Rh(PPh_3)(Me)]^{+}[I]^{-}$, which precipitated from the reaction mixture as a red solid. The $^{31}P\{^{1}H\}$ nmr spectrum of this complex shows a doublet of doublets of doublets at δ186.1 ppm due to $\mu\text{-}PCy_2$, a doublet at δ75.2 ppm due to $pph_3(Fe)$, and a doublet of doublets at δ28.1 ppm due to $PPh_3(Rh)$. The $^{2}J_{\mu P-P_{Rh}}$ coupling constant of 206.5 Hz indicates that $PPh_3(Rh)$ is in the *trans* position. The most unusual property of the spectrum of complex **7** is the J_{P-Rh} coupling constant of 74.3 Hz, which is approximately 30 Hz lower than any other J_{P-Rh} coupling constant. The reasons for this may be the presence of the methyl group at Rh, and the change in oxidation state from Rh(I) to Rh(III). The proposed structure of complex **7** is shown in Figure 4.16.

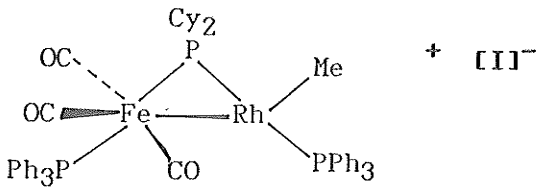

Figure 4.16: Proposed structure of $[(CO)_3(PPh_3)Fe(\mu\text{-}PCy_2)Rh(PPh_3)(Me)]^+[I]^-$, complex 7.

Finally, complex **1** oxidatively-adds HCl to form compound **8**, $(CO)_4Fe(\mu\text{-}PCy_2)Rh(PPh_3)(H)(Cl)$, and **4b** in an approximate 1:2 ratio. The $^{31}P\{^1H\}$ nmr spectrum shows a doublet of doublets at δ188.0 ppm due to $\mu\text{-}PCy_2$, and a doublet of doublets at δ36.9 ppm due to $PPh_3(Rh)$. The $^2J_{\mu P-P_{Rh}}$ coupling constant of 198.0 Hz indicates that PPh_3 is *trans* to $\mu\text{-}PCy_2$. In complex **8**, PPh_3 at Fe has been displaced by CO, unlike complexes **6** and **7**, which retained PPh_3 at Fe.

It would seem that for all three oxidative-addition reactions a competing reaction to form product **4b** is also occurring. This may be because CO is completely removed from Rh in all three reactions, similar to the reaction of **1** with PEt_3. Free CO may then react with **1** to form **4b** in all four reactions. There may also be free CO available in the form of $Fe(CO)_4(PCy_2H)$, as we saw in Chapter Three.

4.7 Preparation and Characterization of $(CO)_4Fe(\mu\text{-}PCy_2)Rh(COD)$ (2)

Complexes such as Wilkinson's catalyst, $RhCl(PPh_3)_3$[63], and $[Rh(\mu\text{-}PPh_2)(COD)]_2$, prepared by Kreter and Meek[19], are known hydrogenation

catalysts. The similarity of compound **2**, $(CO)_4Fe(\mu\text{-}PCy_2)Rh(COD)$, to these complexes warrants its synthesis and the investigation of its reaction properties. Complex **2** contains the easily displaced 1,5-COD ligand, and as was shown in Chapter Three, replacement of 1,5-COD by molecules such as CO and PR_3 provided new compounds with additional side products.

Complex **2** was prepared by reacting two moles $Li[Fe(CO)_4(PCy_2)]$ with one mole $[RhCl(COD)]_2$ as in Equation 4.2. Complex **2** could not be isolated as a solid, but only as a black oil. It was therefore used in situ for reactions with CO, H_2, and PR_3 (R = Et, Cy) with CO.

$$2Li[Fe(CO)_4(PCy_2)] + [RhCl(COD)]_2 \longrightarrow 2(CO)_4Fe(\mu\text{-}PCy_2)Rh(COD) + 2LiCl \quad (4.2)$$

The $^{31}P\{^1H\}$ nmr spectrum shows one doublet downfield at δ142.61 ppm, $J_{\mu P-Rh}$ = 128.8 Hz, indicating that a metal-metal bond may be present. The infrared spectrum of **2** in *n*-hexane solution shows six bands, more than the four expected due to C_{2v} symmetry about the Fe atom. The band at 1837 cm^{-1} may possibly indicate that a semi-bridging carbonyl is present, as was seen for complex **1**. The additional bands may be due to isomerization between a complex that has a semi-bridging carbonyl, and one that does not, and both may exist in solution at room temperature. On the basis of $^{31}P\{^1H\}$ nmr and infrared spectral evidence, the proposed structure of complex **2** is shown in Figure 4.17. Tables 4.4 and 4.5 contain $^{31}P\{^1H\}$ nmr and infrared spectral data, respectively.

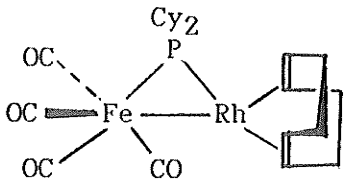

Figure 4.17: Proposed structure of complex 2.

Table 4.4: $^{31}P\{^{1}H\}$ NMR Data[a] for Complex 2 and Derivatives

Complex	$\delta(PCy_2)$[b]	$\delta(P_{Rh})$	$^{2}J_{\mu P-P_{Rh}}$[c]	$J_{\mu P-Rh}$	J_{P-Rh}
2	142.6d[d]			128.8	
8a	217.5d			89.8	
8b	172.9d			103.3	
8c	16.2d			117.9	
9	179.8dd	26.1dd	192.0	81.4	100.8
10	173.1dd	51.9dd	187.1	79.0	99.6
11a	174.9d			99.6	
11b	194.8d			89.9	
11c	216.5d			106.9	

[a]Recorded in toluene solutions at 220K. [b]Chemical shift units: ppm.
[c]Coupling constant units: Hz. [d]Abbreviations: d = doublet.

Table 4.5: Infrared Spectral Data for Complex 2 and Derivatives

Complex	ν_{CO} (cm^{-1})[a]
2	2075(w)[b], 2040(m), 2004(s), 1987(s), 1971(s), 1837(m)
9	2050(w), 2035(w), 2005(w), 1993(s), 1973(s), 1949(m), 1882(m), 1835(m)
10	2033(s), 2004(w), 1985(w), 1970(s), 1963(s), 1949(sh), 1905(w), 1837(w)

[a]Recorded as hexane solutions unless otherwise specified.
[b]Abbreviations: s = strong, m = medium, w = weak.

4.8 Reactions of $(CO)_4Fe(\mu\text{-}PCy_2)Rh(COD)$

As we observed in Chapter Three, the coordinatively unsaturated complex $(CO)_4Fe(\mu\text{-}PCy_2)Ir(COD)$ was easily prepared and reacted with several reagents, including CO, and PR_3 and CO, to displace the labile 1,5-COD ligand. This complex also catalyzed the hydrogenation of styrene to ethyl benzene. Compound **2** should also react with these reagents. Again, reactions can occur at a) the coordinatively unsaturated Rh centre, b) to displace the 1,5-COD ligand, or c) at the metal-metal bond. $^{31}P\{^1H\}$ nmr and infrared spectral data are shown in Tables 4.4 and 4.5 respectively.

Complex **2** was stirred under one atmosphere CO for 30 minutes, during which time the solution turned red-brown in colour. $^{31}P\{^1H\}$ nmr showed three doublets, indicating that three products were formed, **8a-8c**, shown in Figure 4.18.

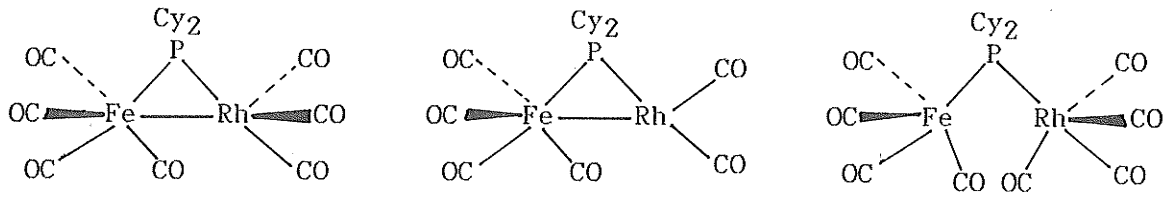

8a **8b** **8c**

Figure 4.18: Proposed structures of complexes 8a-8c.

The $^{31}P\{^1H\}$ nmr spectrum of products **8a-8c** shows a large doublet at δ217.5 ppm due to **8a**, the coordinatively saturated CO adduct. A doublet at δ172.9 ppm is attributed to **8b**, the coordinatively

unsaturated product. Finally, a doublet at δ16.2 ppm is attributed to **8c**.

Formulations of the structures of compolexes **8a-8c** are based on comparing nmr data for **8a-8c** to that of $(CO)_4Fe(\mu\text{-}PCy_2)Ir(CO)_3$, complex **1**, and its CO adduct, **3a**. The $^{13}C\{^1H\}$ nmr spectrum of $(CO)_4Fe(\mu\text{-}PCy_2)Ir(CO)_3$ indicated that 1,5-COD was displaced by CO, and therefore we believe that the same type of reaction with CO at Rh takes place in complex **2**. Product **8a** has a downfield shift of the $\mu\text{-}PCy_2$ ligand, similar to product **3a**, and is therefore believed to be coordinatively saturated. The similar chemical shifts of the $\mu\text{-}PCy_2$ ligands for complex **1** and **8b** indicate that **8b** is probably coordinatively unsaturated. The upfield shift of the resonance due to $\mu\text{-}PCy_2$ in complex **8c** indicates that the Fe-Rh bond has been displaced by CO. This is the first time that reaction of CO with any of the heterobimetallic complexes mentioned here has proceeded to displace the metal-metal bond.

When compound **2** is reacted with PR_3 under one atmosphere CO, the coordinatively saturated products $(CO)_4Fe(\mu\text{-}PCy_2)Rh(PR_3)(CO)_2$ (R = Et (**9**), and Cy (**10**) are formed. The $^{31}P\{^1H\}$ nmr spectra for the complexes are similar: a doublet of doublets at δ179.8 ppm and δ173.1 ppm, and a doublet of doublets at δ26.1 ppm and δ51.9 ppm for **9** and **10** respectively. Both phosphines have *trans* geometry, as shown by $^2J_{\mu P-P_{Rh}}$ coupling constants of 192.0 and 187.1 Hz for **9** and **10** respectively. The infrared spectra for **9** and **10** are also similar, both showing the expected six band pattern. Both Fe and Rh exhibit C_{2v} symmetry, and therefore four bands are expected due to carbonyls attached to Fe, and two bands are expected due to carbonyls attached

to Rh.

Complex **9** is an interesting comparison to the very similar complex **4c**, $(CO)_4Fe(\mu\text{-}PCy_2)Rh(PEt_3)(CO)$. The $\mu\text{-}PCy_2$ $^{31}P\{^1H\}$ nmr chemical shift of **9** is approximately 17 ppm higher than that of **4c**, and the PEt_3 chemical shift of **9** is approximately 10 ppm higher than that of **4c**. Coordinative saturation at Rh then, seems to cause the ^{31}P resonances to shift to lower field. We can use this correlation as a very general indication of coordinative saturation. Using the same arguments, we can say that complex **10** is also coordinatively saturated.

When complex **2** is reacted with H_2, $^{31}P\{^1H\}$ nmr at 220K indicates that three products are formed, **9a-9c**. If the reaction proceeds in a similar manner to that of $(CO)_4Fe(\mu\text{-}PCy_2)Ir(COD)$, then one of the three products may be $(CO)_4Fe(\mu\text{-}PCy_2)Rh(THF)_x$. It is difficult to formulate the structures of any of these complexes solely on the basis of $^{31}P\{^1H\}$ nmr data. ^1H nmr did not show the presence of any metal hydride peaks. Further investigations of these complexes may prove them to be useful hydrogenation catalysts, similar to $(CO)_4Fe(\mu\text{-}PCy_2)Ir(COD)$.

4.9 Summary and Conclusions

Coordinative unsaturation at Rh provided for much more reactive heterobimetallic Fe-Rh complexes when compared to similar Fe-Ir complexes prepared in Chapter Three. Complex **1** reacted with reagents such at PEt_3, CO, and *t*-BuCN resulting in several different types of

substitution and addition products. The Rh atom in **1** also underwent oxidative-addition when reacted with H_2, MeI, and HCl. In all reactions, at least one product was formed in which CO displaced PPh_3 at Fe.

Reactions with complex **2** provced to be less definitive than those observed for similar Fe-Ir complexes. Reactions with phosphines and CO seemed to be relatively straightforward, producing coordinatively saturated complexes in which the 1,5-COD ligand had been displaced by PR_3 and CO. The reaction of complex **2** and CO provided us with the first μ-PCy_2-bridged complex, in this study, in which the metal-metal bond was displaced by CO. When complex **2** was reacted with H_2, three unidentifiable products were formed. However, further investigations into this system may prove it to ba a more uselful hydrogenation catalyst than was $(CO)_4Fe(\mu\text{-}PCy_2)Ir(COD)$, due to the increased reactivity at Rh.

APPENDIX 4.1
SELECTED BOND DISTANCES AND ANGLES FOR $(CO)_3(PPh_3)Fe(\mu\text{-}PCy_2)Rh(PPh_3)(CO)$, (1)

Table 1: Distances (Å)

Rh-Fe	2.660(1)	Fe-P2	2.235(2)
Rh-P1	2.254(2)	Fe-P3	2.259(2)
Rh-P3	2.282(2)	Fe-C2	1.815(9)
Rh-C1	1.896(8)	Fe-C3	1.769(9)
Rh-C2	2.373(8)	Fe-C4	1.773(9)
P1-C11	1.850(6)	P2-C41	1.832(6)
P1-C21	1.850(5)	P2-C51	1.853(8)
P1-C31	1.847(5)	P2-C61	1.836(6)
P3-C71	1.861(8)	C1-O1	1.12 (1)
P3-C81	1.857(8)	C2-O2	1.16 (1)
C3-O3	1.16 (1)	C4-O4	1.17 (1)

Table 2: Angles (degrees)

Fe-Rh-P1	158.8(1)	Rh-Fe-P2	126.4(1)
Fe-Rh-P3	53.7(1)	Rh-Fe-P3	54.5(1)
Fe-Rh-C1	110.7(3)	Rh-Fe-C2	60.6(3)
Fe-Rh-C2	41.8(2)	Rh-Fe-C3	142.8(3)
P1-Rh-P3	106.0(1)	Rh-Fe-C4	80.1(3)
P1-Rh-C1	90.1(3)	P2-Fe-P3	175.6(1)
P1-Rh-C2	135.5(2)	P2-Fe-C2	87.0(2)
P3-Rh-C1	163.0(3)	P2-Fe-C3	89.5(3)
P3-Rh-C2	77.1(2)	P2-Fe-C4	89.7(3)
C1-Rh-C2	95.2(3)	C2-Fe-C3	119.6(4)
Rh-P1-C11	113.2(2)	C2-Fe-C4	127.0(4)
Rh-P1-C21	122.3(2)	C3-Fe-C4	113.3(4)
Rh-P1-C31	111.7(2)	Fe-P2-C41	115.9(2)
C11-P1-C21	100.3(2)	Fe-P2-C51	115.7(2)
C11-P1-C31	105.7(3)	Fe-P2-C61	113.3(2)
C21-P1-C31	101.9(2)	C41-P2-C51	103.7(3)
Rh-P3-C71	120.8(3)	C41-P2-C61	104.9(3)
Rh-P3-C81	120.1(3)	C51-P2-C61	101.8(3)
C71-P3-C81	102.9(3)	Fe-P3-C71	120.6(3)
Rh-C1-O1	174.3(8)	Fe-P3-C81	119.9(3)
Rh-C2-O2	114.8(6)	Fe-C2-O2	167.2(7)
Fe-C3-O3	178.5(7)	Fe-C4-O4	176.4(8)
P1-C11-C12	118.9(4)	P2-C41-C42	117.0(4)
P1-C11-C16	121.1(4)	P2-C41-C46	122.9(5)
P1-C21-C22	121.4(4)	P2-C51-C52	118.7(5)
P1-C21-C26	118.5(6)	P2-C51-C56	121.3(5)
P1-C31-C32	115.2(4)	P2-C61-C62	118.2(3)
P1-C31-C36	124.8(4)	P2-C61-C66	121.7(4)
P3-C71-C72	111.5(5)	P3-C81-C82	114.7(6)
P3-C71-C76	116.3(6)	P3-C81-C86	112.3(6)

REFERENCES

1. J. A. IBERS. Chem. Soc. Rev. **11**, 57 (1982), and references therein.

2. J. M. RITCHEY, D. C. MOODY, and R. R. RYAN. Inorg. Chem. **22**, 2276 (1982).

3. T. YOSHIDA, D. L. THORN, T. OKANO, S. OTSUKA, and J. A. IBERS. J. Amer. Chem. Soc. **102**, 6541 (1980).

4. G. J. KUBAS. J. Chem. Soc. Chem. Comm. 61 (1980).

5. G. J. KUBAS, G. D. JARVINEN, and R. R. RYAN. J. Amer. Chem. Soc. **105**, 1883 (1983).

6. D. A. ROBERTS AND G. L. GEOFFROY, in "Comprehensive Organometallic Chemistry". G. WILKINSON, G. G. A. STONE, AND E. W. ABEL, eds. Pergamon: Oxford (1982). Ch. 40.

7. R. G. FINKE, G. GAUGHAN, C. PIERPONT, and M. E. CASS. J. Amer. Chem. Soc. **106**, 1394 (1981).

8. G. L. GEOFFROY. Acc. Chem. Res. **18**, 469 (1980).

9. M. P. SCHUBERT. J. Amer. Chem. Soc. **55**, 4563 (1933).

10. R. D. ERNST and T. J. MARKS. Inorg. Chem. **17**, 1477 (1978).

11. P. CHINE. 17th Int. Cong. Pure and Applied Chem. (1959).

12. R. T. BAKER, T. H. TULIP, and S. S. WREFORD. Inorg. Chem. **24**, 1379 (1985).

13. a) H. KOPF and R. H. RATHLEIN. Angew. Chem. Int. Ed. Eng. **8**, 980 (1969). b) P. S. BATERMAN, V. A. WILSON, and K. K. JOSHI. J. Chem. Soc. (A) 191 (1971).

14. W. C. FULTZ, A. L. RHEINGOLD, P. E. KRETER, and D. W. MEEK. Inorg. Chem. **22**, 860 (1983).

15. S. A. MacLAUGHLIN, A. J. CARTY, and N. J. TAYLOR. Can. J. Chem. 60, 7 (1982).

16. P. CHINI, G. LONGONI, AND V. G. ALBANO. Adv. Organomet. Chem. **14**, 285 (1976).

17. a) R. G. HAYTER. Prep. Inorg. React. **2**, 211 (1965) and references therein. b) R. G. HAYTER and F. S. HUMIEC. Inorg. Chem. **2**, 306 (1963). c) R. G. HAYTER. Inorg. Chem. **2**, 1031 (1963).

18. a) J. CHATT and J. M. DAVIDSON. J. Chem. Soc. 2433 (1964). b) J. CHATT and D. A. THORTON. J. Chem. Soc. 1005 (1964).

19. P. E. KRETER and D. W. MEEK. Inorg. Chem. **22**, 319 (1983).

20. J. M. RITCHEY, A. J. ZOZULIN, D. A. WROBLESKI, R. R. RYAN, H. J. WASSERMAN, D. C. MOODY, and R. T. PAINE. J. Amer. Chem. Soc. **107**, 501 (1985).

21. A. M. ARIF, D. C. CHANDLER, and R. A. JONES. Inorg. Chem. **26**, 1780 (1987).

22. H. J. LANGENBACK and H. VAHRENKAMP. Chem. Ber. **112**, 3773 (1979).

23. M. J. BREEN, M. R. DUTTERA, G. L. GEOFFROY, D. A. ROBERTS, G. R. STEINMETZ, P. M. SHULMAN, E. D. MORRISON, C. W. DeBROSSE, and R. R. WHITTLE. Organometallics **2**, 846 (1983).

24. a) H. VAHRENKAMP. Angew. Chem. Int. Ed. Engl. **17**, 379 (1978). b) W. L. GLADFELTER AND G. L. GEOFFROY. Adv. Organomet. Chem. **18**, 207 (1980). c) C. W. ABEL and S. P. TYFIELD. Adv. Organomet. Chem. **8**, 117 (1970).

25. P. C. STEINHARDT, W. L. GLADFELTER, A. D. HARLEY, J. R. FOX, and G. L. GEOFFROY. Inorg. Chem. **19**, 332 (1980).

26. J. P. COLLMAN and L. S. HEGEDUS. "Principles and Applications of Organotransition Metal Chemistry". University Science Books: Mill Valley, California (1980).

27. J. A. OSBORN, F. H. JARDINE, J. F. YOUNG, and G. WILKINSON. J. Chem. Soc. (A) 1711 (1966).

28. L. VASKA. Acc. Chem. Res. **9**, 175 (1976).

29. F. NOBILE, G. VARAPOLLO, P. GIANNOCCARO, AND A. SACCO. Inorg. Chim. Acta. **48**, 261 (1981).

30. T. S. TARGOS, R. P. ROSEN, R. R. WHITTLE, AND G. L. GEOFFROY. Inorg. Chem. **24**, 1375 (1985).

31. C. H. TOLMAN. Chem. Rev. **77**, 313 (1977).

32. J. C. BAILAR JR., and H. ITANANI. Inorg. Chem. **4**, 1618 (1965). ($PdCl_2(PPh_3)_2$ is prepared by the same method, producing yellow crystalline solid in 75% yield.)

33. L. M. VENANZI. J. Chem. Soc. 719 (1958).

34. D. J. DARENSBOURG and R. L. KUMP. Inorg. Chem. **17**, 2680 (1978).

35. D. F. SHRIVER. "The Manipulation of Air-Sensitive Compounds". McGraw-Hill: New York (1969).

36. E. D. MORRISON, A. D. HARLEY, M. A. MARCELLI, G. L. GEOFFROY, A. L. RHEINGOLD, and W. C. FULTZ. Organometallics **3**, 1407 (1984).

37. M. J. BREEN and G. L. GEOFFROY. Organometallics **1**, 1437 (1982).

38. Phosphido ligands are not always inert and unreactive. a) G. L. GEOFFROY, S. ROSENBERG, P. M. SHULMAN, and R. R. WHITTLE. J. Amer. Chem. Soc. **106**, 1519 (1984). b) R. J. CROWTE and J. EVANS. J. Chem. Soc. Chem. Comm. 1332 (1984).

39. a) J. L. PETERSON and R. P. STEWART JR. INorg. Chem. **19**, 186 (1980). b) A. J. CARTY, S. A. MacLAUGHLIN, and N. J. TAYLOR. J. Organomet. Chem. **204**, C27 (1981). c) A. J. CARTY. Adv. Chem. Ser. **196**, 163 (1982).

40. P. S. PREGOSIN and R. W. KUNZ. "Phosphorous-31 and Carbon-13 Nuclear Magnetic Resonance Studies of Transition Metal Complexes Containing Phosphorous Ligands". Springer-Verlag: New York (1979).

41. K. F. PURCELL and J. C. KOTZ. "Inorganic Chemistry". W. B. Saunders Company: Philadelphia (1977).

42. D. E. SANDS. "Introduction to Crystallography". W. A. Benjamin Inc.: New York (1969).

43. a) M. PFEFFER, J. FISCHER, A. MITSCHLER, and L. RICHARD. J Amer. Chem. Soc. **102**, 6338 (1980). b) M. PFEFFER, D. GRANDJEAN, and G. LeBORGNE. Inorg. Chem. **20**, 4226 (1981). c) R. BENDER, P. BRAUNSTEIN, Y. DUSAUSORY, and J. PROTAS. Angew. Chem. Int. Ed. Engl. **17**, 596 (1978).

44. Z. Z. ZHANG, H. K. WANG, H. G. WANG, and R. J. WANG. J. Organomet. Chem. **314**, 357 (1986).

45. W. W. PORTERFIELD. "Inorganic Chemistry, a Unified Approach". Addison Wesley: Don Mills, Ontario (1983).

46. a) R. A. JONES, J. G. LASCH, N. C. NORMAN, A. L. STUART, T. C. WRIGHT, and B. R. WHITTLESEY. Organometallics **3**, 114 (1984). b) R. A. JONES, A. L. STUART, J. L. ATWOOD, W. E. HUNTER, and T. C. WRIGHT. Organometallics **1**, 1721 (1982). c) R. A. JONES and T. C. WRIGHT. Organometallics **2**, 1842 (1983). d) D. J. CHANDLER, R. A. JONES, A. L. STUART, and T. C. WRIGHT. Organometallics **3**, 1830 (1984).

47. W. C. MERCER, G. L. GEOFFROY, and A. L. RHEINGOLD. Organometallics **4**, 1418 (1985).

48. M. J. BREEN, P. M. SHULMAN, G. L. GEOFFROY, A. L. RHEINGOLD, and W. C. FULTZ. J. Amer. Chem. Soc. **105**, 1069 (1983).

49. R. A. JONES, T. C. WRIGHT, J. L. ATWOOD, and W. E. HUNTER. Organometallics **2**, 470 (1983).

50. a) R. REGRAGUI, P. H. DIXNEUF, N. J. TAYLOR, and A. J. CARTY. Organometallics **5**, 1, (1986). b) S. ROSENBERG, W. S. MAHONEY, J. M. HAYES, and G. L. GEOFFROY. Organometallics **5**, 1065 (1986). c) G. L. GEOFFROY, S. ROSENBERG, A. W. HERLINGER, and A. L. RHEINGOLD. Inorg. Chem. **25**, 2916 (1986). d) R. A. JONES, A. L. STEWART, J. L. ATWOOD, and W. E. HUNTER. Organometallics **2**, 1437 (1983). e) R. A. JONES, A. L. STUART, J. L. ATWOOD, and W. E. HUNTER. Organometallics **2**, 874 (1983). f) S. J. LOEB, H. A. TAYLOR, L. GELMINI, and D. W. STEPHAN. Inorg. Chem. **25**, 1977 (1986).

51. S. ROSENBERG, G. L. GEOFFROY, A. L. RHEINGOLD, W. S. MAHONEY, and J. M. HAYES. Organometallics **5**, 1065 (1986).

52. W. C. MERCER, G. L. GEOFFROY, and A. L. RHEINGONLD. Organometallics **4**, 1418 (1985).

53. W. C. MERCER, R. R. WHITTLE, E. W. BURKHARDT, and G. L. GEOFFROY. Organometllics **4**, 68 (1985).

54. K. VRIEZE, J. P. COLLMAN, C. T. SEARS JR., and M. KUBOTA. Inorg. Synth. **11**, 101 (1968).

55. J. L. HERDE, J. C. LAMERT, C. V. SENOFF, and M. A. CUSHING. Inorg. Synth. **15**, 18 (1974).

56. P. M. TREICHEL, W. K. DEAN, and W. M. DOUGLAS. Inorg. Chem. **11**, 1609 (1972).

57. See reference 23 and Chapter Four.

58. J. F. NIXON and A. PIDCOCK. Ann. Rev. NMR. Spectrosc. **2**, 345 (1969).

59. N. C. PAYNE and D. W. STEPHAN. Can. J. Chem. **58**, 15 (1980).

60. J. R. SHAPELY, R. R. SCHROCK, and J. A. OSBORN. J. Amer. Chem. Soc. **91**, 2816 (1969).

61. R. H. CRABTREE, H. FELKIN, and G. E. MORRIS. J. Organomet. Chem. **141**, 205 (1977).

62. M. D. FRYZUK. Can. J. Chem. **61**, 1347 (1983).

63. K. C. DEWHIRST, W. KEIM, and C. A. REILLY. Inorg. Chem. **7**, 546 (1968).

64. D. EVANS, J. A. OSBORN, and G. WILKINSON. Inorg. Synth. **11**, 99 (1968).

65. J. CHATT and L. M. VENANZI. J. Chem. Soc. 4753 (1957).

66. Prepared as described in Section 3.2.ii of this text.

67. a) M. R. CHURCHILL and M. V. VEIDIS. J. Chem. Soc. (A) 2170 (1971). b) M. R. CHURCHILL and M. V. VEIDIS. J. Chem. Soc. Chem. Comm. 1470 (1970).

68. A. A. HOCK and O. S. MILLS. Acta. Crystallogr. **14**, 139 (1961).

69. F. A. COTTON and G. WILKINSON. "Advanced Inorganic Chemistry, A Comprehensive Text. John Wiley and Sons: New York (1980).